

AD-A088 765

SOUTHWEST RESEARCH INST SAN ANTONIO TEX
SPECIAL ENGINEERING SERVICES TO ESTABLISH INSPECTION CRITERIA F--ETC(U)
DEC 79 F N KUSENBERGER, J R BARTON

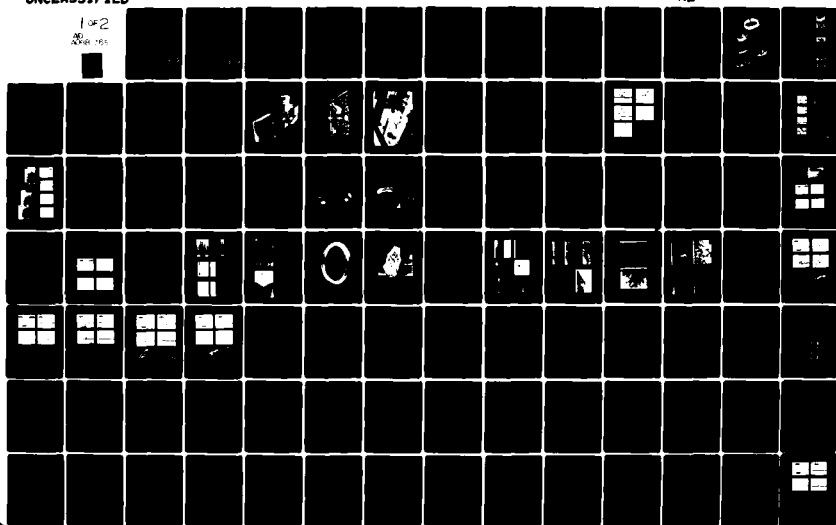
F/G 13/9

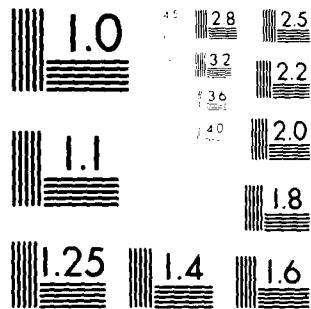
F09603-74-C-5158

NL

UNCLASSIFIED

1 of 2
208 165





MICROCOPY RESOLUTION TEST CHART
NATIONAL BUREAU OF STANDARDS-1963-A

APPROVED FOR PUBLIC RELEASE: DISTRIBUTION UNLIMITED

LEVEL II **①**

**SPECIAL ENGINEERING SERVICES TO
ESTABLISH INSPECTION CRITERIA FOR
BEARINGS TO IMPROVE LIFE PREDICTION**

AD A088765

FINAL ENGINEERING REPORT

(1 July 1974 — 30 November 1979)

SwRI Project 15-4012

Contract No. F09603-74-C-5158

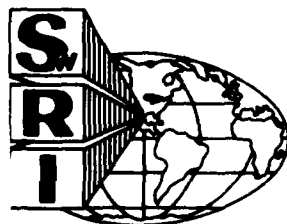
Prepared for

Warner Robins Air Logistics Command
Directorate of Materiel Management
Robins Air Force Base, Georgia 31093

December 1979

DTIC
ELECTE
S SEP 3 1980 **D**
D

DDC FILE COPY



SOUTHWEST RESEARCH INSTITUTE
SAN ANTONIO HOUSTON

80 8 29 086

SOUTHWEST RESEARCH INSTITUTE
Post Office Drawer 28510, 6220 Culebra Road
San Antonio, Texas 78284

**SPECIAL ENGINEERING SERVICES TO
ESTABLISH INSPECTION CRITERIA FOR
BEARINGS TO IMPROVE LIFE PREDICTION.**

by

10) Felix N. Kusenberger, Felix N.
John R. Barton, John R.

FINAL ENGINEERING REPORT

(1 July 1974 — 30 November 1979)

SwRI Project 15-4012

15) Contract No. F09603-74-C-5158

1) Final report.

1 Jul 74 - 30 Nov 79

Prepared for

Warner Robins Air Logistics Command
Directorate of Materiel Management
Robins Air Force Base, Georgia 31093

"The investigation reported in this document was requested by WRALC of the Directorate of Materiel Management, Robins AFB, Georgia 31093 under contract no. F09603-74-C-5158; however, it does not necessarily bear the endorsement of the requesting agency."

December 1979

Approved:

John R. Barton

John R. Barton, Vice President
Instrumentation Research Division

| | |
|----------------------------|-------------------------------------|
| Accession For | |
| NTIS GRA&I | <input checked="" type="checkbox"/> |
| DDC TAB | <input type="checkbox"/> |
| Unannounced | <input type="checkbox"/> |
| Justification | <input type="checkbox"/> |
| By <u>Per Ltr. on file</u> | |
| Distribution/ | |
| Availability Codes | |
| Dist. | Avail and/or special |
| A | |

DTIC
ELECTE
SEP 3 1980

328200

ABSTRACT

The CIBLE (Critical Inspection of Bearings for Life Extension) program concept for quantitative nondestructive evaluation of bearing components is briefly reviewed and the automatic inspection equipment used to acquire the data presented in this report is described. Many examples of significant crack networks detected in the races of vendor reworked bearings as well as subsurface flaw indications in a new bearing are illustrated. The savings realized by elimination of the potential for inclusion nucleated failure from the group of CIBLE inspected bearings is estimated, and the future economic benefits of removing potential failures from the J57-#2 and J57-#4 engine bearings currently in the fleet are also projected. The results of endurance testing bearings with service-induced cracks at low stress levels and flaw indications at higher levels are presented and discussed. The results of metallurgical examination of service-induced cracked regions as well as other flaw regions are illustrated, and the results from 1000 balls inspected at the Oklahoma City Air Logistics Center (OCALC) are summarized. A preliminary serviceability criteria for races is outlined and implementation of the criteria is discussed.

FOREWORD

The work reported herein was conducted under a program sponsored by the United States Air Force, Warner Robins Air Logistics Command, Directorate of Material Management. The authors express their appreciation to Messrs. K. E. Dammann, P. L. Hampton, L. Schaefer, and W. G. Webb of WRALC, and Messrs. E. Ansley, D. Barclay and R. Caldwell of OCALC for encouragement, aid, and enthusiastic participation in this program. The authors gratefully acknowledge the significant contributions by Mr. C. R. McGinnis and Mr. D. H. Heihn through their meticulous acquisition and filing of data, Mr. A. S. Lozano for his many extra hours spent in generating software, Mr. W. B. Tarver for his aid in signature processing concept formulation and development, and Mr. B. B. Baber for conducting the endurance testing efforts.

TABLE OF CONTENTS

| | <u>Page</u> |
|---|-------------|
| LIST OF ILLUSTRATIONS | vi |
| LIST OF TABLES | viii |
| I. INTRODUCTION | 1 |
| A. Background and Significance | 1 |
| B. Inspection Equipment | 7 |
| C. Highlights of Flaw Signature Response | 11 |
| 1. Typical Signature Responses | 11 |
| 2. Significant Flaw Responses | 16 |
| II. SUMMARY OF WORK ACCOMPLISHED | 19 |
| A. CLIN 0001AE, June 1974 - June 1975 | 19 |
| B. CLIN 0001AF (new), July 1975 - June 1977 | 20 |
| C. CLIN 0001AH, July 1977 - June 1978 | 20 |
| D. CLIN 0001AJ, July 1978 - November 1979 | 21 |
| III. SUMMARY OF RESULTS | 25 |
| A. Bearing Population Inspected | 25 |
| B. Significant Flaw Results | 29 |
| 1. Races | 29 |
| 2. Balls | 39 |
| C. Preliminary Serviceability Criteria | 50 |
| IV. CONCLUSIONS AND RECOMMENDATIONS | 52 |
| A. Conclusions | 52 |
| B. Recommendations | 52 |
| V. REFERENCES | 53 |
| APPENDIX A "CIBLE" CONCEPT | |

TABLE OF CONTENTS (continued)

| | |
|------------|---|
| APPENDIX B | IMPLEMENTATION OF "CIBLE" (Preliminary) |
| APPENDIX C | SUMMARY REPORT ON CIBLE BALL INSPECTION |
| APPENDIX D | TABLE OF ENDURANCE TEST RESULTS |
| APPENDIX E | TABLE OF METALLURGICAL RESULTS |
| APPENDIX F | CIBLE RESULTS ON RACES |

LIST OF ILLUSTRATIONS

| <u>Figure</u> | <u>Title</u> | <u>Page</u> |
|---------------|---|-------------|
| 1 | Typical Anti-Friction Bearing Components | 2 |
| 2 | J57 Bearings with Service Induced Cracks | 3 |
| 3 | Bearing Inspection System | 8 |
| 4 | Race Inspection Unit | 9 |
| 5 | Ball/Roller Inspection Unit | 10 |
| 6 | CIBLE System Diagram | 12 |
| 7 | Signatures and Computer Printout from a Ref. Component | 14 |
| 8 | CIBLE Results Showing Surface Photomicrograph (~100x) of Crack Network and Associated Circumfer- ential Flux Signatures | 17 |
| 9 | CIBLE Results on New J57-#4 Bearing (S/N 534A-1) Inner Race, Loaded Half (S12671-2) | 18 |
| 10 | Photograph Illustrating Relationship between Loaded and Inspected Regions on an Inner Race | 23 |
| 11 | Photograph Illustrating Relationship between Loaded and Inspected Regions on an Outer Race | 24 |
| 12 | Bar Graph Showing Distribution of Service Hours, on J57-#2 Serviceable Bearing Population Inspected | 26 |
| 13 | Bar Graph Showing Distribution of Service Hours on J57-#4 Serviceable Bearing Population Inspected | 27 |
| 14 | Bar Graph Showing Distribution of Service Hours on J85-#2 Bearing Population Inspected | 28 |
| 15 | CIBLE Results on J57-#4 Bearing (S/N 219A-2) Inner Race, Nonloaded Half (S12052-1), 3761 hrs. Service, Vendor Reworked | 31 |
| 16 | CIBLE Results on J57-#2 Bearing (S/N Y704-2RM) Outer Race (S01692-5), 8296 hrs. Service, Vendor Reworked | 33 |
| 17 | Graph of Magnetic Perturbation Signature Amplitude as a Function of Applied Magnetization Current for Flaws with and without Cracking | 34 |
| 18 | CIBLE Results on J57-#2 Bearing S/N 144D-2 Inner Race, Loaded Half (S00762-3), 6965 hrs. Service (Vendor Reworked) Before and After Endurance Testing | 35 |

LIST OF ILLUSTRATIONS (continued)

| <u>Figure</u> | <u>Title</u> | <u>Page</u> |
|---------------|---|-------------|
| 19 | Surface Photomicrographs of Flaw Signature Region Before and After Failure (30 Hrs.) Endurance Test Time, J57-#4 Bearing, S/N 219A-2 Inner Race (S12052) | 36 |
| 20 | Very Small Spall which Developed after 30 hours Total Endurance Test Time, J57-#4, S/N 219A-2 (S12052-1) | 37 |
| 21 | Surface Photomicrograph of Spall Region on J57-#4 Inner Bearing Race, S/N 219A-2 (S12052-1) | 38 |
| 22 | Metallurgical Examination of Crack Network on J57-#2 Bearing (S/N 144D-2), Inner Race, Loaded Half at BR2291 Location (S00762-3) | 40 |
| 23 | Metallurgical Examination of Regions Corresponding to Signatures A and B on J57-#2 Bearing (S/N 144D-2), Inner Race Loaded Half (S00762-3) | 41 |
| 23A | Metallurgical Examination of Regions Corresponding to Signatures A and B on J57-#2 Bearing (S/N 144D-2), Inner Race Loaded Half (S00762-3) (continued) | 42 |
| 23B | Metallurgical Examination of Regions Corresponding to Signatures A and B on J57-#2 Bearing (S/N 144D-2), Inner Race Loaded Half (S00762-3) (continued) | 43 |
| 24 | CIBLE Inspection Signatures and Surface Photomicrographs Showing Corresponding Surface Flaws on Ball with 3230 hrs. Service, J57-#4 Bearing S/N 9117-2 | 45 |
| 25 | CIBLE Inspection Signatures and Corresponding Surface Photomicrograph Showing Gouges on Ball with 3230 hrs. Service, J57-#4 Bearing S/N P9117-2 | 46 |
| 26 | CIBLE Inspection Signatures and Corresponding Surface Photomicrograph Showing Inclusion on Surface of New Ball from Vendor Reworked J57-#4 Bearing S/N 3453-2 | 47 |
| 27 | CIBLE Inspection Signatures and Corresponding Surface Photomicrographs Showing Pits and Cracks on New Ball From Vendor Reworked J57-#4 Bearing S/N 395-2 | 48 |
| 28 | CIBLE Inspection Signatures and Corresponding Surface Photomicrographs Showing Crack Network on New Ball From Vendor Reworked J57-#4 Bearing S/N 395-2 | 49 |
| 29 | Serviceability Criteria (preliminary), Races and Rolling Elements | 51 |

LIST OF TABLES

| <u>Table</u> | <u>Title</u> | <u>Page</u> |
|--------------|---|-------------|
| I | Statistical Summary of (CH*) Flaw Printouts | 4 |
| II | Estimated Savings Based on J57 #2 and #4 Bearings Inspected | 5 |
| III | CIBLE - Automated Bearing Inspection System | 13 |
| IV | Statistical Summary of (CH*) Flaw Printouts | 30 |
| V | Summary of Balls (J57 #4 Bearing) Inspected and Magnetic Printouts Obtained | 44 |

I. INTRODUCTION

A. Background and Significance

The primary purpose of the CIBLE (Critical Inspection of Bearings for Life Extension) program is to provide improved nondestructive methods for inspecting new and used rolling element bearing components to ensure a high degree of uniformity and reliability and to provide a basis for forecasting bearing life based on measured material conditions of individual bearing components (the reader is referred to Appendix A of this report for a more detailed description of the CIBLE concept.) Typical bearing components are shown in Figure 1. As part of the overall CIBLE program, computer-assisted automated equipment for quantitative nondestructive evaluation inspection of ball and roller bearing components was delivered to the Air Force Logistics Center at Tinker AFB in Oklahoma City (OCALC) under Contract No. F09650-74-C-0200. This bearing inspection equipment was selected as one of the 100 most significant new technical products in the 1977 IR-100 competition sponsored by Industrial Research magazine in April 1977. A similar system at Southwest Research Institute was used for the data acquisition and signature investigations conducted on the CIBLE inspection program under this Contract No. F09603-74-C-5158.

As a direct result of this CIBLE inspection program, service-induced cracks* in seven serviceable main shaft vendor reworked bearings were detected and other significant flaws (undetected by inspection procedures presently used at the original manufacturer, the overhaul depot, and a rework vendor) were found in many new and serviceable races. It is emphasized that this is the first time quantitative examination with the required resolution and capability of detecting tiny flaws, including subsurface inclusions (0.001 - 0.003 in. dia.), has been completed on a large population of bearing components. Furthermore, analysis of results provides, for the first time, hard data that inclusions and inclusion nucleated cracks can occur even in premium quality aircraft gas turbine engine bearings.

Table I presents a concise statistical summary of flaw printouts obtained with one of the magnetic methods. From these data an appraisal of the potential for inclusion nucleated failures being eliminated and the associated direct economic significance for the J57 #2 and #4 bearings inspected is presented in the data of Table II. It is possible that a few of the inclusion nucleated potential failures would be discovered by SOAP, excessive vibration, etc. However, since extensive subsurface crack networks and material transformations often develop (see Figures 23 & 23A, pp. 41, 42) before any significant material spalls out to cause surface roughness and oil debris, it is more reasonable to assume that most instances would be "sudden type" failures. Support for this idea that subsurface cracking may cause sudden type failures is provided by several

* See Figure 2, arrows point out crack networks

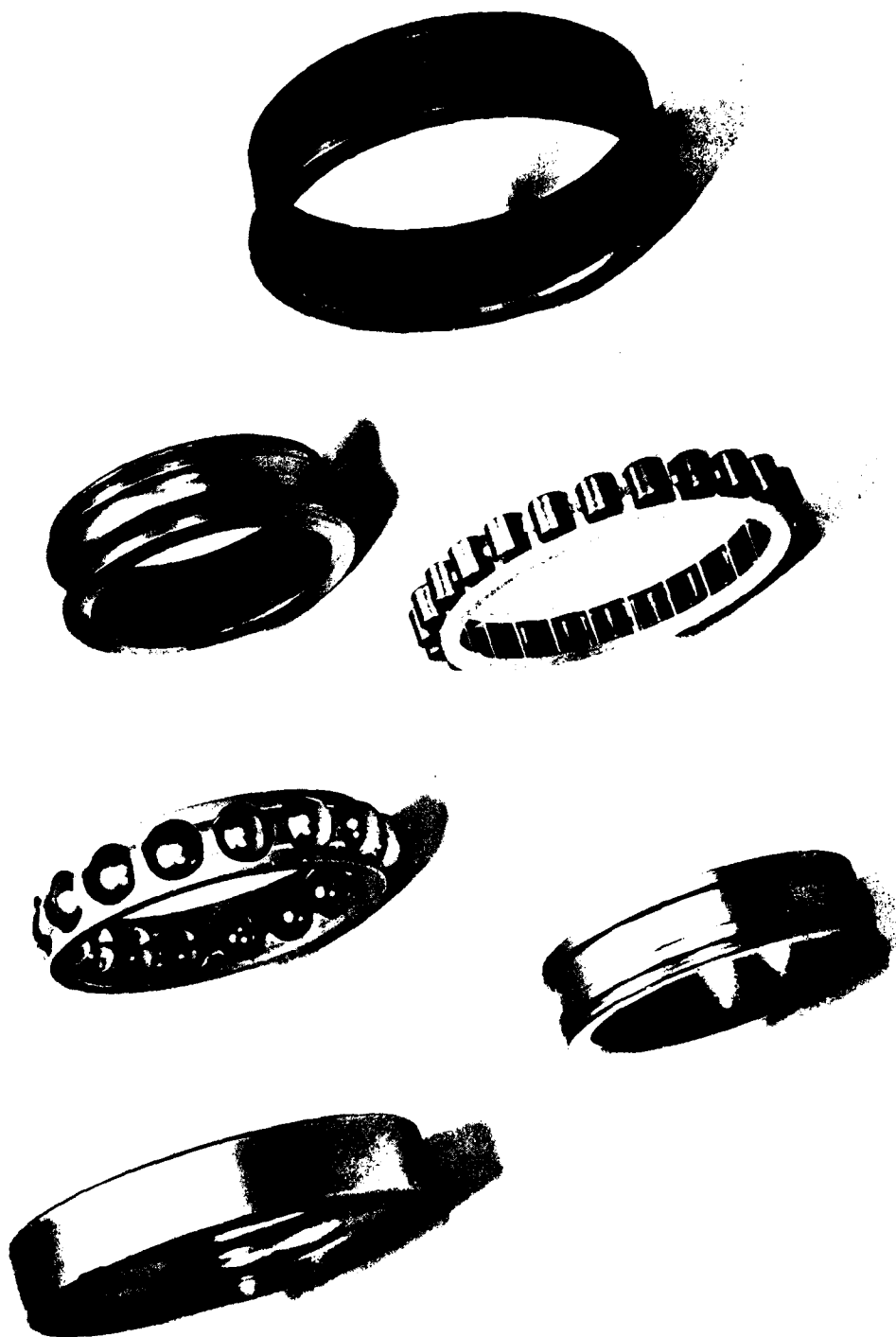


FIGURE 1. TYPICAL ANTI-FRICTION BEARING COMPONENTS

Bearing Position,
S/N, and Mfgr. Code

Service
Hours

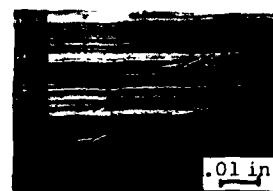
Photomicrograph
of Cracked Region

5547

#2, Outer Race
Y635-2(S01682)
Mfgr. (5)

1108

A.



#4, Inner Race
685D-1(S11281)
Mfgr. (0)

1668

B.



#2, Inner Race
B1274-2(S00032)
Mfgr. (5)

2053

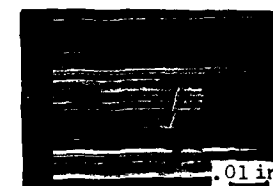
C.



#2, Inner Race
A984-1(S00591)
Mfgr. (5)

2752

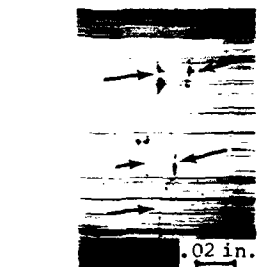
D.



#2, Inner Race
144D-2(S00762)
Mfgr. (0)

6965

E.



#2, Outer Race
Z916-2(S00722)
Mfgr. (5)

7259

F.



#2, Outer Race
Y704-2RM(S01692)
Mfgr. (5)

8296

G.



FIGURE 2. J57 BEARINGS WITH SERVICE INDUCED CRACKS
(Vendor Refurbished bearings accepted by
Air Force for reuse in engines)

TABLE I
STATISTICAL SUMMARY OF (CH*) FLAW PRINTOUTS

| <u>Bearing Type</u> | <u>Bearing Condition</u> | <u>Bearings Inspected</u> | <u>No. with CH Printout</u> | <u>% with CH Printout</u> |
|-------------------------|------------------------------|-------------------------------|---------------------------------|-------------------------------|
| J57-#2 | New | 80 | 1 | 1.3 |
| | Serviceable | 320 | 57 | 17.8 |
| J57-#4 | New | 194 | 12 | 6.2 |
| | Serviceable | 358 | 21 | 5.9 |
| J85-#2 | New | 45 | 4 | 8.9 |
| | Serviceable | 95 | 17 | 17.9 |
| TOTALS | | 1092 | 112 | 10.3 |

*CH = magnetic perturbation, circumferential flux, high field inspection
(This inspection mode detects surface and subsurface inclusions,
cracks, and severe mechanical surface damage)

TABLE II

ESTIMATED SAVINGS BASED ON J57 #2 and #4

BEARINGS INSPECTED

| <u>ASSUMPTION</u> | <u>NUMBER FAILURES</u> | | <u>AVERAGE COST/ FAILURE</u> | <u>SAVINGS</u> |
|-------------------|------------------------|---------|----------------------------------|----------------|
| A | 16 | (1.68%) | \$25,000 | \$ 400,000 |
| | 16 | (1.68%) | \$50,000 | \$ 800,000 |
| B | 27 | (2.84%) | \$25,000 | \$ 675,000 |
| | 27 | (2.84%) | \$50,000 | \$1,350,000 |

TOTAL BEARINGS 952

ASSUMPTIONS:

- A ALL CRACKED BEARINGS AND 25% OF BEARINGS WITH INCLUSIONS
IN LOADED REGION CAUSE FAILURE
- B ALL CRACKED BEARINGS AND 50% OF BEARINGS WITH INCLUSIONS
IN LOADED REGION CAUSE FAILURE

recent inflight engine bearing failures:

- 1977-1978 five compressor bearing failures before 500 hours in large commercial engines - neither SOAP nor vibration monitors warned of impending failure before extensive damage;
- July 1978 KC 135 in-flight engine failure caused by compressor bearing failure;
- Aug 1978 B52 mission abort because of J57#2 engine bearing failure - 256.6 hours since overhaul.

The preceding indicates that a significant economic savings has already been realized from the CIBLE program. In addition, an analysis based on the data of Figure 2 and Table II, indicates that the approximately 6600 J57 and TF33 engines in B52's, KC135's, and C141's presently in use potentially have 244 #2 and 36 #4 bearings with cracks. Total service hours on the seven (7) cracked bearings (Figure 2) is 28,433 hours or an average of 4062 hours. Assuming that these average service hours are accumulated on each engine at the rate of 300 hours/yr. then average service time on each cracked bearing is 13.54 years and the 280 potentially cracked bearings in the total J57 #2 and #4 bearing population (26,000) can be expected to fail at the rate of approximately 21 bearings/yr.

If all these bearings with cracks, as well as those with potential crack nucleating inclusions in the loaded regions, could be removed from service before failure by using the CIBLE inspections, major economic benefits, possible ranging from \$11 X 10⁶ to as great as \$37 X 10⁶, could result. Such inspections would require several years to process the approximately 26,000 bearings (#2 and #4 are duplex sets) but could easily be accommodated by the available equipment. In fact three shift operation of the equipment at OALC and at SwRI could process all 26,000 of these bearings in approximately one year if the bearings were available in such a short time.

Highlights of the voluminous data and results obtained are presented in this report; technical foundations for the inspection methods (1-28)* and a concise summary of the CIBLE concepts (29-33,36)* have been presented previously. A cardinal element of the program has been the acquisition of a comprehensive data base from a large fraction of several in-service bearing populations (for example, J57 engine main shaft ball bearings No. 2 and No. 4 positions) during service lives. Computer processing the extensive data acquired (from components of individual bearings) will aid in development of trend analysis based on characteristic signature changes associated with service-induced bearing deterioration or changes which ultimately would result in failure of the bearing component. The service data base accumulated thus far has been augmented by metallurgical investigations and controlled endurance testing investigations of selected service components. Use of actual engine service instead of the usual laboratory

* Superscript numbers in parentheses refer to list of references at the end of this report.

endurance testing ensures realistic conditions and also eliminates the unacceptable high cost associated with laboratory testing of large numbers of main shaft bearings over intervals commensurate with actual service times. As will become evident in this report, there are significant differences in failure development between service-induced and laboratory-induced damage. An initial serviceability criteria has been developed under the CIBLE program which has been implemented on the CIBLE System at OALC recently (October 1979). Ultimately, a refined serviceability criteria can be evolved using the computer-assisted multiple parameter analyses already implemented by establishing correlations between individual bearing data profiles based on trends in bearing performance with increasing service hours.

For the benefit of the reader, the CIBLE inspection equipment will be briefly described and highlights of flaw responses will be presented before presenting more detailed results.

B. Inspection Equipment

The CIBLE equipment provides a completely integrated nondestructive inspection methodology using non-contacting sensors with precision tracking of individual probes. Accordingly, it is possible to correlate results from several sensor channels, thereby providing a basis for more completely defining and quantifying signature sources. Sensitive quantitative nondestructive examinations of the active race and ball/roller surfaces of individual ball and roller bearing components are accomplished rapidly and automatically under the supervision of a minicomputer. Three different NDE methods are used; namely, magnetic perturbation, Barkhausen noise analysis and scattered laser radiation. A photograph of the overall system is shown in Figure 3, and a description of the methods is presented elsewhere (31-34,36)*. The computer, data terminal, magnetic recorder, power supplies, electronics, etc., are housed in the center consoles; the inner and outer race inspection module is in the cabinet at the left and the ball/roller inspection module is in the cabinet at the right for the Air Force system. A photograph of the race inspection assembly is shown in Figure 4, and Figure 5 is a view of the ball/roller inspection assembly.

Precision fixtures and associated software are required for each different configuration component; change-over from one configuration component to another is simple and can be accomplished in approximately 5 minutes. Fixtures essentially consist of precision air-operated chucks for positioning the bearings during inspection and magnetic pole pieces to guide the flux to the inspection region. The pole pieces also support and precisely position the magnetic perturbation and Barkhausen probes which are air-cushion floated on the race surface. Stepper motors under supervision of the computer automatically index the probes to inspect the active raceway surfaces during high-speed rotational scans of the bearing component. An optical sensor acquires a permanently engraved reference mark on a non-critical surface of the bearing race and this mark is tracked continuously by the computer to provide precise signature azimuthal information. The laser inspection requires no special fixtures and only a software change is required to accommodate different components. After the

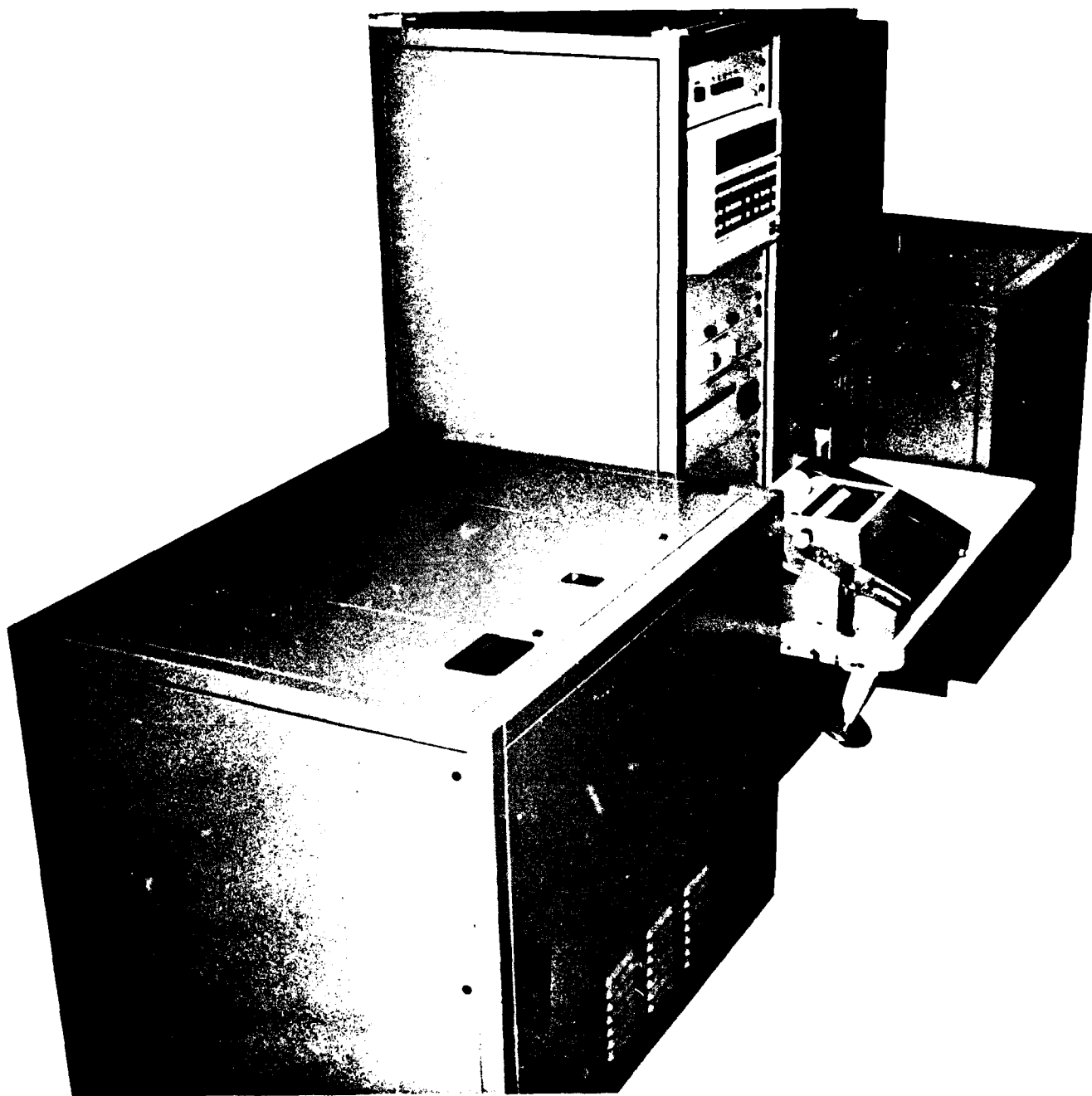


FIGURE 3. BEARING INSPECTION SYSTEM

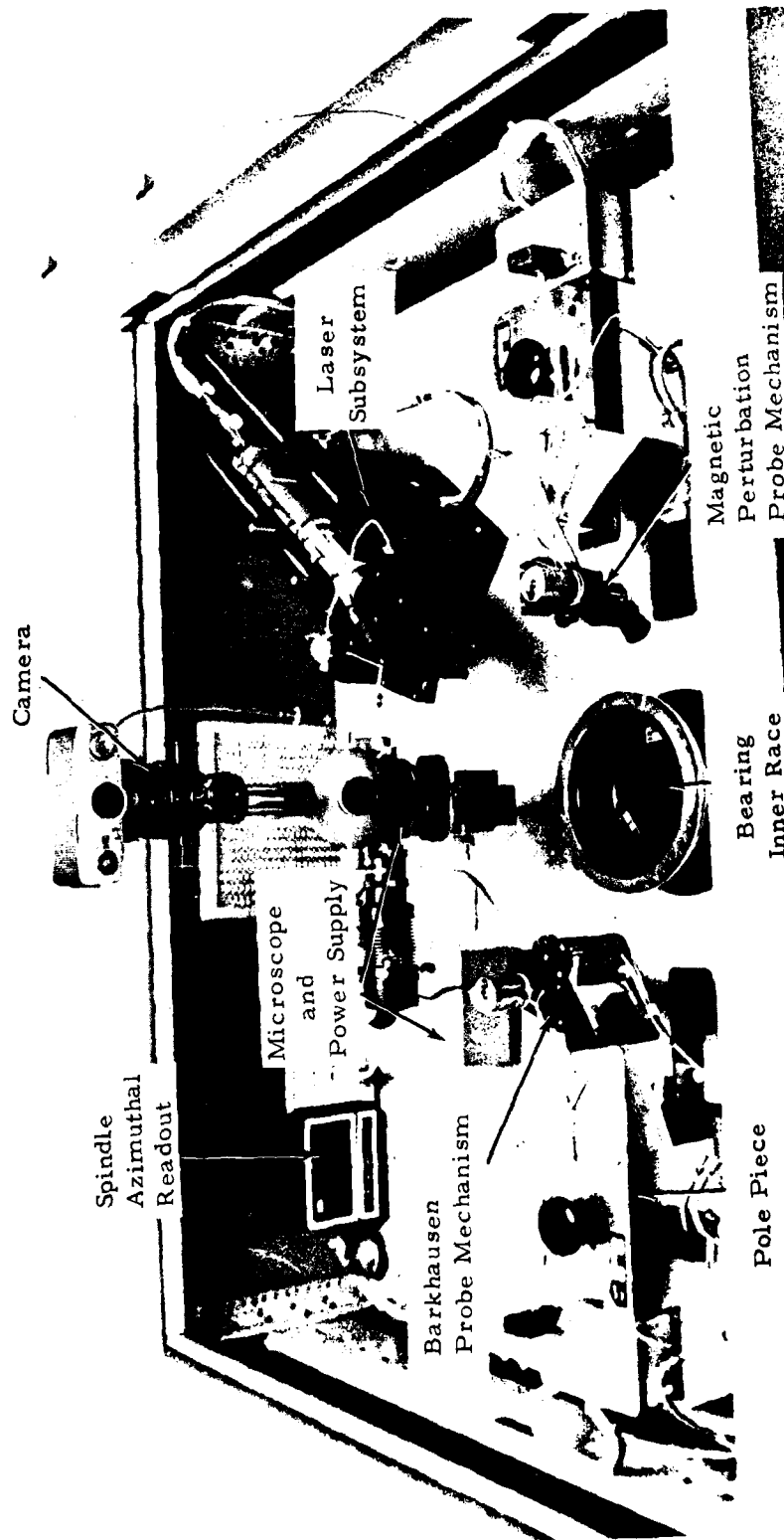


FIGURE 4. RACE INSPECTION UNIT

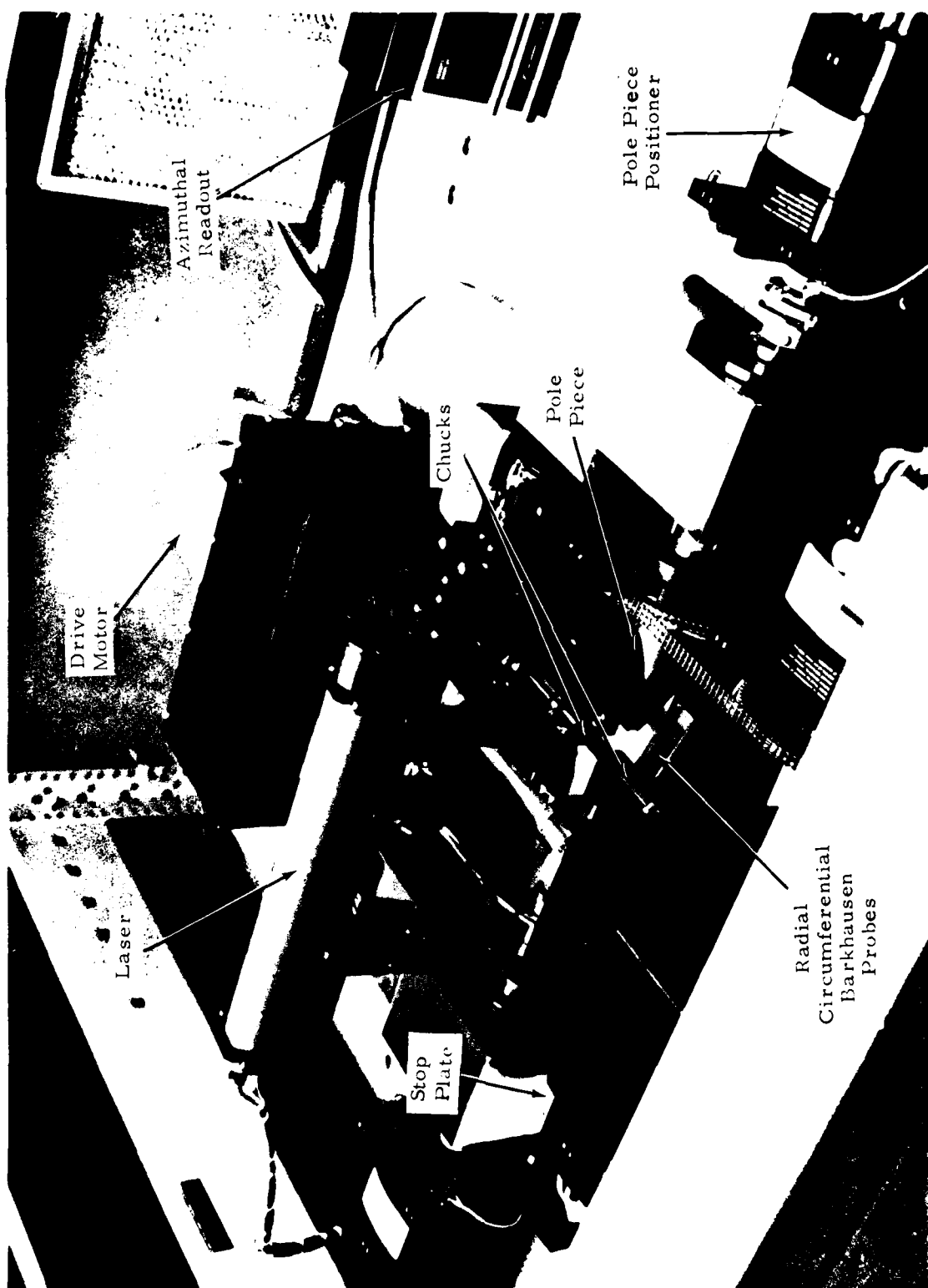


FIGURE 5. BALL/ROLLER INSPECTION UNIT

inspection is completed, the components are automatically demagnetized. Signature information is stored in the computer memory during inspection and data processing and output to a digital tape for later transfer to a data base. The serviceability of the bearing is computed for each component immediately after inspection is completed. A microscope mounting fixture, azimuthal digital display and adjustment procedures are also provided which permits precise location positioning of signature regions in the field of view of a microscope; a camera attachment facilitates photographing the surface. All inspection parameters, for example, rotational speed, positioning sequences, magnetic field sequences, etc., are automatically controlled by the computer during inspection. Figure 6 is a system diagram and the black lines indicate routine functions of the operator; a terminal/calculator is used for operator-computer communication. The shaded blocks indicate recently added functions to facilitate automated signature processing and bearing serviceability computation.

Selected equipment features and a concise summary of the inspections performed are presented in Table III. One of the magnetic inspection examinations is capable of resolving minute subsurface inclusions as small as 0.001 in. (0.025 mm) in diameter which is far beyond the capabilities of other nondestructive inspection methods. During the laser scan the total active surface of the raceway is examined as compared to isolated tracks normally examined with conventional surface-roughness measuring devices. The Barkhausen noise analysis method of residual stress measurement is a state-of-the-art development capable of sensing subsurface stress changes caused by service⁽³⁵⁾ and associated material transformations which occur during extended severe loading of ball bearing components; this is the only known, completely nondestructive method of sensing such stresses.

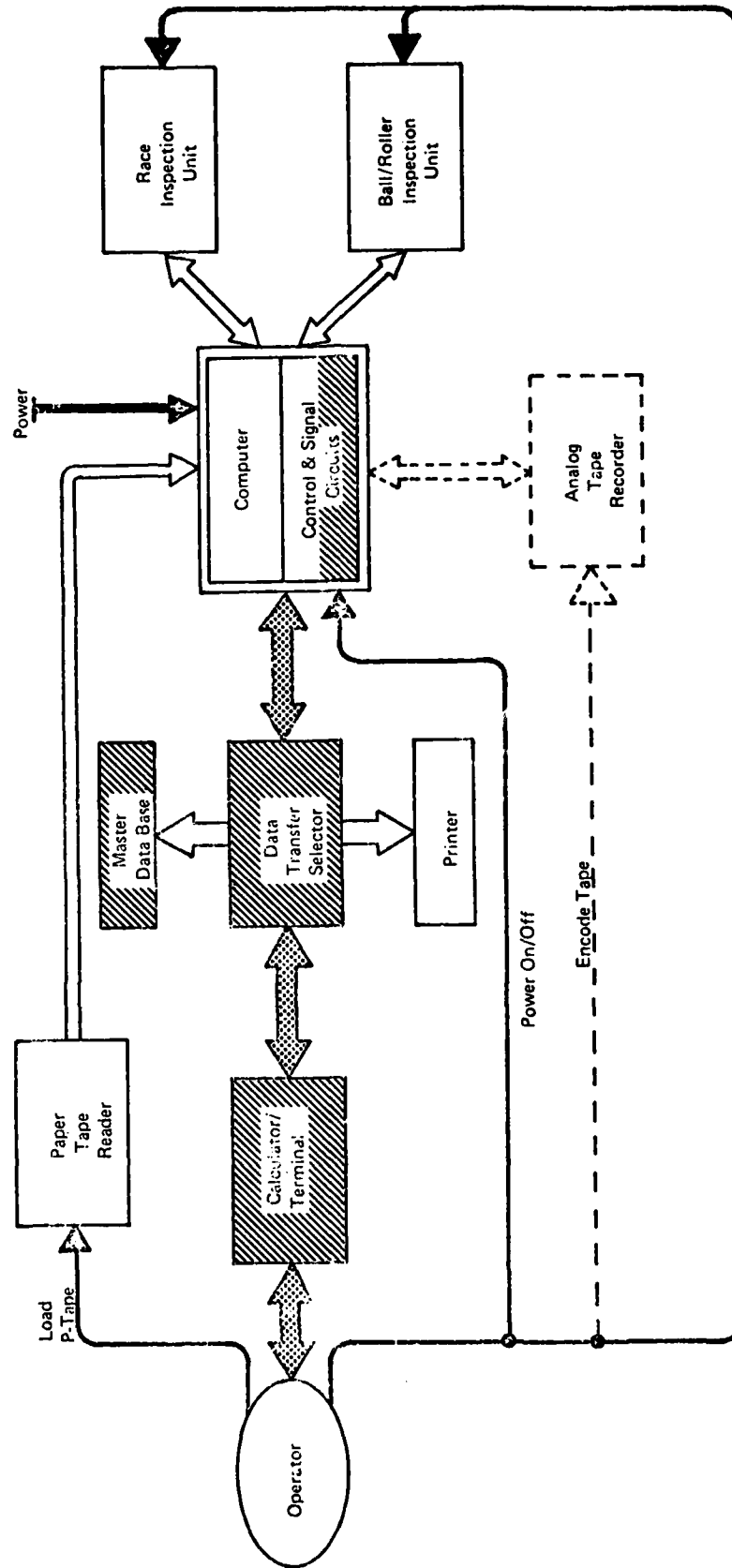
C. Highlights of Flaw Signature Response

1. Typical Signature Responses

Typical signature responses are illustrated in Figure 7; sources a and c are lapped holes and source b is an indent. The responses are those from a reference bearing component used to check overall functioning of the equipment; such a reference bearing is provided with each set of fixtures. The hard copy printout and Polaroid photographs of actual signatures were obtained from test flaws - a lapped hole (a geometric void simulating an inclusion) and a mechanical indent (this is a very shallow geometric void with pronounced localized surface contour change and localized stresses and strains). A detailed review of the information in Figure 7 follows, and although the reader may find this review tedious, it is essential for a clear understanding of information that follows in subsequent sections.

The characteristic signatures obtained with circumferential flux orientation are shown in Figure 7A; note the "downward and then upward" sequence and the symmetrical shape of signatures a and c. Such a signature is characteristic of a symmetrically shaped void or inclusion and the peak-to-peak separation in the scan direction (which can readily be measured on an expanded horizontal axis sweep record) indicates the

353/2



Install Fixtures, Load/Unload Specimens, Visual Observation;
Mount Microscope, Rotate Spindle

FIGURE 6. CIBL SYSTEM DIAGRAM



CIBLE

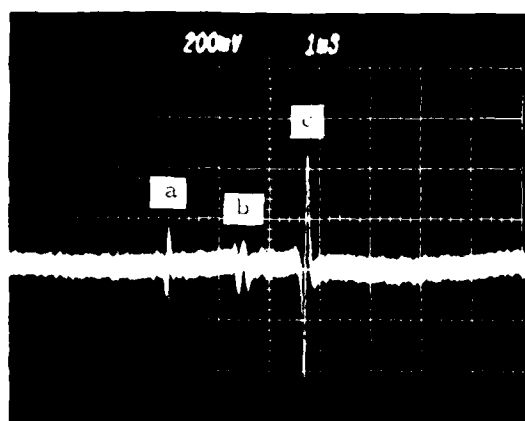
(Critical Inspection on Bearings for Life Extension)

AUTOMATED BEARING INSPECTION SYSTEM**FEATURES**

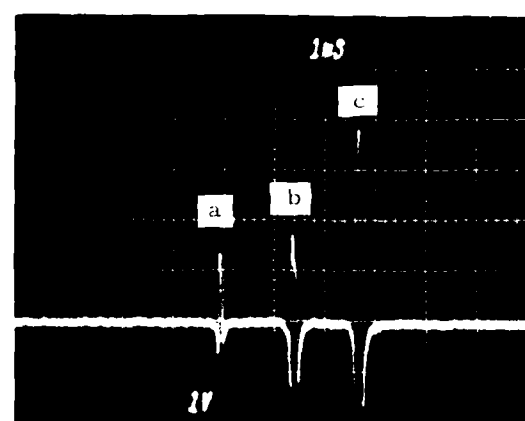
COMPUTER SUPERVISED AND CONTROLLED INSPECTION
 RAPID FIXTURING CHANGEOVER FOR DIFFERENT BEARINGS
 COMPUTER SETUP OF PARAMETERS FOR DIFFERENT BEARINGS
 COMPUTER PRINTOUT OF SIGNAL LOCATIONS
 PERMANENT RECORD ON MAGNETIC TAPE
 DIAGNOSTIC PRINTOUTS AND SAFETY INTERLOCKS

SPECIFICATIONS

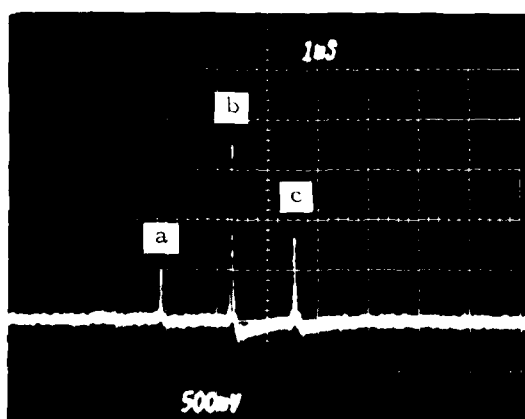
| INSPECTION METHODS | CONDITIONS DETECTABLE | SCAN PATTERN |
|---|-----------------------|--------------|
| <u>MAGNETIC PERTURBATION</u> | | |
| <div><div><div><u>RADIAL FLUX</u></div><div><ul style="list-style-type: none">● HIGH FIELD● LOW FIELD</div></div><div>SURFACE PITS, INCLUSIONS, SPALLS AND INDENTATIONS</div><div><div>0.025-INCH WIDE CIRCUMFERENTIAL STRIPS WITH 20% OVERLAP</div></div></div> | | |
| <div><div><div><u>CIRCUMFERENTIAL FLUX</u></div><div><ul style="list-style-type: none">● HIGH FIELD● LOW FIELD</div></div><div>SUBSURFACE INCLUSIONS, AND SPALLS AND DEEPER SURFACE ANOMALIES</div><div>FATIGUE DAMAGED REGIONS AND INDENTATIONS</div><div>12 TO 60 SCANS PER INSPECTION METHOD</div></div> | | |
| <u>LASER-SCATTERED LIGHT</u> | | |
| <div><div><div><u>SURFACE ANOMALY</u></div><div><u>SURFACE FINISH</u></div></div><div>SURFACE SCRATCHES, PITS, SPALLS, AND INDENTATIONS</div><div>RELATIVE SURFACE FINISH</div><div><div>SYNCHRONIZED SCANS</div></div></div> | | |
| <u>BARKHAUSEN NOISE</u> | | |
| <div><div><div>RELATIVE SURFACE AND NEAR-SURFACE RESIDUAL STRESS CONDITIONS</div><div>SERVICE MODIFICATION OF RESIDUAL STRESS</div></div><div>PROGRAMMED SAMPLING 0.050 × 0.050- INCH REGIONS 9 TO 15 LOCATIONS</div></div> | | |



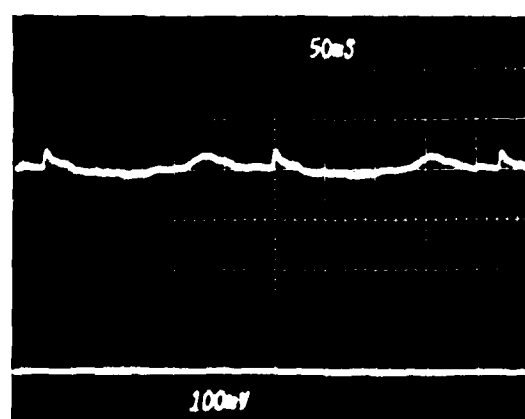
A - CH Signatures



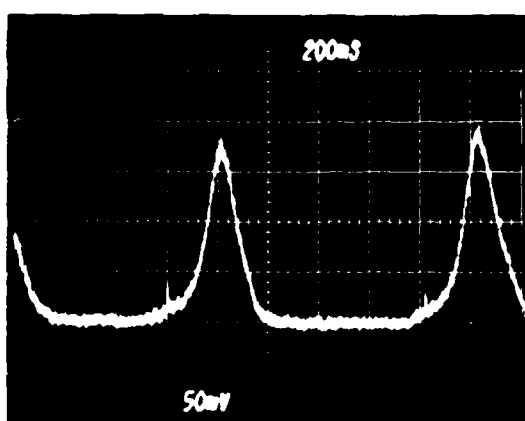
B - RH Signatures



C - LA Signatures



D - LD (Surface Finish)

E - Barkhausen Noise Signature
Legend:

R - radial flux
C - circumferential flux
H - high flux density
L - low flux density

FLAWS

| TY | S | T | B | R | S | R |
|----|------|------|------|---|---|---|
| RH | 0005 | 0001 | 0024 | | | |
| RH | 0005 | 0032 | 0055 | | | |
| RH | 0005 | 0059 | 0082 | | | |
| CH | 0005 | 0060 | 0083 | | | |
| RL | 0005 | 0001 | 0024 | | | |
| RL | 0005 | 0032 | 0055 | | | |
| RL | 0005 | 0060 | 0083 | | | |
| CL | 0005 | 0060 | 0083 | | | |
| LA | 0005 | 0031 | 0054 | | | |
| LA | 0005 | 0059 | 0082 | | | |

Signature

a } B
b }
c }
c } A

b } C
c }

Note: Signatures not printed are below threshold settings.

LA - laser, pit imperfection
ST - probe location across race groove
BR - azimuthal location of signature from reference mark on race (1 rev = 5000)

FIGURE 7. SIGNATURES AND COMPUTER PRINTOUT FROM A
REFERENCE COMPONENT

depth from the scan surface to the geometric centroid of the flaw. The peak-to-peak vertical amplitude of the signature is directly related to the volume of the flaw and the polarity of the signature also provides significant information concerning the signature source. A downward and then upward sequence is classed as void polarity and is associated with inclusion signatures. An upward and then downward sequence is often associated with indents and other types of metallurgical anomalies and is classed as opposite polarity, i.e., opposite to a void. Furthermore, comparisons of the signatures obtained at high magnetic field with those obtained at low magnetic field provide additional information. For example, the signature from a geometric discontinuity such as an inclusion will increase continuously and monotonically with applied magnetic field increases. In contrast, indents which are usually very shallow have only a small contribution from the geometric void, but usually a large component from the localized stress and strains and this contribution is most pronounced at relatively low magnetic field conditions; the signature does not increase monotonically with increasing magnetic field. Examples in which the CH/CL signature ratio is used to classify flaws (service-induced cracking) will be shown later in this report. The flaw location coincides precisely with the zero crossing point of the circumferential signature and the symmetry of a flaw volume influences the symmetry of the signature.

The signatures a, b, and c presented in Figure 7B were obtained with radial flux orientation and the change in localized surface contour is the primary factor producing these signatures. The characteristic shape consists of: a relatively slow, downward going segment followed by a rapid upward going segment to a prominent peak, then a rapid downward segment to a peak in the opposite direction, and then a relatively slow return to the baseline. Overall amplitude of the signature is related to the surface flaw size and the center of the flaw is coincident with the location of the upward or positive prominent peak. A monotonic increase of signature amplitude with increasing magnetic field is obtained.

Laser signatures are presented in Figure 7C for the pit or surface anomaly inspection mode and for the surface finish mode in Figure 7D. The characteristic spike signatures for the surface anomaly inspection mode are influenced by several different parameters. In the surface finish inspection mode the upward departure of the signal trace from the baseline is associated with increasing surface roughness of the component.

In the present equipment configuration, the residual stress measurement is not made in a scanning mode, but at selected locations including the center of the load track and at locations near the extremities of the load track. Characteristic Barkhausen signatures obtained from the reference component are shown in Figure 7E. The two signatures shown were obtained from the same location but on successive cycles of the magnetic field sweep. This characteristic shape is obtained from races with high residual compression stresses; low amplitude signatures are obtained from compression regions and high amplitude signatures are obtained from tension regions. For material in tension, the signature consists of a leading edge spike joined to the triangular shaped segment of the records in Figure 7E. Examples have been presented in previous reports. (24,32,33)

2. Significant Flaw Responses

For the approximately 1204 bearings inspected (997 new and serviceable, 145 reject and time limited and 62 PACER RESTORE), about 10% produced magnetic perturbation, circumferential flux, high field signatures which were above the alarm threshold level and produced CH (circumferential flux, high field) printouts. Such CH signatures have been confirmed to be associated with significant, critical flaws, prominent examples of which are shown in Figures 8 and 9. A brief discussion of each of these figures follows.

Figure 8 dramatically illustrates the capability of CIBLE to detect the presence of critical fatigue damage in bearing race components. The large crack network (~ 0.1 in. or 2.5 mm, transversely across the race) detected in the loaded half of an inner race of a J57-#2, vendor reworked bearing (S/N 144D-2). Typical CH signatures included in Figure 8 correspond with the programmed scan tracks from which the signatures were obtained. The bearing race was subsequently endurance tested for a total of 3 hours at a maximum Hertz stress of 204 ksi*. These test conditions were selected to minimize the probability of a failure. Fortunately, spall-type failure did not result from the 3 hour endurance test; however, significant, visually evident crack propagation did occur and it is estimated that the remaining life of this component in an engine would be only a few hours. Subsequent to the endurance test, metallurgical investigation of the cracked region illustrated in Figure 8 was completed and confirmed that inclusions were the nucleating source for the cracks; detailed results are presented later in this report.

The results in Figure 9 illustrate, equally dramatically, that significant inclusions are present, occasionally, in new bearings fabricated from premium quality steel which can lead to the initiation and propagation of cracks such as previously shown in Figure 8. Again in Figure 9, significant CH signatures are presented which correspond to apparently innocuous surface indications. The surface indications illustrated in the photomicrograph A of Figure 9 suggest a long ($\sim .025$ in. or 0.64 mm in length) stringer type inclusion. If the inclusion were superficial only radial flux signatures would be generated; however, the significant CH signatures in Figure 9 confirm that a large inclusion extends beneath the surface. These CIBLE results were obtained from the inner race half which would be loaded in engine service of a J57-#4 bearing (S/N 534A-1). It is anticipated that the life of this component in engine service would be severely limited by the presence of the flaw indicated in Figure 9.

* 204 ksi was the minimum Hertz stress which could be applied without a high probability of ball skidding.

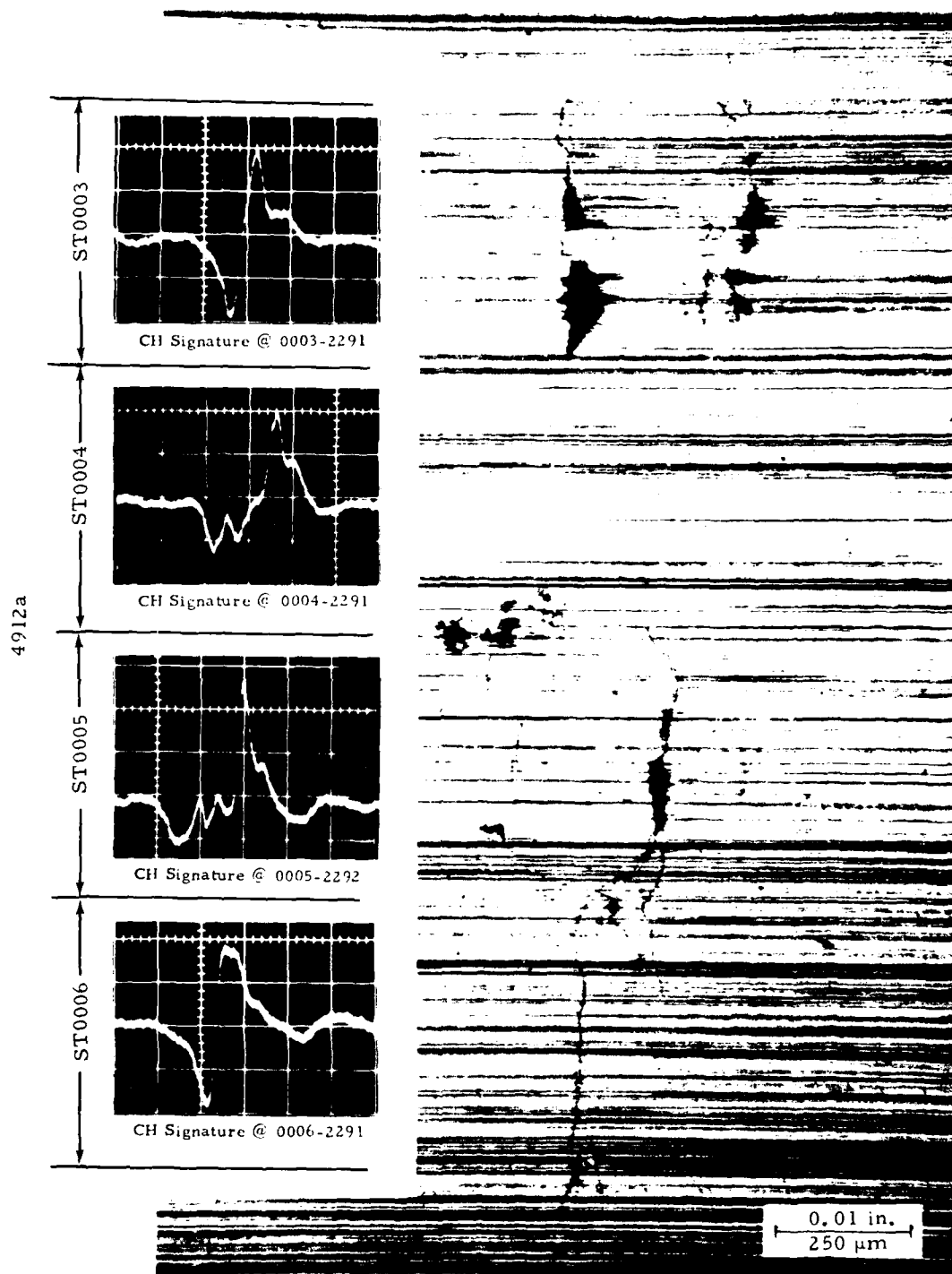
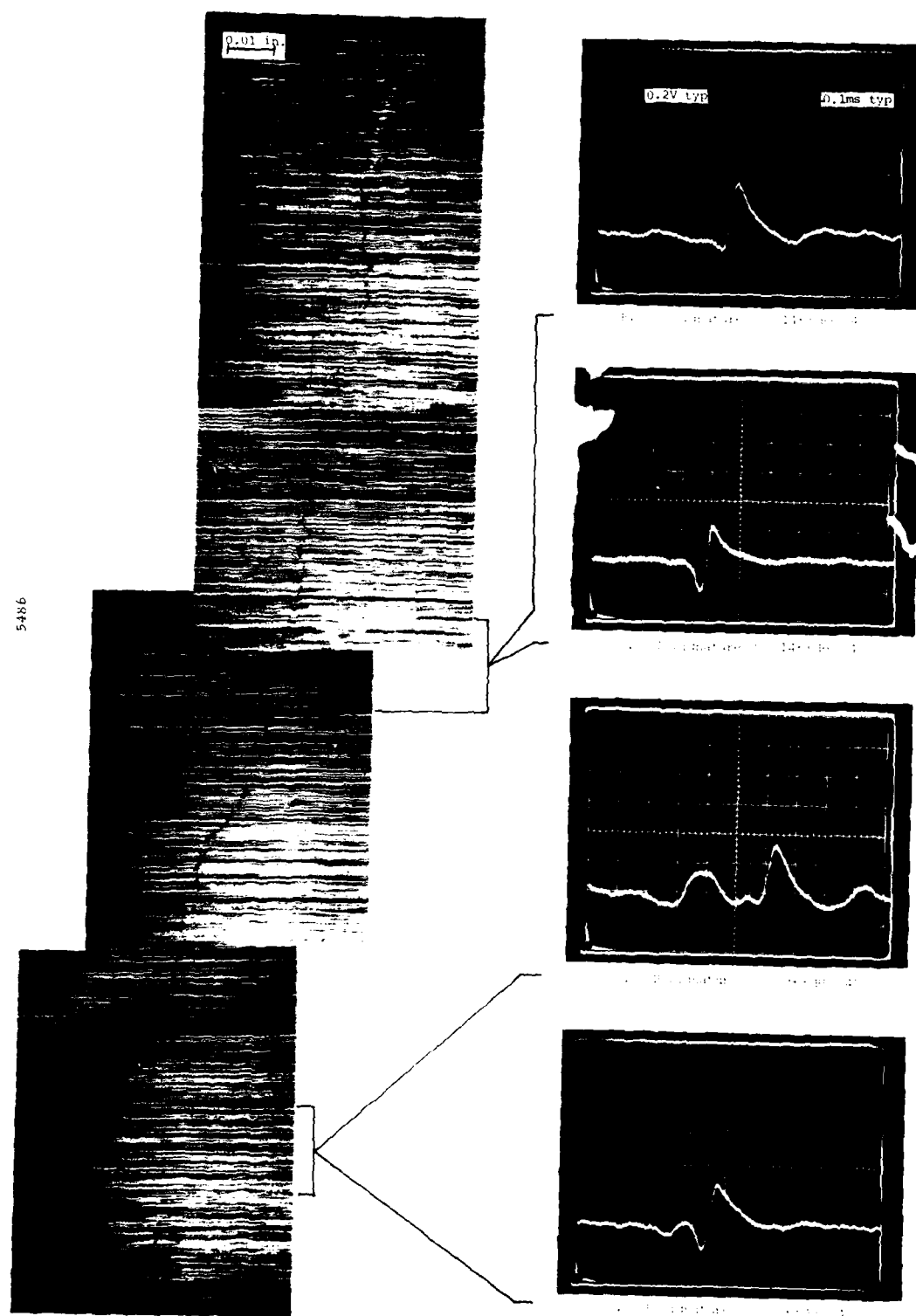


FIGURE 8. CIBLE RESULTS SHOWING SURFACE PHOTOMICROGRAPH ($\times 100$) OF CRACK NETWORK AND ASSOCIATED CIRCUMFERENTIAL FLUX SIGNATURES



A. Magnified View of CIBLE Data
 9.0000-0010, 10.0000-0010

FIGURE 9. CIBLE RESULTS ON NEW J57-#4 BEARING (S/N 534A-1)
 INNER RACE, LOADED HALF (S12671-2)

II. SUMMARY OF WORK ACCOMPLISHED

This section briefly summarizes the types and extent of efforts accomplished by Contract Line Item Number (CLIN) and calendar time.

A. CLIN 0001AE, June 1974 - June 1975

The program was initiated and assigned to a program manager with a broad technical background in NDE to direct and coordinate the team. The project team included personnel: i) for the design, fabrication, and assembly of inspection fixturing and sensors, ii) competent in the area of endurance testing, iii) with computer, electronic circuitry, and signature analysis backgrounds, iv) competent in the acquisition and analysis of magnetic perturbation, Barkhausen noise, and laser scattered light inspection data.

Work space and facilities were allocated for:

- i) bearing handling and storage;
- ii) bearing inspection;
- iii) endurance testing;
- iv) data storage.

Facilities for bearing inspection consisted of SwRI-furnished bearing race inspection hardware incorporating magnetic perturbation, Barkhausen noise, and laser scattered light methods. SwRI also furnished two machines for endurance testing.

A number of bearing types were considered by cognizant Government and SwRI technical personnel as candidates for inspection; factors which influenced selection included: i) bearing availability, ii) rapidity of expected "turn-around" of bearings in service, and iii) bearing failure statistics. In subsequent discussions, it became evident that it would be beneficial to the Government and to the technical effectiveness of the overall program to use J57-#2, J57-#4, J79-#2 and J85-#2 main shaft bearings as the items for inspection testing. Accordingly, the design of fixturing for the J57-#2, J57-#4, J79-#2 and J85-#2 main shaft bearing inner and outer races was completed and fabrication and assembly of fixturing for these bearing races was undertaken. SwRI-funded inspection equipment and endurance test machines, as well as bearing processing facilities, were made available for the inspection and testing of the bearing types selected.

Procedures were established for the cleaning, preservation, storage, packaging, and shipment of bearings to be inspected. In addition, the format and procedures for identifying and marking the bearings were formulated and documented.

Procedures were also established for the acquisition, filing, easy tracking, and convenient retrieval and filing of inspection data including the cataloging of bearings (and all significant accompanying service history information) and the filing of the accompanying inspection data.

Long-range data handling, processing and analysis requirements were outlined, and initial signal analysis considerations and approaches were established. A signal data storage system was implemented which permits the future playback and analysis of all bearing data acquired from the subject program.

B. CLIN 0001AF (new)*, July 1975 - June 1977

Bearing inspection was conducted on all bearings received during the subject period which included J57-#2 new and reworked races, J-57#4 new, reworked, and reparable reject races, and J85-#2 new, reworked, and time-limited races. Detailed documentation and data examination were conducted based on printouts from the initial automated inspections. These efforts included examination of flaw signatures correlating with printout locations, surface photomicrography, replication, etc.

Metallurgical investigations were undertaken at selected locations; evidence of inclusions was found with microcracking and "flaking out" of material.

Endurance testing was also undertaken on selected bearings, and two failures were obtained which correlated with specific signatures; one of these failures occurred after only 16 hours endurance testing and was initiated at a subsurface inclusion.

Reclamation investigations were initiated and coordinated with metallurgical and endurance test efforts. Such efforts were concentrated on bearings reworked by a vendor (a presently implemented reclamation procedure). Reworked bearings dominated the bearing population inspected and results showed that significant and critical flaws can pass current rework (and inspection) procedures "undetected".

Construction of a master data base was initiated. A sample data base was constructed and tested to provide a basis for a full-scale data base system. The initial description and formatting for the full-scale system was completed. These data base efforts included initial flaw parameter identification.

C. CLIN 0001AH, July 1977 - June 1978

Work efforts during the subject period were scheduled according to the amended schedule of the subject contract. Bearing inspection was completed on a total of 766 bearings (~2300 race components) including J57-#2 new and reworked races, J57-#4 new, reworked, and reparable reject races, and J85-#2 new, reworked, and time-limited races. In addition,

* Difficulties in obtaining delivery from the Government of bearing drawings and bearings to initiate inspection resulted in a modification of the work schedule.

inspection was conducted on 1000 each J57-#4 balls at Tinker Air Force Base in Oklahoma City. Detailed documentation and data examinations were continued based on printouts from the initial automated inspections and included the recording of flaw signatures, correlation with print-out locations, surface photomicrography, replication, SEM micrography, etc.

Metallurgical investigations were continued on selected surface flaw locations (pits, dig nicks, and indents). No evidence of either surface or subsurface cracking was observed; these surface flaws were located in the loaded region of the raceway in service.

Endurance testing was also continued on bearings selected on the basis of specific inspection signatures and/or surface flaw conditions. Three additional spall-type failures were obtained and indications of imminent spall-type failures were obtained on five other bearings.

Reclamation investigations were continued in coordination with overall inspection, metallurgical, and endurance test activities. Outstanding and significant results were obtained which confirmed that very critical flaw conditions can pass, "undetected", current rework and inspection procedures performed by an Air Force vendor. These critical flaws were detected and rejected during routine automatic inspection by the CIBLE Equipment.

Construction of a master data base (MDB) was continued. The tentative description and format of the MDB compatible for interfacing with automated inspection/signature analysis routines was formulated. An overall CIBLE integrated inspection input/output data plan was outlined which incorporated pre-inspection descriptive and historical data input, MDB data acquisition, signature characterization, and the application of a serviceability criteria. Interfacing circuitry to facilitate signature analysis was breadboarded and checked out and preliminary signature characterization tests were conducted.

D. CLIN 0001AJ, July 1978 - November 1979

Inspection was completed on a total of 1,204 bearings (997 new and serviceable, 145 reject and time-limited, and 62 PACER RESTORE) which included J57-#2, J57-#4, and J85-#2 type bearings. Detailed documentation and data examination for selected bearing races and balls (from the 1,000 balls inspected during the latter part of 0001AH OCALC) were also completed. Metallurgical examinations were completed on additional selected locations for a total of 44 locations. The latter locations were selected, dominantly on the basis of subsurface flaw indications and surface fatigue cracks. Significant evidence of subsurface inclusions with material transformation and subsurface cracking was observed.

Endurance testing was completed on a total of 44 bearings (25 each J57-#2, 15 each J57-#4, and 4 each J85-#2); candidates were selected on the basis of specific inspection signatures and/or surface flaw conditions. Spall-type failures were developed on 11 bearings. Endurance testing was conducted over periods extending from 1 hour to slightly over

500 hours and for maximum Hertz stress values extending from 204 ksi to 332 ksi. Figures 10 and 11 illustrate the regions typically loaded on inner and outer races and the associated scan track inspection region as well as the track region in which the initiating failure sources occurred.

Reclamation investigations were completed concurrently with overall inspection, metallurgical, and endurance test activity. Again, outstanding and significant results were obtained which further confirmed that very critical flaw conditions can pass, undetected, current rework and inspection procedures performed by an Air Force bearing rework vendor. Vendor reworked bearings are being accepted by the Air Force as serviceable and are restocked in overall depot inventory.

Definition of the Master Data Base (MDB) structure was completed. Automated signature processing including data input and output and serviceability computations was integrated with the CIBLE inspection procedures. Signal analysis hardware and software for supervision of the CIBLE equipment was completed and delivered to OCALC, Tinker Air Force Base (TAFB). The signal analysis system was installed and operated at TAFB which included troubleshooting and training.



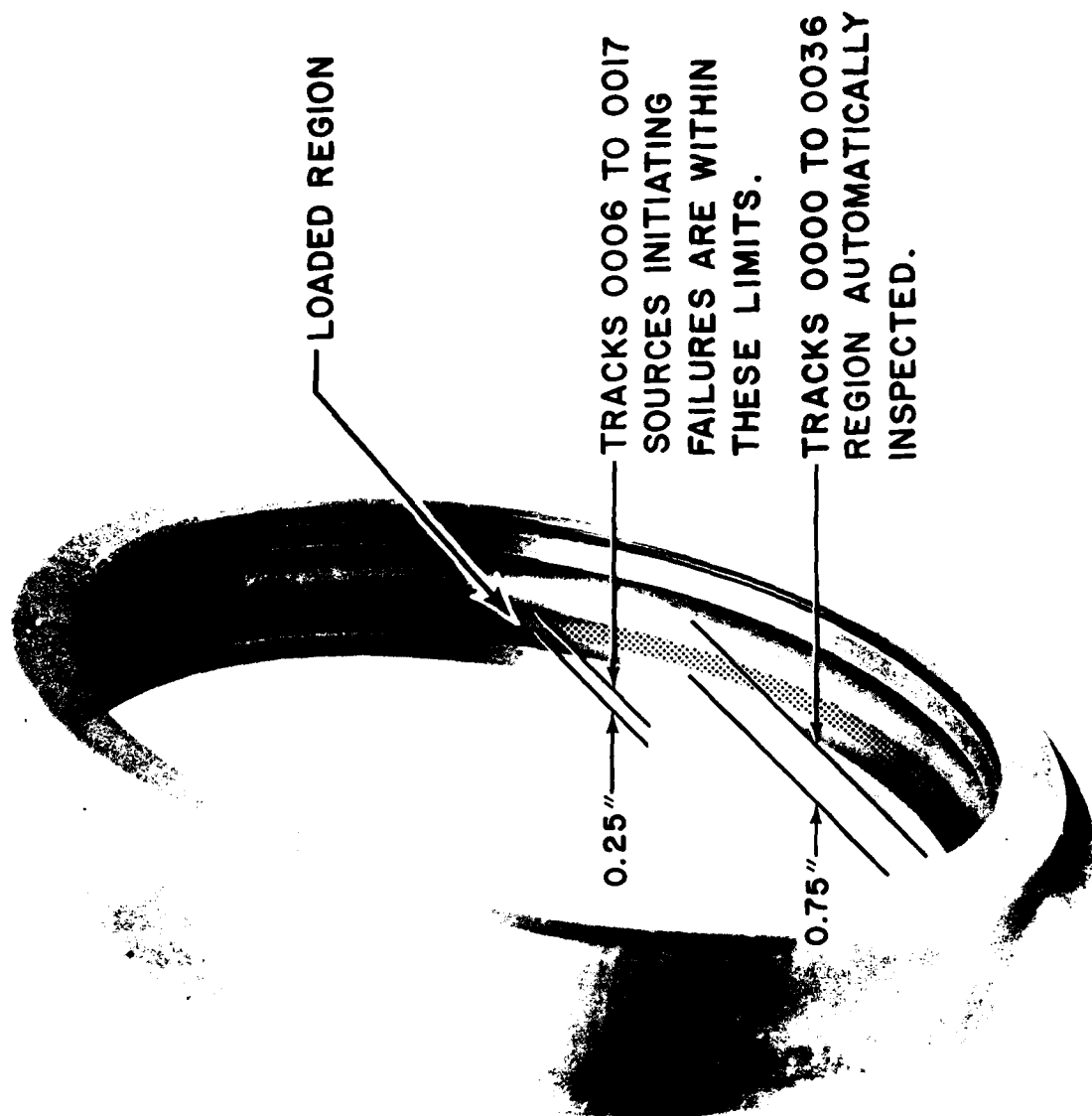


FIGURE 11. PHOTOGRAPH ILLUSTRATING RELATIONSHIP BETWEEN LOADED AND INSPECTED REGIONS ON AN OUTER RACE

III. SUMMARY OF RESULTS

This section summarizes data acquired from the population of bearings inspected, and the significant flaw printout, endurance tests and metallurgical examination results obtained. In addition, a preliminary serviceability criteria related to J57-#2, J57-#4, and J85-#2 bearing races is outlined. A very preliminary criteria for J57-#4 balls is also included.

A. Bearing Population Inspected

A total of 1,092 new and serviceable (total components) bearings were inspected; 400 J57-#2 bearings, 552 J57-#4 bearings, and 140 J85-#2 bearings (50 each J57-#4 reparable rejects and 62 each PACER RESTORE were also inspected, but are not included in this discussion of new and serviceable bearings). Figures 12, 13, and 14 are bar graphs illustrating the service time distribution for the population of each of the three bearing types. It is noted in the case of J57-#2 and J57-#4 bearings that service times greater than 13,000 hours have been accumulated. It is interesting that while J85-#2 bearings are time-limited to 1200 hours service, there are bearings which have accumulated as high as 3500 hours; those bearings having service times in excess of 1200 hours, generally, although not in all cases, were observed to have been vendor reworked at 1199 hours. All serviceable bearings (other than those indicated as new) inspected included both non-reworked and vendor reworked bearings.

In addition to the bearing population presented in Figures 12 through 14, 50 each J57-#4 reparable reject bearings and 62 each J57-#4 bearings, which were set aside at OCALC for the PACER RESTORE* program, were also inspected.

CIBLE inspections were initially conducted in the automated, threshold-alarm detection mode, and the printouts therefrom retained. Subsequently, the flaw printout types and locations were reviewed and bearings were selected on the basis of signature type and location for detailed data acquisition which included the recording of Polaroid photographs of the signatures, and visual examination and photomicrographs of the signature region. In many cases, plastic replicas of the surface were made for SEM (scanning electron microscopy) examination. Magnetic perturbation signatures were usually documented for radial as well as circumferential high and low field magnetization, irrespective of which of the magnetic perturbation conditions was responsible for the printout. Bearing races and locations for metallurgical examination were selected based on the recorded signature characteristics and the visual surface indications in the signature region.

The total data acquired under the subject program is too voluminous to present in its entirety here; however, selected results are summarized below. For more extensive examples of signatures as well as the

* PACER RESTORE bearings are a group of bearing races set aside at OCALC to be retrofitted with a new complement of balls.

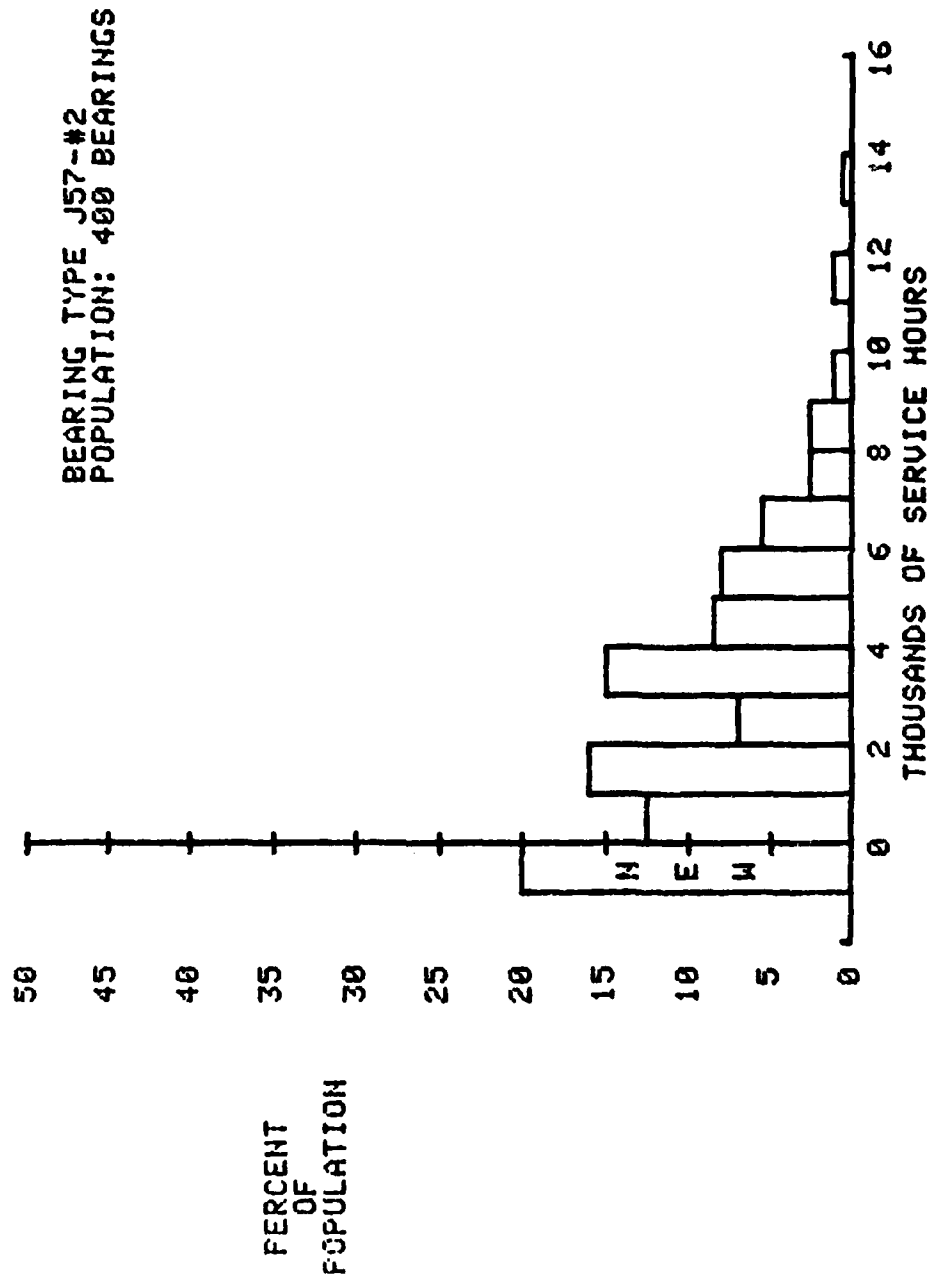


FIGURE 12. BAR GRAPH SHOWING DISTRIBUTION OF SERVICE HOURS ON J57-#2 SERVICEABLE BEARING POPULATION INSPECTED.

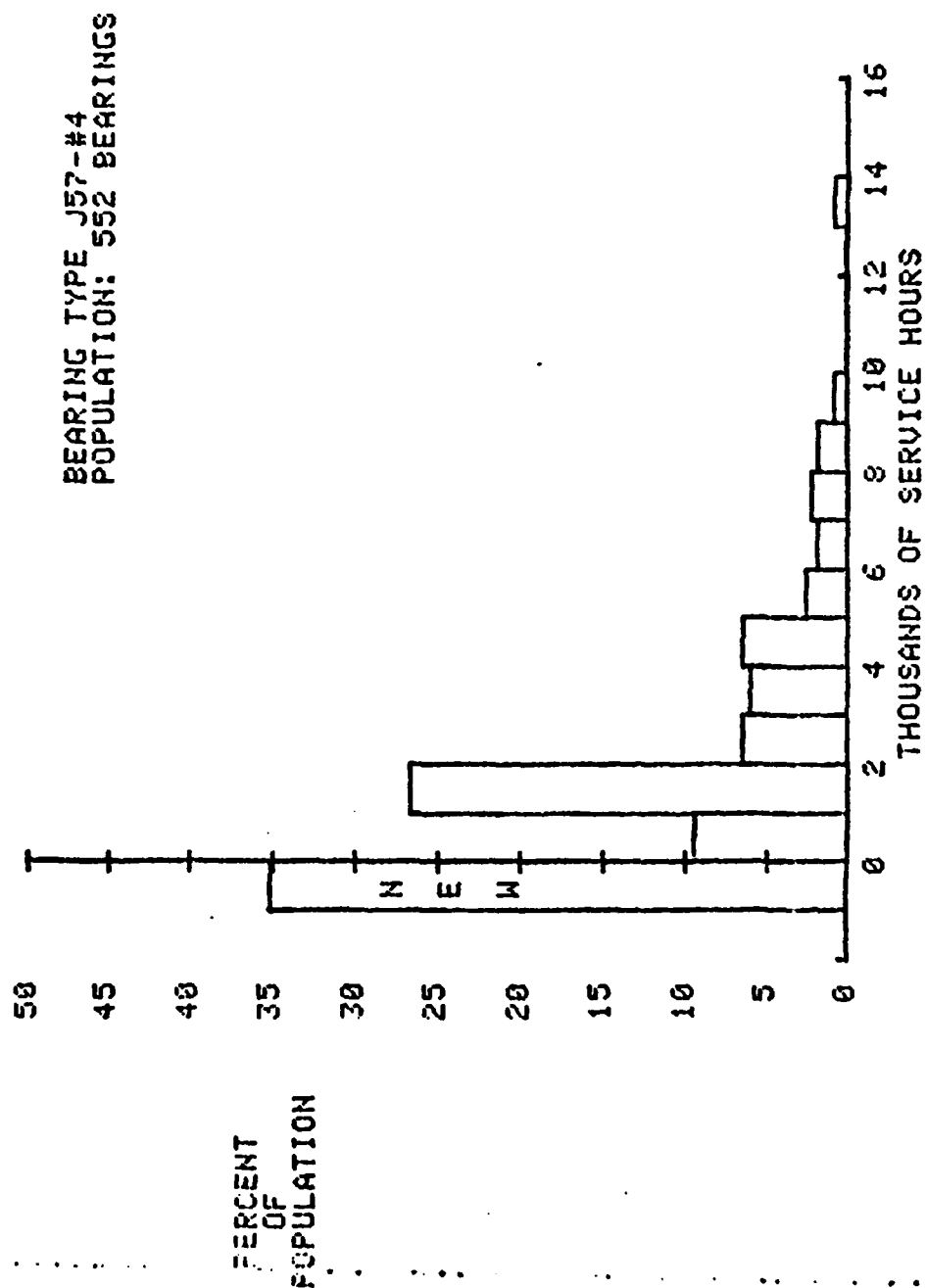


FIGURE 13. BAR GRAPH SHOWING DISTRIBUTION OF SERVICE HOURS ON J57-#4 SERVICEABLE BEARING POPULATION INSPECTED.

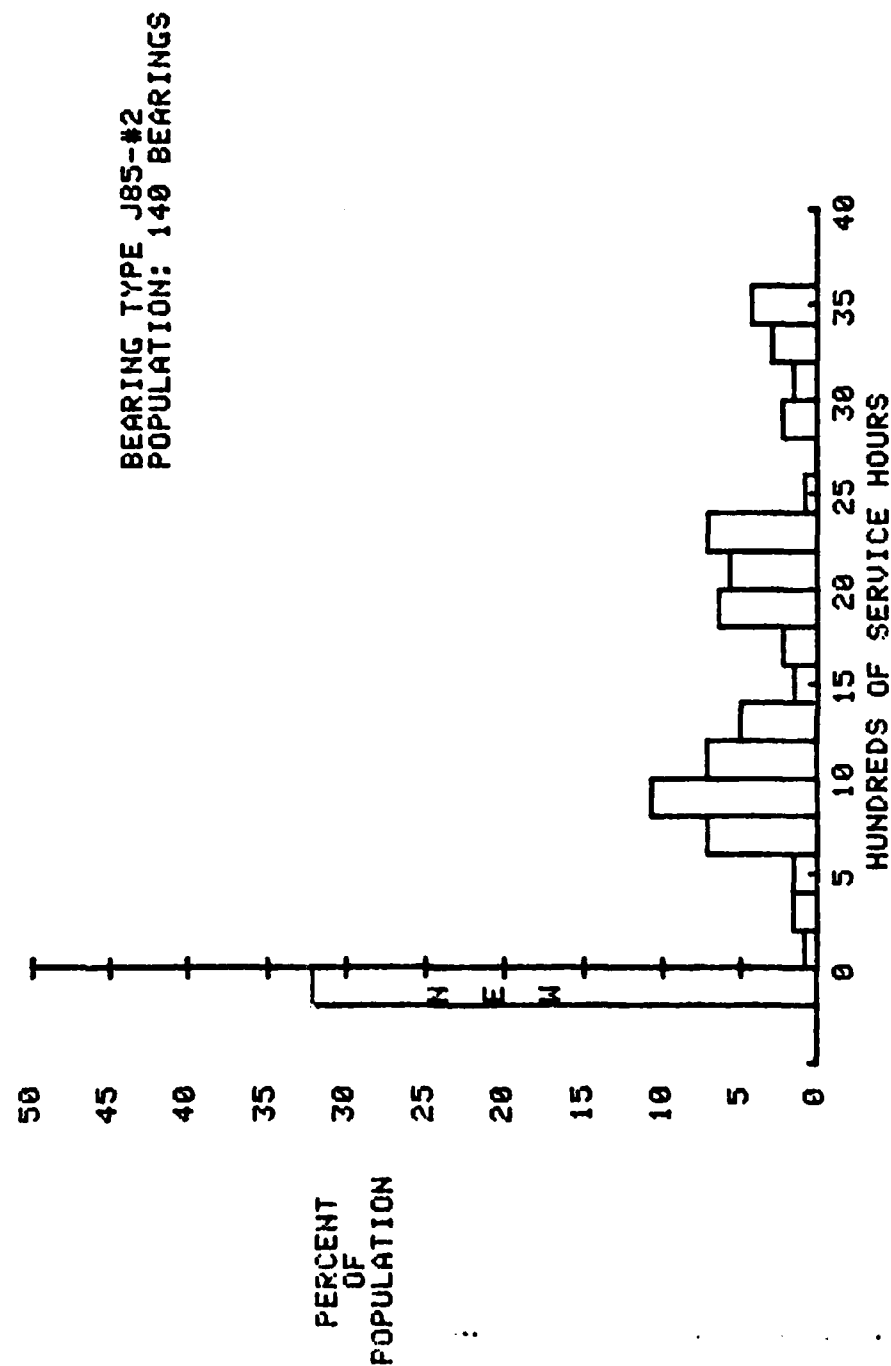


FIGURE 14. BAR GRAPH SHOWING DISTRIBUTION OF SERVICE HOURS ON J85-#2 BEARING POPULATION INSPECTED.

corresponding surface indications and/or metallurgical examination results, the reader is referred to Appendix F of this report and prior reports (31-33) issued under the contract.

B. Significant Flaw Results

A summary of inspection, endurance testing, and metallurgical results are presented in this section of the report for races and balls.

1. Races

Results obtained on this program and prior programs confirm that inclusions are a dominant source from which cracks and spalls initiate. Such inclusions, particularly if they are slightly subsurface, can only be detected by magnetic perturbation circumferential flux high field inspection (CH). Accordingly, particular attention was given to the number of bearings producing CH printouts during the routine, automatic CIBLE inspection. Table IV presents a summary of such printouts for the bearing populations previously shown in Figures 12 through 14.

Examination of the data presented in Table IV indicates relatively similar percentages of CH signature printouts on new bearings for the three bearing types inspected, and in all cases less than 10%. Significantly higher percentages of CH printouts are obtained for J57-#2 and J85-#2 serviceable bearings, while the percentage for serviceable J57-#4 bearings is approximately 6% which is one-third of that for J57-#2 and J85-#2. In the case of the J57-#2 and J57-#4 bearings, approximately 90% of the serviceable bearing population consisted of vendor reworked bearings, and less than 50% of the J85-#2 bearing population consisted of reworked bearings. While the results in Table IV from an overall viewpoint of signature printouts indicate the presence of possible critical flaws for 1% to 18% of the bearings, it should be remembered that only those flaws in the loaded regions of the races are potential failure initiation sites. Accordingly, the nonloaded half of the inner race and almost half of the outer raceway could be eliminated from consideration. Nevertheless, the preliminary results in Table IV indicate a variation in bearing quality. It is informative to next examine some of the specific signature characteristics and the related flaws and conditions which produce them.

One of the more significant signature features is the magnetic perturbation, circumferential flux, signal response from flaw regions in which microcracking has initiated as compared to flaw regions in which cracking is not present. For example, in Figure 15 (upper left), corresponding CH, RH, and RL printouts at ST 0013 and BR 1760-1761, indicate that the same flaw generates these printouts. The depth of the centroid of the flaw beneath of the surface in this case is estimated to be 0.002 inches (50 μ m); the fact that the flaw is near the surface is further confirmed by the presence of an outstanding radial flux signature. Note that a comparison of the CH signature amplitude, 480 mV, with the CL signature amplitude, 120 mV, yields a CH/CL signature amplitude ratio of 4. It is pointed out there is no evidence of cracking at the surface in this region (see photomicrograph in Figure 15); also precision location procedures confirms that the CH signature does not coincide with any of the surface anomalies visible in the photomicrograph. While service time on the bearing is 3761 hours, these signatures were obtained on the nonloaded half of the inner race and load stresses would be far below the values to initiate cracking.

TABLE IV
STATISTICAL SUMMARY OF (CH*) FLAW PRINTOUTS

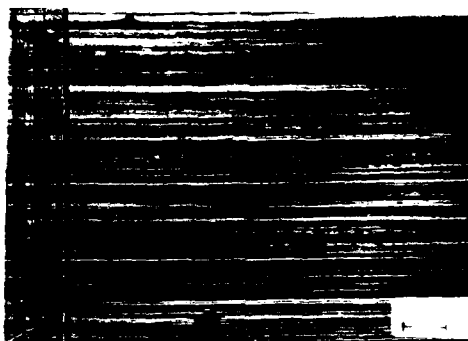
| <u>Bearing Type</u> | <u>Bearing Condition</u> | <u>Bearings Inspected</u> | <u>No. with CH Printout</u> | <u>% with CH Printout</u> |
|---------------------|--------------------------|---------------------------|-----------------------------|---------------------------|
| J57-#2 | New | 80 | 1 | 1.3 |
| | Serviceable** | 320 | 57 | 17.8 |
| J57-#4 | New | 194 | 12 | 6.2 |
| | Serviceable | 358 | 21 | 5.9 |
| J85-#2 | New | 45 | 4 | 8.9 |
| | Serviceable | 95 | 17 | 17.9 |
| TOTALS | | 1092 | 112 | 10.3 |

*CH = magnetic perturbation, circumferential flux, high field inspection
(This inspection mode detects surface and subsurface inclusions, cracks, and severe mechanical surface damage)

** All bearings were considered suitable for reuse in engines under present acceptance criteria.

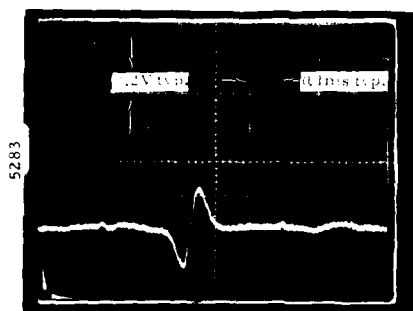
FLAWS
 TY ST BR SR
 RH 0006 1198 1216
 RH 0013 1761 1779
 CH 0013 1760 1778
 RL 0006 1198 1216
 RL 0013 1761 1779

Legend:
 C - circumferential flux
 R - radial flux
 H - high flux density
 L - low flux density
 ST - probe location across race groove
 BR - azimuthal location of signature
 from reference mark on race
 (1 rev = 5000)

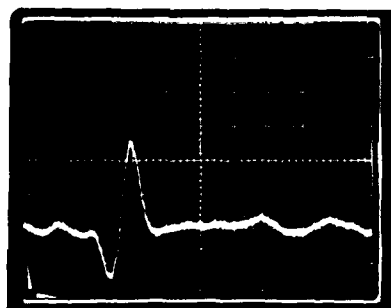


Flaw Printout Obtained
 During Automatic Inspection

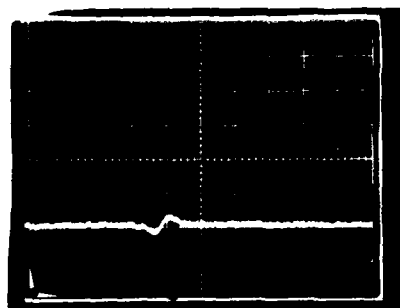
Magnified (x4 - X) View of Surface @ 0013-1761



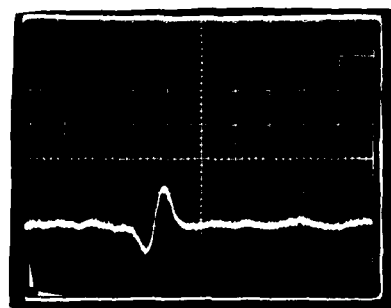
CH Signature @ ST0013+4 BR1760



RH Signature @ ST0013+4 BR1761



CL Signature @ ST0013+4 BR1760



RL Signature @ ST0013+4 BR1761

FIGURE 15. CIBLE RESULTS ON J57-#4 BEARING (S/N 219A-2)
 INNER RACE, NONLOADED HALF (S12052-1), 3761 HRS.
 SERVICE, VENDOR REWORKED.

An analysis similar to the preceeding of data from the J57-#2 bearing shown in Figure 16 with a crack (see photomicrograph) reveals a significantly different ratio; the ratio of CH/CL signature amplitude for the crack region in Figure 16 is approximately 520 mV/400 mV, or 1.3. The graphs in Figure 17 relating circumferential signature amplitude from flaws as a function of magnetization level illustrates the significantly different signature behavior for a flaw with cracking as compared with one when cracking is not present. Note the significantly greater signal amplitude in the case of the crack at lower magnetizing current levels (in the range between 0 and 2 Amperes (low field) of Figure 17). A similar behavior is also indicated for radial flux, however, defect geometry factors can contribute to a similar behavior in the case of radial signatures.

Further, direct confirmation of the behavior of the circumferential signature from cracked versus uncracked regions is demonstrated by the CIBLE results in Figure 18. A comparison of the CH/CL ratio for signature A (see Records C and D in Figure 18) versus a similar ratio for signature B indicates a crack would be anticipated in the region of signature A. Photomicrograph E, however, visually shows no evidence of a crack at regions corresponding to signatures A or B. Since it is possible to "smear" metal over the top of a tightly closed crack in rework polishing operations, it was decided to endurance test this bearing (S/N 144D-2) for 2 hours at a low stress level (maximum Hertz stress of 204 ksi) to repropagate the crack through the repolished surface, if one were present. Photomicrograph F in Figure 18 shows the appearance of the signature region of interest after the endurance test. Importantly, a tightly closed crack is now visually evident at signature A corresponding with the signature behavior previously described; no crack is evident at the signature B location. In summary, the ratio of HF to LF signatures is approximately 4 or more for flaws without associated cracking and this ratio is approximately 2 or less for flaws with associated cracking. This circumferential flux high field - low field signature behavior for cracks is a significant factor in the formulation of a serviceability criteria.

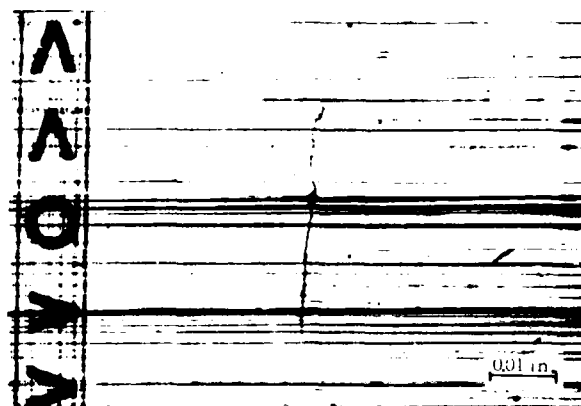
The reader is now referred to the previously presented Figure 15 in which significant circumferential and radial signatures were obtained from a region where no visual surface indication was present. This bearing, J57-#4 (S/N 219A-2) was endurance tested after the initial inspection. A spall-type failure was obtained after 30-hours endurance test time (at a maximum Hertz stress of 332 ksi). The failure was initiated at a location corresponding with the flaw signature previously illustrated in Figure 15; precise correspondence of the failure initiation site and the signature is confirmed in Figure 19. The leading edge of the spall (upstream side relative to ball movement) is shown in photomicrograph A of Figure 19 where several "landmarks" are indicated by arrows. Photomicrograph B, Figure 19, was obtained 11 hours before failure (after 19 hours endurance test time) and arrows point out the same "landmarks" as those indicated in photomicrograph A; an irregular line has been superposed on photomicrograph B representing the leading edge of the spall shown in photomicrograph A for reference purposes. Figures 20 and 21 show an overall view of the race component containing the spall and a macro-view of the spall, respectively.

FLAWS

| TY | S | T | S | R | S | R |
|----|------|------|------|----|------|-----------|
| RH | 0005 | 1666 | 1665 | RL | 0002 | 2636 2635 |
| CH | 0003 | 2500 | 2499 | RL | 0005 | 1666 1665 |
| RH | 0009 | 2504 | 2503 | CL | 0003 | 2500 2499 |
| CH | 0009 | 2500 | 2499 | RL | 0009 | 2504 2503 |
| CH | 0010 | 2500 | 2499 | CL | 0002 | 2500 2499 |
| | | | | CL | 0010 | 2500 2499 |

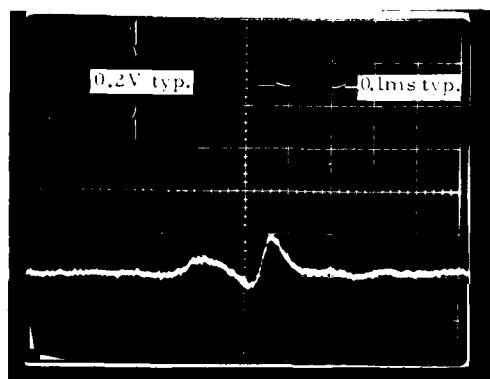
Legend:

C - circumferential flux
 R - radial flux
 H - high flux density
 L - low flux density
 ST - probe location across race groove
 BR - signature azimuthal location from
 reference mark on race (1 rev = 5000)



Magnified (~50X) View of Surface @ 0009-2500

Flaw Printout Obtained
 During Automatic Inspection

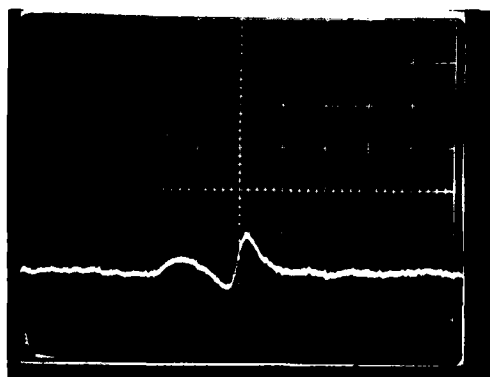


RH Signature @ ST0009+2 BR2504

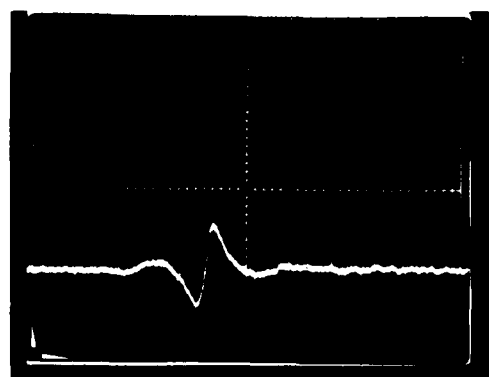


CH Signature @ ST0009+2 BR2500

5303



RL Signature @ ST0009+2 BR2504



CL Signature @ ST0009+2 BR2500

FIGURE 16. CIBLE RESULTS ON J57-#2 BEARING (S/N Y704-2RM)
 OUTER RACE (S01692-5), 8296 HRS. SERVICE, VENDOR
 REWORKED

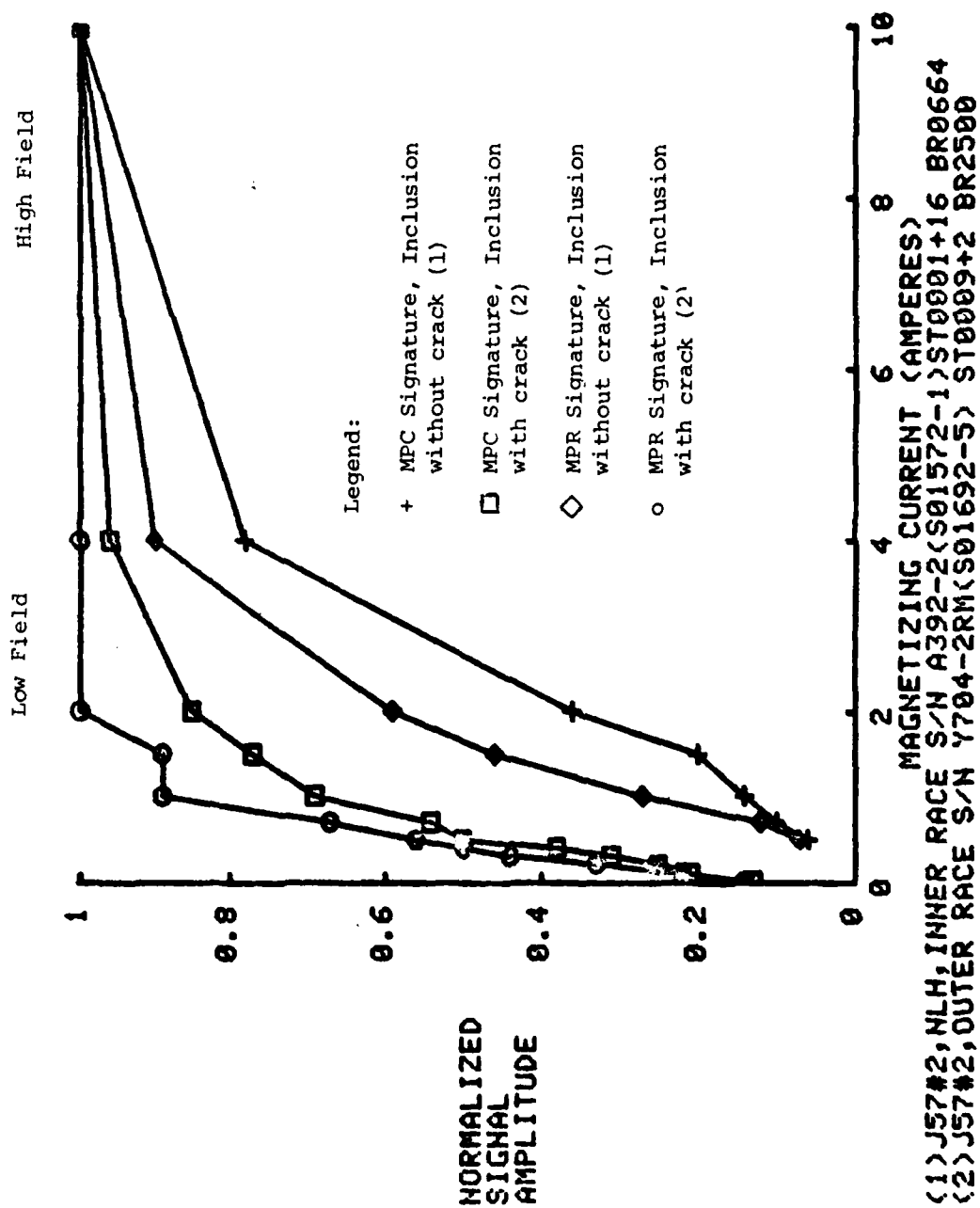
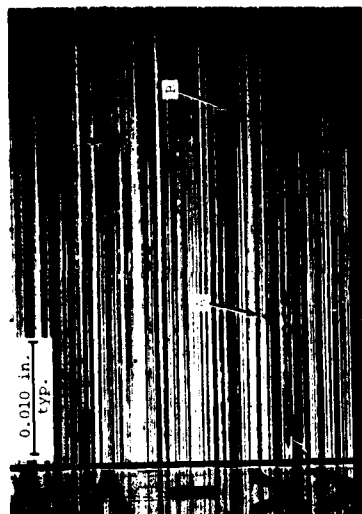


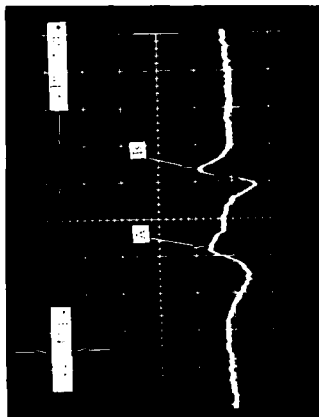
FIGURE 17. GRAPH OF MAGNETIC PERTURBATION SIGNATURE AMPLITUDE AS A FUNCTION OF APPLIED MAGNETIZATION CURRENT FOR FLAWS WITH AND WITHOUT CRACKING.



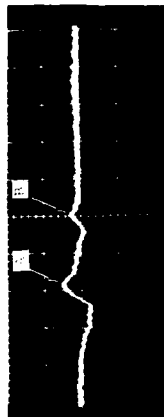
1. Magnified (100x) View of Surface a
0008-1041 Before Endurance Test



2. Magnified (100x) View of Surface a
0008-1041 After Endurance Test
2 Hours @ 204 ksi

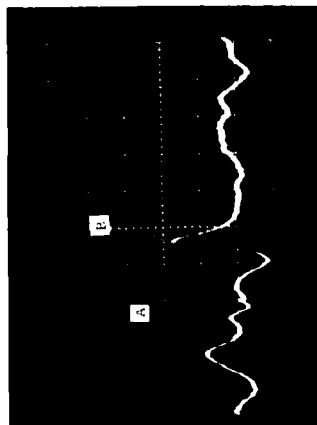


3. RH Signature a ST0008+8 BR1041



4. CL Signature a ST0008+8 BR1041

Magnetic Perturbation Signatures Before Endurance Test



5. RH Signature a ST0008+8 BR1041



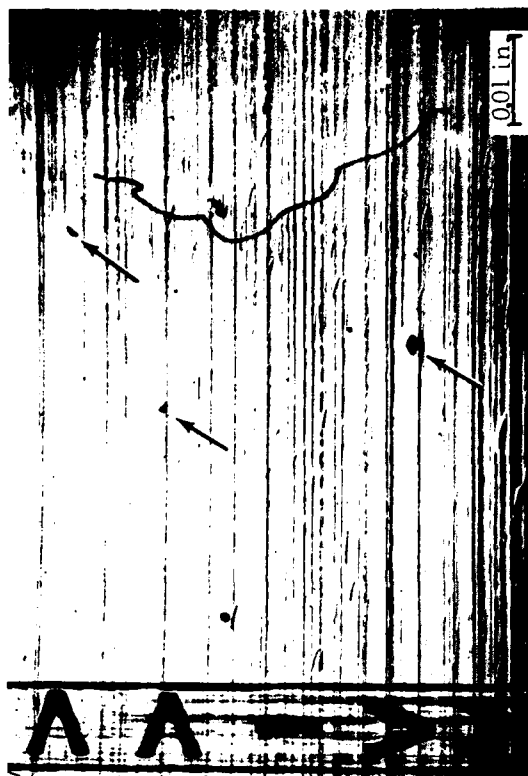
6. CL Signature a ST0008+8 BR1041

FIGURE 18. CIBL RESULTS ON J57-#2 BEARING S/N 144D-2 INNER RACE, LOADED HALF (S00762-3),
6965 HRS. SERVICE (VENDOR REWORKED) BEFORE AND AFTER ENDURANCE TESTING

5281



A. Magnified View (~50X) of Surface at 0013-1760
30 Hrs. Endurance Test Time



B. Magnified View (~50X) of Surface at 0013-1760
19 Hrs. Endurance Test Time

Note: Small arrows identify "landmarks" used to establish "spall front" outline in Photograph B.

FIGURE 19. SURFACE PHOTOMICROGRAPHS OF FLAW SIGNATURE REGION BEFORE (19 HRS.) AND AFTER FAILURE (30 HRS.) ENDURANCE TEST TIME, J57-#4 BEARING, S/N 219A-2 INNER RACE (S12052)

5099

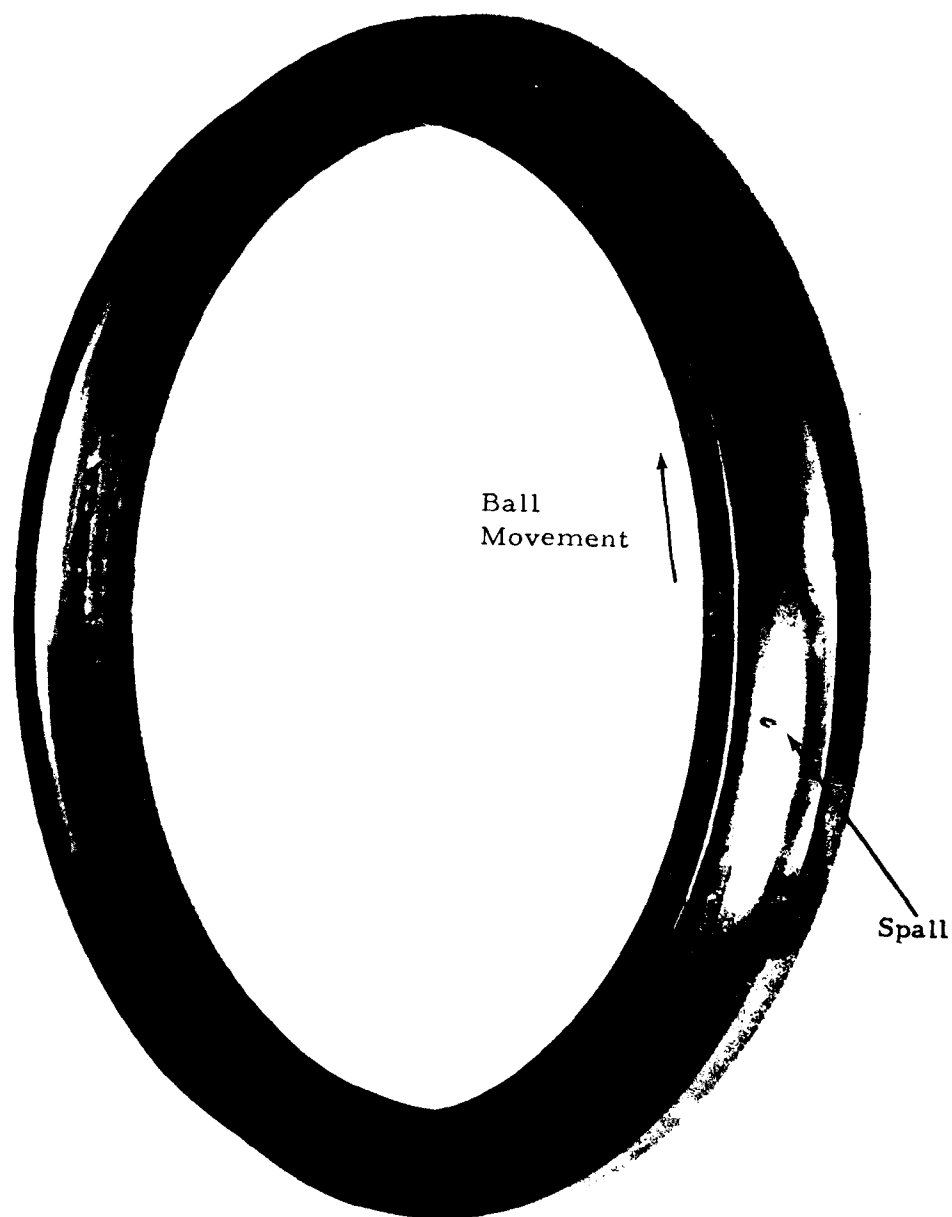


FIGURE 20. VERY SMALL SPALL WHICH DEVELOPED AFTER 30 HOURS TOTAL ENDURANCE TEST TIME, J57-#4, S/N 219A-2 (S12052-1)

5282



FIGURE 21. SURFACE PHOTOMICROGRAPH OF SPALL REGION ON
J57-#4 INNER BEARING RACE, S/N 219A-2 (S12052-1).

If the failure was a truly randomly originated event, there would be approximately 400,000 unit cells (0.003 in. by 0.003 in.) at the surface within which the failure could have initiated. The fact that it was possible to forecast the precise initiation location even though no prominent anomaly was observed on the surface demonstrates the effectiveness of the CIBLE inspection methodology.

The presence of critical flaws corresponding with signatures and/or service-induced cracking have also been confirmed through metallurgical examinations. For example, Figure 22 summarizes the results of metallurgical investigations in the region of the extensive, service-induced crack network previously illustrated in Figure 8 of this report. The sectioning planes illustrated in photomicrographs B through F of Figure 22 are referenced to the sectioning plane locations indicated in photomicrograph A of the same figure. Even though the sectioning planes illustrated in Figure 22 are near one edge of the damaged region, note the significant flaws and subsurface cracking present; material transformation was also extensive in the region investigated.

Figure 23 summarizes metallurgical results in the regions of signatures A and B previously presented in Figure 18 from the inner race, loaded half of J57-#2 bearing, S/N 144D-2. Note the extensive material transformation present in the flaw region corresponding with the cracking (signature A, see Figure 18) as shown by photomicrographs B through E in Figure 23 as well as A and B of Figure 23A. It is pointed out that such extensive transformation is not evident in the flaw region corresponding with signature B (see Figure 18) as shown in photomicrographs A through D of Figure 23B.

Many figures depicting other results from race inspection, endurance testing, and metallurgical examination have been presented in prior reports (31-33) and are also presented in Appendix F of this report.

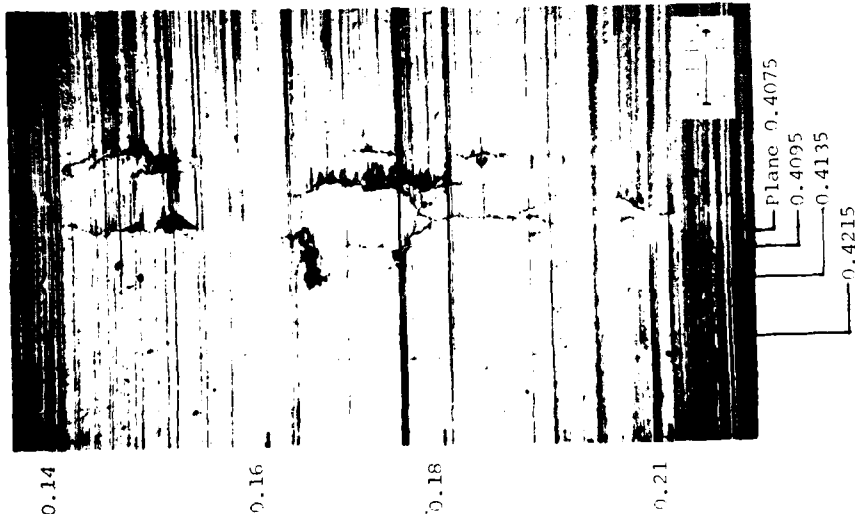
2. Balls

The inspection of 1,000 balls from J57-#4 main shaft engine bearings was completed during the latter part of 1978 at OCALC, TAFB, using the CIBLE Air Force bearing inspection system at TAFB*. Ball inspection was accomplished by routinely removing the balls from the retainer of each bearing and storing them as sets for inspection. Table V below summarizes the ball population inspection and the magnetic perturbation printouts obtained.

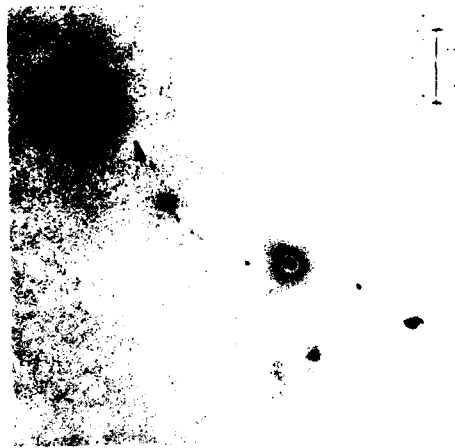
* The ball inspection unit was used for ball inspection at OCALC, TAFB since it is the only such unit available; the CIBLE bearing inspection facility at SwRI is for races only.

5483

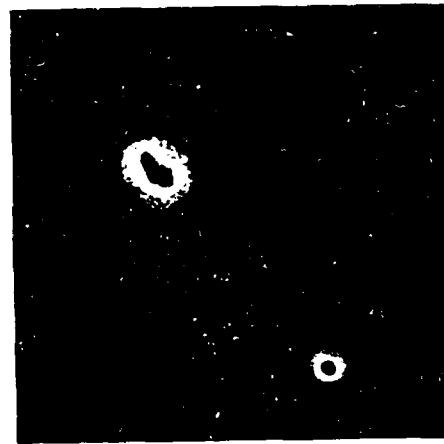
Transverse
Location



A. Magnified View of Surface (50x)
@ 0004-2291



B. Plane 0.4215 500x (0.16)
(2% nital etch)



C. Plane 0.4215 500x (0.16)
(2% nital etch)



D. Plane 0.4140 100x (0.18)

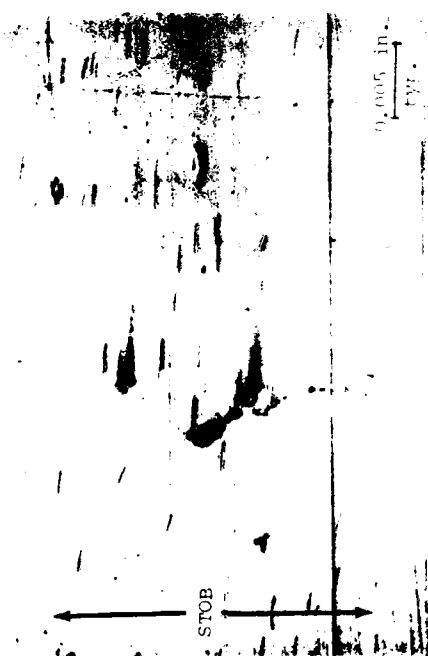


E. Plane 0.4140 100x (2% nital etch)



F. Plane 0.4140 500x (0.18)

FIGURE 22. METALLURGICAL EXAMINATION OF CRACK NETWORK ON J57-#2 BEARING S/N 144D-2),
INNER RACE, LOADED HALF AT BR2291 LOCATION (500762-3), (6965 SERVICE HOURS).



A. Magnified View of Surface (x100x) @ 0008-1011
 Signature A region
 Signature B region
 Plane 0.3915
 0.3850
 0.3930
 0.3710
 0.3680
 0.005 in.
 1 μm



B. Plane 0.3915 (2x nital etch)



C. Plane 0.3850 (2x nital etch)



D. Plane 0.3650 (2x nital etch)



E. Plane 0.3850 (2x nital etch)

FIGURE 23. METALLURGICAL EXAMINATION OF REGIONS CORRESPONDING TO SIGNATURES A AND B ON J57-#2 BEARING (S/N 144D-2), INNER RACE LOADED HALF (S00762-3)

0.002 in.
typ.

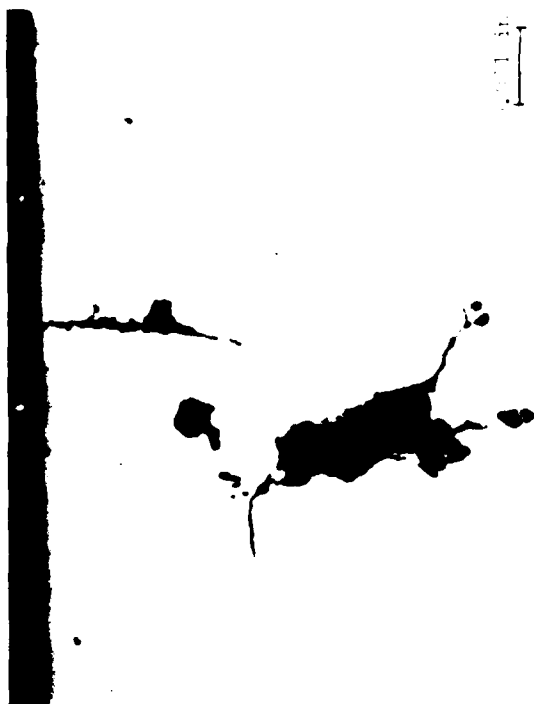
A. Plane 0.3830 $\times 250$



B. Plane 0.3830 $\times 250$ (2% nital etch)

FIGURE 23A. METALLURGICAL EXAMINATION OF REGIONS CORRESPONDING TO SIGNATURES A AND B ON J57-#2 BEARING (S/N 144D-2), INNER RACE LOADED HALF (S00762-3) (continued)

5546a



A. Plane 0.3680, area a 500x



B. Plane 0.3680, area a 500x (2% nital etch)



C. Plane 0.3680, area a 500x



D. Plane 0.3680, area a 500x

FIGURE 23B. METALLURGICAL EXAMINATION OF REGIONS CORRESPONDING TO SIGNATURES A AND B ON J57-#2 BEARING (S/N 144D-2), INNER RACE LOADED HALF (S00762-3) (continued)

TABLE V

SUMMARY OF BALLS (J57-#4 BEARING) INSPECTED
AND MAGNETIC PRINTOUTS OBTAINED

| <u>Quantity of Balls</u> | <u>Bearing Condition</u> | <u>Ball Condition</u> | <u>Percent with RH* Printouts</u> | <u>Percent with CH* Printouts</u> |
|------------------------------|------------------------------|---------------------------|---------------------------------------|---------------------------------------|
| 200 | Serviceable** | Serviceable** | 89 | 4 |
| 800 | Vendor Reworked | New | 33 | 12 |

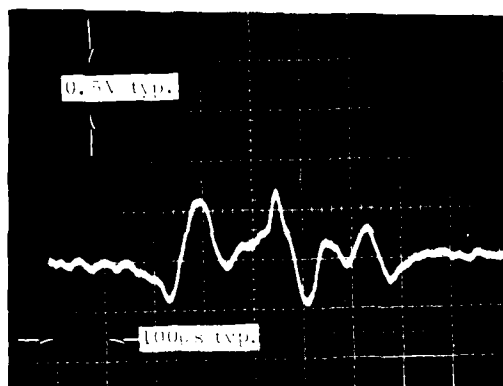
* RH - Magnetic Perturbation, radial flux, high field
CH - Magnetic Perturbation, circumferential flux, high field

** The term serviceable refers to a bearing which has been removed from an engine at overhaul and processed through the OALC bearing shop and accepted as serviceable without being vendor reworked. Vendor reworked bearings are, of course, also serviceable but have been processed through vendor facilities, and a complement of new balls installed in each bearing (as determined by visual examination).

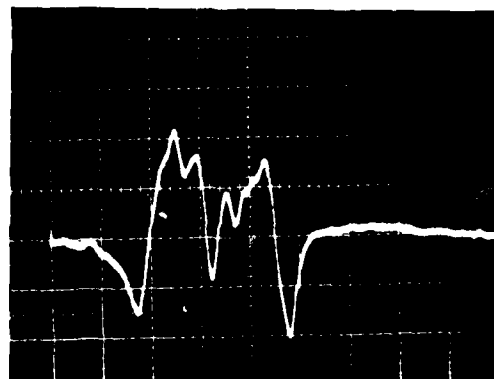
The magnetic perturbation radial and circumferential flux printouts are of special interest since these indicate the probable presence of surface and near-surface flaws. Note that the service balls (balls with service time) have almost 3 times the number of radial flux, high field (i.e., RH) printouts as that for new balls. Conversely, the new balls have three times the number of circumferential high field printouts as the balls with service time. Through computer-assisted, manual mode operation of the ball inspection system, a number of balls with printouts were sampled for recording of flaw signatures and marked for subsequent visual examination. The details of this sampling procedure and the marking of the balls for subsequent visual examination is presented in a more detailed discussion of the ball inspection effort presented in Appendix C of this report.

Figures 24 and 25 show the outstanding radial signatures obtained from surface damage in OALC-processed service balls. Figures 26, 27, and 28 show an inclusion, pitting and cracks and a substantial crack network with loss of material, respectively, from vendor processed bearings, apparently new balls. While the data presented above for balls is not from sampling a large part of the overall ball population, it does clearly show the extent of flaw conditions present in balls from serviceable bearings. Many other examples of signatures and corresponding flaws are presented in Appendix C.

Although the data base available for developing a serviceability criteria on balls is not adequate, a very preliminary criteria which may be used as a "starting point" is discussed in the section to follow on serviceability criteria along with that for the races.

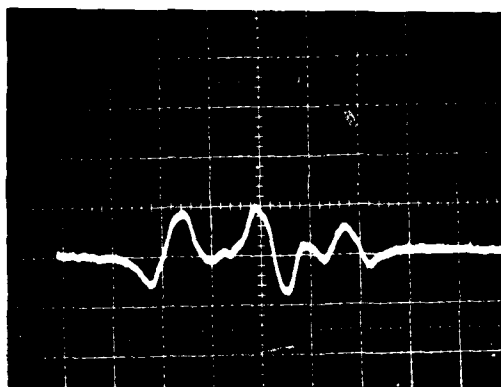


A. RH Signature, Defect #1

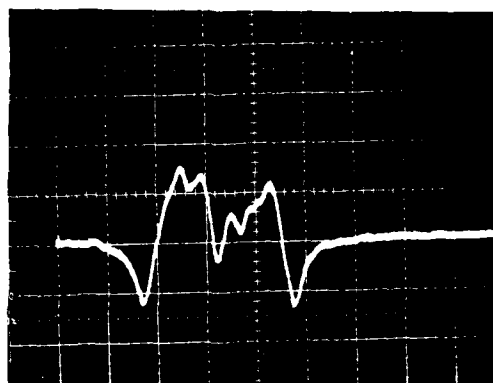


D. RH Signature, Defect #2

5162



B. EL Signature, Defect #1



E. EL Signature, Defect #2

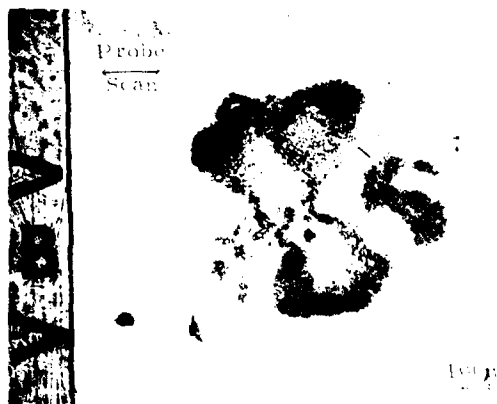
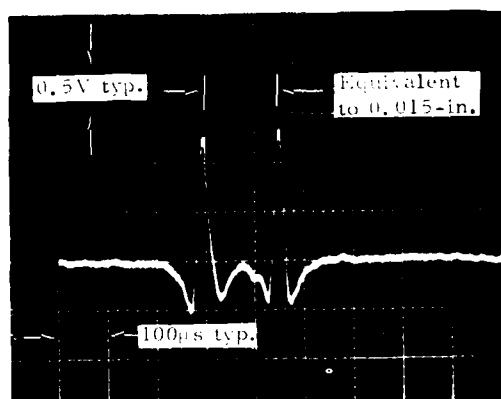
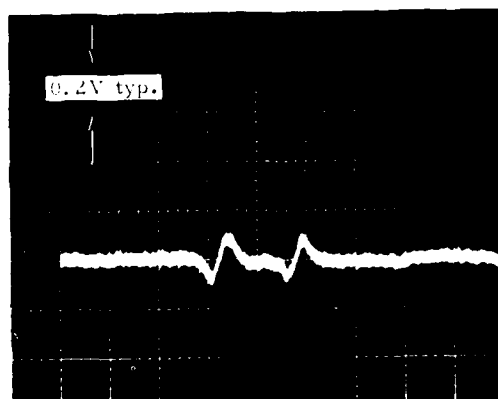
C. Surface Photomicrograph
(~50X), Defect #1F. Surface Photomicrograph
(~100X), Defect #2

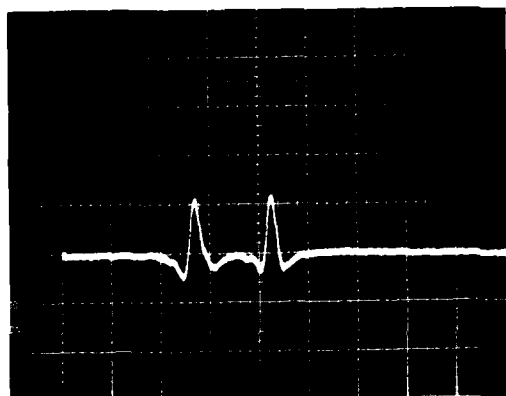
FIGURE 24. CIBLE INSPECTION SIGNATURES AND SURFACE PHOTOMICROGRAPHS
SHOWING CORRESPONDING SURFACE FLAWS ON BALL WITH 3230 HRS.
SERVICE, J57-#4 BEARING S/N 9117-2 (Ball #20, Defects 1 and 2).



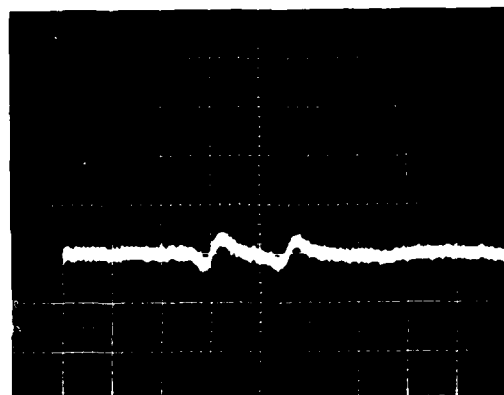
A. RH Signature



C. CH Signature (typ. peak separation, typ.)



B. RL Signature



D. CL Signature

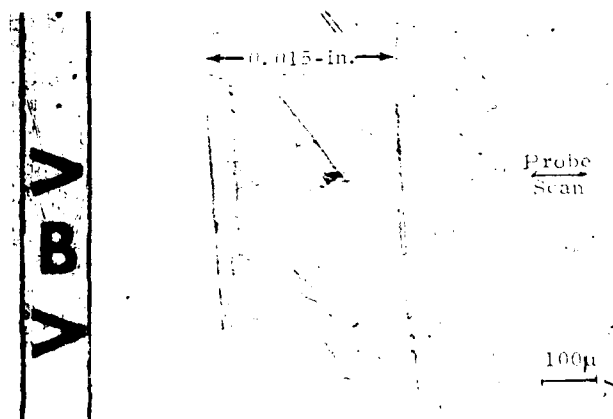
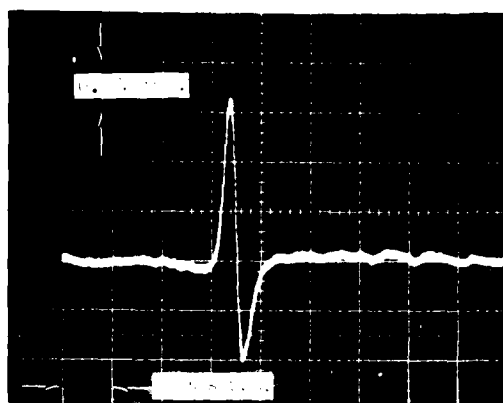
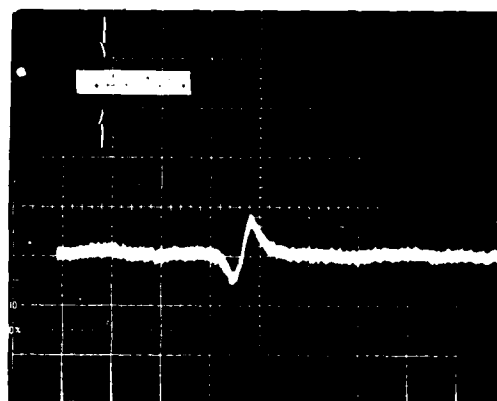
E. Surface Photomicrograph ($\sim 100\times$)

FIGURE 1. THERMAL INSPECTION SIGNATURES AND CORRESPONDING SURFACE PHOTO MICROGRAPH SHOWING GOUGES ON BALL WITH 4230 HRS SERVICE, 357-#4 BEARING S/N P9117-2 (Ball #30, Defect #3).

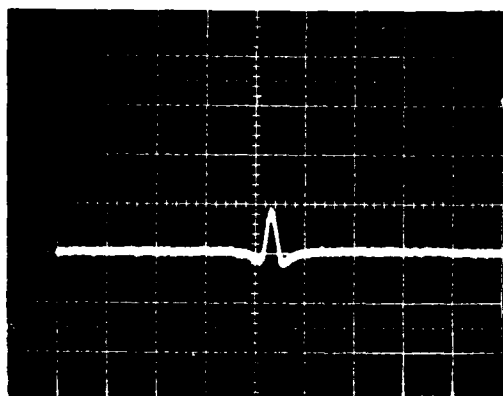
5161



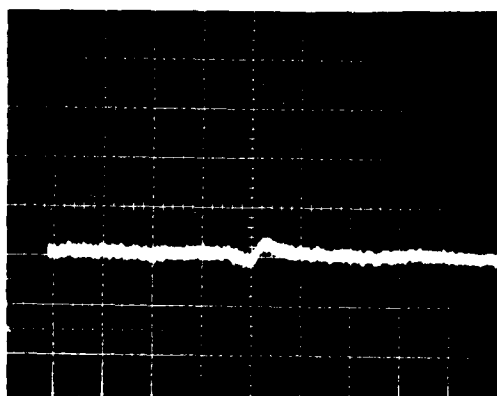
A. RH Signature



C. CH Signature (75μ peak separation)



B. RL Signature



D. CL Signature

V B V

Probe
Scan

6

1.1

E. Surface Photomicrograph ($\approx 100\times$)

FIGURE 26. CIBLE INSPECTION SIGNATURES AND CORRESPONDING SURFACE PHOTOMICROGRAPH SHOWING INCLUSION ON SURFACE OF NEW BALL FROM VENDOR REWORKED J57-#4 BEARING S/N 3453-2, 5940 HRS (Ball #12, S11092).

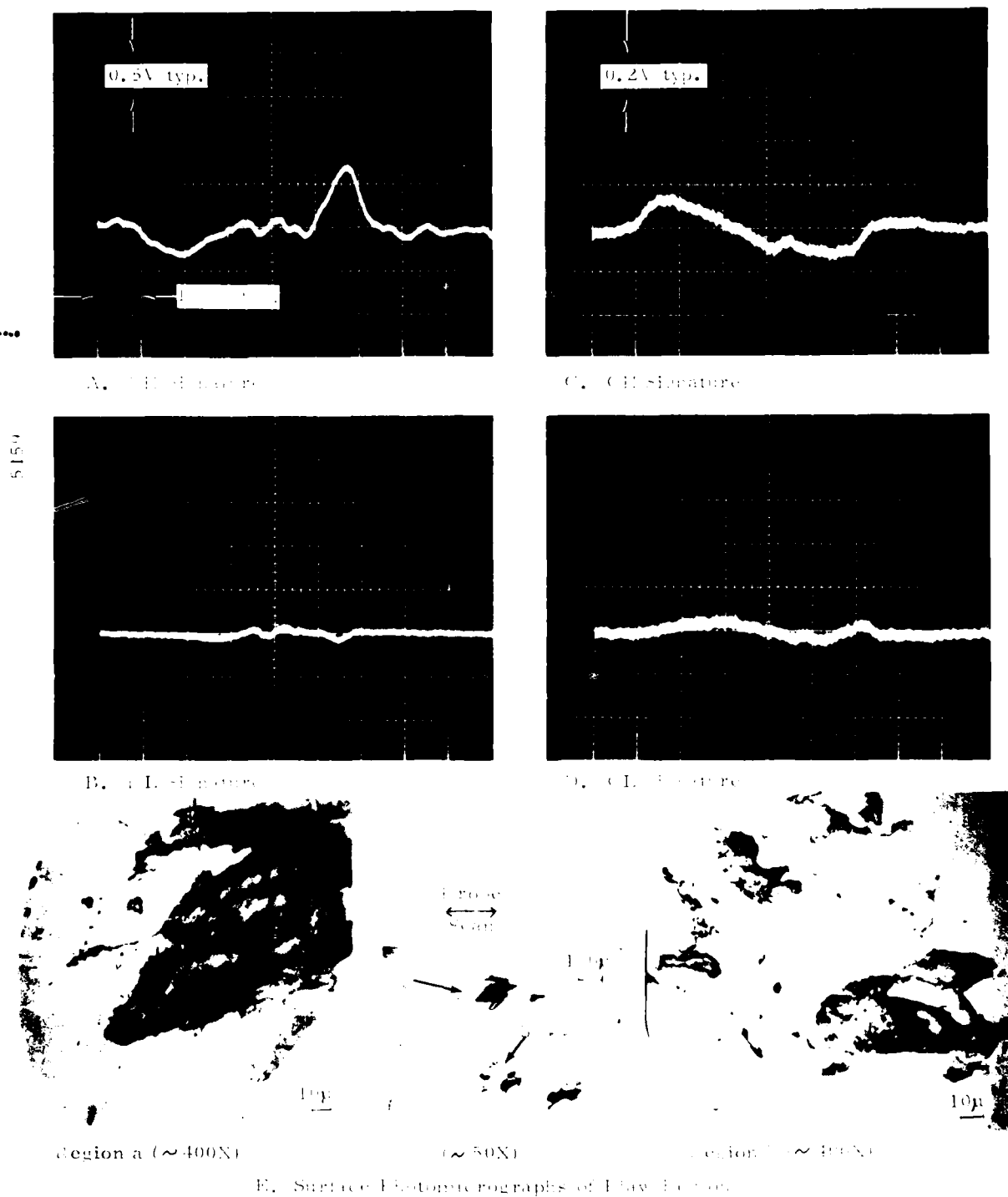


FIGURE 27. CIBL INSPECTION SIGNATURES AND CORRESPONDING SURFACE PHOTOMICROGRAPHS SHOWING PITS AND CRACKS ON NEW BALL FROM VENDOR REWORKED J57-#4 BEARING S/N 395-2, 4362 HRS (Ball #11, S11672).

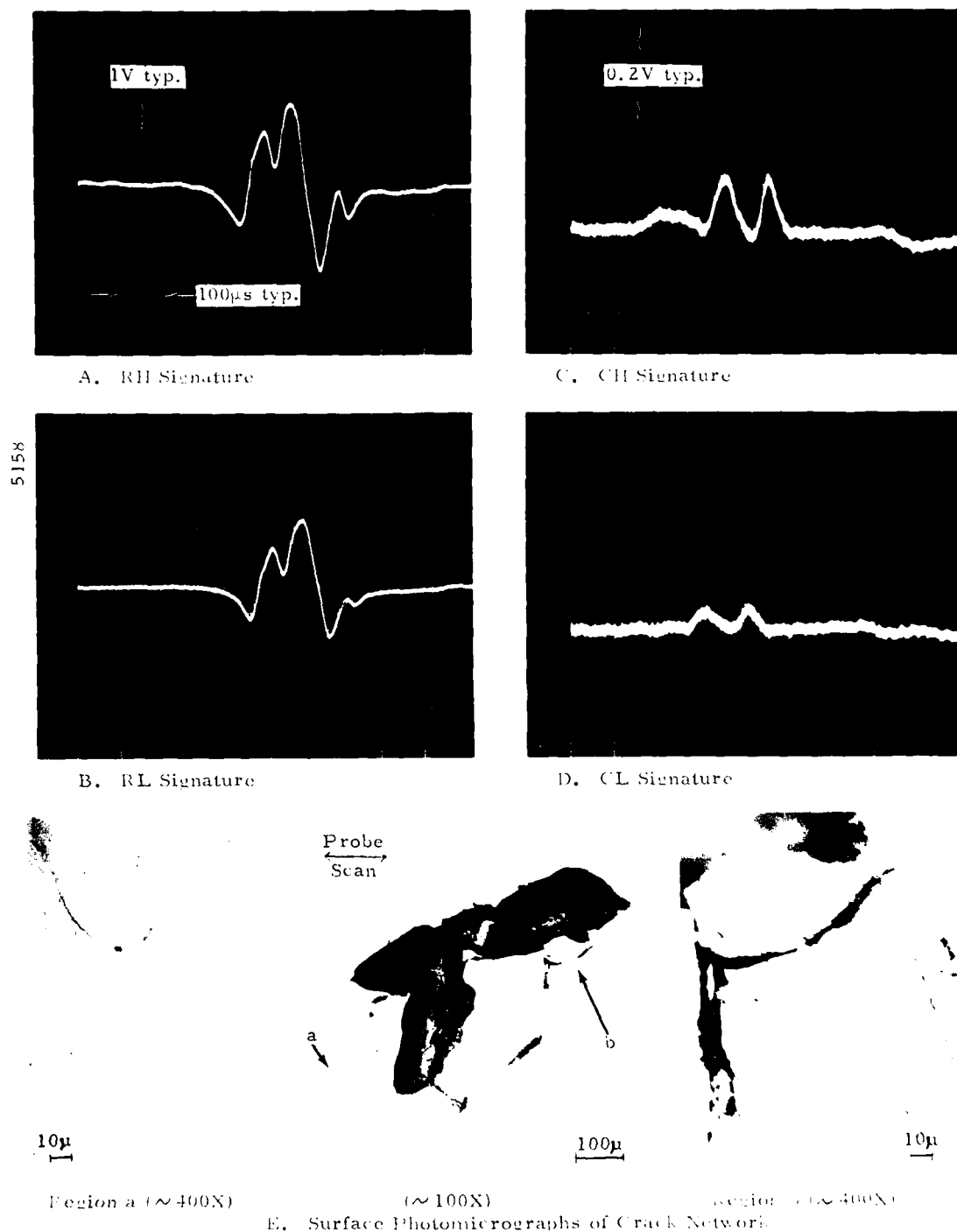


FIGURE 28. CIBL INSPECTION SIGNATURES AND CORRESPONDING SURFACE PHOTOMICROGRAPHS SHOWING CRACK NETWORK ON NEW BALL FROM VENDOR REWORKED J57-#4 BEARING S/N 395-2, 4362 HRS (Ball #3, S11672).

C. Preliminary Serviceability Criteria

Based upon the type of results presented above on races, a serviceability criteria was developed by examining the voluminous Polaroid records of signatures, surface photomicrographs, endurance test results, and metallurgical results. In addition, 64 bearings released after inspection were returned to the OCALC bearing inspection shop with accompanying notes as well as copies of signatures, printouts, surface photomicrographs, etc. to determine if the bearing race components would be accepted under current OCALC bearing inspection procedures. All but one bearing (S/N 144D-2 with the large crack network (see Figure 22)) would have been accepted. Importantly, two of the bearings sent to OCALC contained service-induced cracks which were not detected by the routine bearing inspection procedures presently used at TAFB. The bulk of the bearings shipped to OCALC with notes were ones on which radial signatures were obtained (with no accompanying outstanding circumferential signatures) and a corresponding visual pit was noted; in some cases, the pits were greater than 0.005 in. (125 μ m) in diameter.

Figure 29 presents the preliminary serviceability criteria developed for J57-#2 races (values for other races are shown in Appendix B of this report) and this criteria has been programmed into the Air Force CIBLE equipment at OCALC. Currently, the serviceability criteria for the rolling elements (balls or rollers) of each of the bearing types is the same as that for the races since experience to date on rolling elements is not adequate to develop an independent set of criteria item values.

| <u>Item*</u> | *CIBLE automatically checks that CH peak-to-peak amplitude is ≥ 80 mV+ and CL peak-to-peak amplitude is ≥ 40 mV+ before applying criteria. |
|--------------|--|
| A | Reject all with CL peak-to-peak amplitude ≥ 100 mV+ |
| B | Reject all CH with CH/CL ratio < 2.0 . ≥ 0 |
| C | Reject all CH with peak-to-peak amplitude ≥ 200 mV+ and peak separation < 150 μ m |
| D | Reject all CH with peak-to-peak amplitude ≥ 200 mV+ and RH peak amplitude ≥ 600 mV+ |
| E | Reject if CH ≥ 200 mV+ for BR XXXX + (0050) for 3 or more ST |
| F | Reject all RH with peak amplitude ≥ 1000 mV+ |
| G | If flaw buffer overloads |
| H | BK reject, if SLP1 LOC < 560 ms, SLP1 ≥ 50 and EXTR1AMP ≥ 100 mV |
| I | Reject, if laser EXTR1 AMP ≥ 3900 mV+ |
| J | LD AVG MEAN ≥ 720 mV |

IF REJECTED GIVEN ITEM(S)

Notes:

| | | |
|-------------|--------------------------------------|--|
| + | Absolute magnitudes | |
| CH | Circumferential flux, high field | |
| CL | Circumferential flux, low field | |
| RH | Radial flux, high field | |
| BR | Bearing reference azimuthal location | |
| ST | Scan track | |
| BK | Barkhausen noise signature | |
| SLP1 LOC | | } See Appendix B, Figures B-4 through B-7. |
| SLP1 | | |
| EXTR1 AMP | | |
| LD AVG MEAN | | |

FIGURE 29. SERVICEABILITY CRITERIA (PRELIMINARY), RACES AND ROLLING ELEMENTS

IV. CONCLUSIONS AND RECOMMENDATIONS

A. Conclusions

The following major conclusions are based on the voluminous data acquired and the wide range of significant results obtained on this program.

1. Service-induced cracking occurs in bearings.
2. A small percentage of in-service bearings with cracks are missed during depot and rework inspections (under the current, routinely employed inspection procedures).
3. Cracks are initiated at inclusion sites in the bearing material.
4. Endurance testing and metallurgical examination of service bearings confirms crack initiation at inclusion sites.
5. The small percentage of new bearings with subsurface, incipient failure sites (inclusions) are missed by presently used inspection methods.
6. CIBLE inspection procedures can identify and eliminate bearings with service-induced cracks and new bearings with inclusions. In fact, CIBLE employs the only known NDE method, magnetic perturbation, which is capable of detecting tiny subsurface inclusions.
7. CIBLE can directly contribute to the investigation and explanation of failure mechanisms and processes in bearings.

B. Recommendations

Based on the many important and significant results obtained under this program, the following major recommendations are made:

1. Expand the present CIBLE data base and further develop a serviceability criteria for rolling elements.
2. Expand the inspection and serviceability criteria to include other bearing types.
3. Initiate efforts to integrate the advanced methodology of CIBLE into the activities of prime bearing manufacturers and rework vendors.
4. Finally, but not least to those above, it is strongly recommended that a program be established with a contractor immediately for the CIBLE inspection of all critical main shaft bearings if the internal organizational structure and procedures presently employed at the overhaul depot prevent rapid integration of the CIBLE system with on-going bearing inspection activities.

V. REFERENCES

1. Barton, J. R., "Early Fatigue Damage Detection in 4140 Steel Tubes", Proc. Fifth Annual Symposium on NDE of Aerospace and Weapons Systems Components and Materials, South Texas Chapter ASNT, San Antonio, Texas, April 1965.
2. Kusenberger, F. N., Leonard, B. E., Barton, J. R., Donaldson, W. Lyle, "Nondestructive Evaluation of Metal Fatigue", Air Force Office of Scientific Research, Scientific Report AFOSR 67-1288, April 1967.
3. Barton, John R., Donaldson, W. Lyle, Kusenberger, F. N., "Nondestructive Evaluation of Metal Fatigue", Proceedings of the Office of Aerospace Research, Research Applications Conference, Arlington, Virginia, March 1969.
4. Kusenberger, F. N., Francis, P. H., Leonard, B. E., Barton, John R., "Nondestructive Evaluation of Metal Fatigue", AFOSR Scientific Report 69-1329TR, April 1969.
5. Barton, John R., Kusenberger, Felix N., "Magnetic Perturbation Inspection to Improve Reliability of High Strength Steel Components", Paper 69-DE-58, Design Engineering Conference of ASME, New York, New York May 1969.
6. Kusenberger, F. N., Lankford, Jr., J., Francis, P. H., Barton, J. R., "Nondestructive Evaluation of Metal Fatigue", Air Force Office of Scientific Research, AFOSR 70-1206 TR, March 1970.
7. Barton, John R., Kusenberger, Felix N., "Fatigue Damage in Gas Turbine Engine Materials", Chapter on Fatigue Damage Detection, ASTM STP 495, pp. 193-208, 1971.
8. Kusenberger, F. N., Lankford, Jr., J., Francis, P. H., Barton, J. R., "Nondestructive Evaluation of Metal Fatigue", Scientific Report, AFOSR-TR-71-1965, April 1971.
9. Barton, J. R., Lankford, J., Hampton, P. L., "Advanced Non-destructive Testing Methods for Bearing Inspection", SAE Paper No. 720172, Automotive Engineering Congress, Detroit, Michigan, January 1972.
10. Kusenberger, F. N., Lankford, Jr., J., Francis, P. H., Barton, J. R., "Nondestructive Evaluation of Metal Fatigue", Scientific Report AFOSR-TR-72-1167, April 1972.
11. Barton, J. R. and Lankford, J., "Magnetic Perturbation Inspection of Inner Bearing Races", NASA CR-2055, May 1972.

12. Kusenberger, F. N., Ko, W. L., Lankford, Jr., J., Francis, P. H., Barton, J. R., "Nondestructive Evaluation of Metal Fatigue", Scientific Report AFOSR-TR-73-1070, April 1973.
13. Lankford, J. and Kusenberger, F. N., "Initiation of Fatigue Cracks in 4340 Steel", Met. Trans., 4, 1973, pp. 553.
14. Barton, J. R., Kusenberger, F. N., Francis, P. H., Ko, W. L., Lankford, Jr., J., "Nondestructive Evaluation of Metal Fatigue", Scientific Report AFOSR-TR-74-0820, February 1974.
15. Barton, J. R., "Quantitative Correlation between Magnetic Perturbation Signatures and Inclusions", ASTM International Symposium on Rating of Nonmetallic Inclusions in Bearing Steels, Boston, Mass., May 1974.
16. Barton, J. R., "Advanced Magnetic Methods of Flaw Detection", Workshop for NDE Sponsored jointly by ARPA and AFML, Thousand Oaks, California, June 1974. Technical Report AFML-TR-74-238, Nov. 1974.
17. Gardner, C. G., Barton, J. R., "Recent Advances in Magnetic Field Methods of Nondestructive Evaluation for Aerospace Applications", Propulsion and Energetics Panel Advisory Group for Aerospace Research and Dev., London, England, April 1970.
18. Lankford, J. and Francis, P. H., "Magnetic Field Perturbation Due to Metallurgical Defects", Int. J. NDT, Vol. 3, 1971, pp. 77.
19. Pasley, R. L., "Barkhausen Effect - An Indication of Stress", Materials Evaluation, Vol. 28 (1970), p. 157.
20. Gardner, C. G., Matzkanin, G. A. and Davidson, D. L., "The Influence of Mechanical Stress on Magnetization Processes and Barkhausen Jumps in Ferromagnetic Materials", Int. J. Non-destructive Testing, Vol. 3, 1971, pp. 131-169.
21. Barkhausen, H., "ZWEI mit Hilfe der neuen Verstärker entdeckte Erscheinungen", Physik, Z. Vol. 20 (1919).
22. Parker, R. J., "Correlation of Magnetic Perturbation Inspection Data with Rolling-Element Bearing Fatigue Results", ASME Journal of Lubrication Technology, April 1975.
23. Barton, J. R., "Residual Stresses in Gas Turbine Engine Components from Barkhausen Noise Analysis", Gas Turbine Conference ASME, Zurich, Switzerland, March-April 1974. Published in Journal of Engineering for Power, October 1974.

24. Kusenberger, F. N. and Barton, John R., "Barkhausen Noise Stress Measurements on Bearing Races Before and After Service", Final Report, SwRI Project No. 15-2888, AF Contract No. F09603-70-D-5547, June 1974.
25. Barton, John R., "Magnetic Perturbation Inspection of J85 Main Shaft Inner Bearing Races", SwRI Project No. 15-2654, AF Contract No. F09603-69-C-5101, June 1975.
26. Beissner, R. E., Cerwin, S. A., "Inspection of J-57 and J-85 Engine Bearings Using Conventional and Laser Light Techniques", Final Report, SwRI Project No. 15-3133, AF Contract No. F09603-71-C-4538, October 1972.
27. Kusenberger, Felix N., Bradshaw, William W., Barton, John R., "Inspection of Refurbished Helicopter Engine and Transmission Bearings Using Magnetic Perturbation, Barkhausen Noise, and Laser Light Methods", Inspection Report, SwRI Project No. 15-4018, Army Contract No. DAAG46-74-C-0143, January 1975.
28. Kusenberger, Felix N., Barton, John R., "Development of Diagnostic Test Equipment for Inspecting Antifriction Bearings", Final Report, SwRI Project Nos. 15-3764 and 15-4052, Army Contract Nos. DAAG 46-74-C-0012 and DAAG46-75-C-0001, March 1977.
29. Barton, J. R., Ku, P. M., Gardner, C. G., "A Proposal for Use of New Nondestructive Evaluation Procedures for Predicting Bearing Service Life", SwRI Proposal 15-7888-3, 6 May 1971.
30. Barton, John R., Kusenberger, Felix N., Hampton, P. L., Bull, Hugh, "Critical Inspection of Bearings for Life Extension (CIBLE)", Proc. Tenth Symposium on Nondestructive Evaluation, South Texas Section, ASNT and Southwest Research Institute, April 1975, pp. 310-331.
31. Kusenberger, Felix N., Baber, Burl B., Barton, John R., "Special Engineering Services to Establish Inspection Criteria for Bearings to Improve Life Prediction", Interim Report for Period 1 July 1974-30 June 1975, SwRI Project No. 15-4012, AF Contract No. F09603-74-C-5158, August 1975.
32. Kusenberger, Felix N., Baber, Burl B., Barton, John R., and Tarver, Wilson B., "Special Engineering Services to Establish Inspection Criteria for Bearings to Improve Life Prediction", Interim Report 1 July 1975-30 June 1977, SwRI Project No. 15-4012, AF Contract No. F09603-74-C-5158, August 1977.
33. Kusenberger, Felix N., Baber, Burl B., Barton, John R., and Lozano, Albert S., "Special Engineering Services to Establish Inspection Criteria for Bearings to Improve Life Prediction", Interim Engineering Report 1 July 1977-30 June 1978, SwRI Project No. 15-4012, AF Contract No. F09603-74-C-5158, July 1978.

34. "Operating Instruction Manual for Bearing Inspection System", (15-3976-001A, Option C) Contract No. F09603-74-C-5158, SwRI Project No. 15-4012, September 1979.
35. Bohm, K., et al., "Nonmetallic Inclusions and Rolling Contact Fatigue", Symposium on Bearing Steels: The Rating of Nonmetallic Inclusion, ASTM, Boston, Mass., 22-24 May 1974. ASTM STP 575.
36. Barton, John R., Kusenberger, Felix N., "CIBLE Data Base Acquisition on New and Used Bearings", Proc. Eleventh Symposium on Nondestructive Evaluation, San Antonio, Texas, April 1977, pp. 130-149.

APPENDIX A
"CIBLE" CONCEPT

A. Description of Concept

A descriptive title for the overall program is:

CRITICAL INSPECTION OF BEARINGS FOR LIFE EXTENSION
(CIBLE)

The closed loop flow diagram in Figure A1 helps to clarify the program concepts and functional relationships of important elements.

- Starting at the upper left, new bearings from the manufacturer and bearings from service engines are processed at the overhaul facility using presently established procedures (no change). A large fraction of service bearings and all new bearings (of the specific type) are routed to SwRI for examination and data acquisition.
- Comprehensive magnetic perturbation and Barkhausen stress data are recorded from races and balls of each bearing; high magnification surface photographs, plastic replicas, ultrasonic, optical (holographic contouring when developed), and other supplementary data are obtained on selected specimens.
- Data (from SwRI, overhaul facility and other sources) are permanently retained on punched cards, magnetic tape, etc.
- Initially, the serviceability criteria will pass all bearings which are acceptable under present overhaul criteria, and all bearings will be returned to the overhaul facility for normal use (upper right). However, when inspection results indicate critical flaws, recommendations will be made to postpone installation. (Transit and turn around time will be minimized to a few days by air shipment and rapid processing.)
- Gradually, as more definitive information enters the data storage from repeated inspections (first, second, and third service tours), early indications of impending spalls, rig runs, metallographic examinations, oil analysis, sonic analysis, on-board condition monitoring systems, failed bearings, etc., computer assisted analysis will be used to develop individual bearing data profiles, to disclose important trends, to select specific precursors of impending failures, etc.
- The data base, analysis, and serviceability criteria (lower right) will be refined on a continuing basis.
- Correlations of the complete individual bearing data profile with performance of bearings in actual service will be the major determinant of serviceability criteria.

Critical Inspection of Bearings for Life Extension (CIBLE)

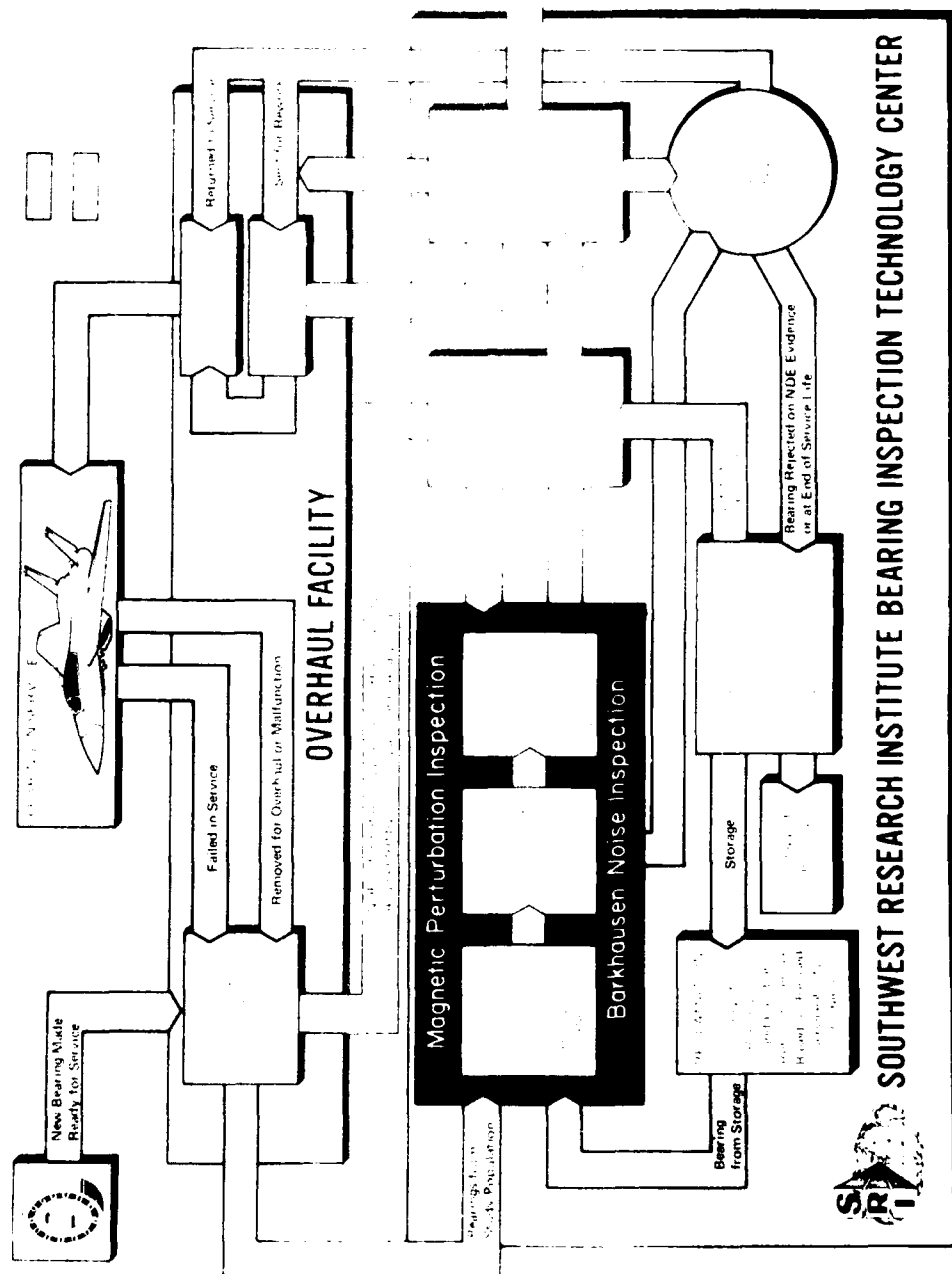


FIGURE A1. BLOCK DIAGRAM OF CIBLE CONCEPT

- Bearings rejected on NDE evidence (both current and advanced) and those reaching the end of service life (lower right) will be stored for reclamation investigations; many of these bearings may eventually be completely validated for further service.
- Overhaul facility personnel will be progressively integrated into the program and trained to routinely accomplish all major functions including data acquisition, data storage and processing, computer analysis, etc., by the end of the program. The complete inspection process would then be routinely accomplished at the overhaul facilities.

B. Features of Concept

Features of the concept program are:

- Advanced methods of nondestructive characterization and evaluation (NDE) will be applied to a controlled, statistically significant population of bearings of selected types (location); inspections will be performed on new and service bearings at Southwest Research Institute in coordination with periodic overhaul procedures.
- Advanced state-of-the-art data acquisition, storage, and analysis procedures will be employed to produce permanent, individualized NDE profiles for each bearing component inspected.
- Automation of inspection hardware and data processing will be developed.
- Rational criteria for acceptance, rejection, or service restriction for individual bearings will be developed and validated.
- Performance of bearings in actual service will be the dominant factor in establishing the criteria.
- Individual bearings will be reinspected and reevaluated each time they are returned to the overhaul facility; deterioration, changes, and failure trends can therefore be established.
- Information from supplementary sources such as spectrometric oil analysis, sonic engine analyzers, failure reporting systems, postfailure investigations, etc., will be incorporated into the data base used for the development of serviceability criteria.
- Close, continuous liaison will be maintained between Southwest Research Institute and cognizant personnel at overhaul facilities (as well as superior administrative levels) to insure timely exchange of pertinent information and smooth, effective transfer of new technology and procedures from the laboratory to the shop.

- As an integral part of the program, selected overhaul facilities will participate by using online inspection and data acquisition hardware fabricated by Southwest Research Institute and installed at the selected overhaul facilities.

C. Technical Payoff

Short-Term Payoff:

- A decrease of premature in-service failure rate by immediate elimination of individual components with critical subsurface and surface flaws and with detrimental surface tension stresses (beyond capability of ALL present inspection procedures).

Long-Term Payoff:

- Substantial and continued decrease in service bearing failures.
- Elimination of time-consuming, meticulous, visual examinations and associated subjective variations.
- Improved procurement specifications and NDE procedures to ensure conformance of bearing components - this would eliminate variability presently encountered with similar products procured from different sources.
- Early alerting to possible detrimental affects on bearings caused by changes in mission profile and environment.
- Improved reliability of critical bearing components used in advanced technology development programs.
- Establishment of an extensive, actual-service, data base which is readily accessible for new design considerations, etc.
- Early appraisal of the affect of engineering and/or product improvement changes on bearing reliability.
- Provide a basis for improved projections of stocking levels.
- Provide definitive, valid criteria for reliable "life extensions" based on measured material characteristics of individual bearings.

APPENDIX B

IMPLEMENTATION OF "CIBLE"
(Preliminary)

The hardware and software elements required to upgrade the basic inspection system (developed under specification WRAMA/MME4940-526) presently at the Oklahoma City Air Logistics Center, TAFB, are shown in a block diagram of Figure B1, along with the interrelationships to the basic system. The basic system is outlined by the dashed-line block; the hardware elements added primarily consist of a signal conditioner module and computer interface (indicated within the block entitled, "Additions to HP 2100 Computer for Signal Analysis/Data Management"), high speed terminal w/tape cartridge storage (for operator interaction with the system), and the telephone communication link adapter (MODEM) to facilitate linkup with an off-site data base management network.

The signal conditioner, a block diagram of which is shown in Figure B2, consists of circuitry to facilitate the sampling or digitization of the analog inspection signatures (magnetic perturbation, radial and circumferential channels including background, Barkhausen noise, laser pit signals, and laser surface finish); digitization of these channels is accomplished by using a single analog-to-digital converter (Biomation Model 805) through the use of a multiplexer under computer control. Auto-scaling of the signatures for conversion is also accomplished under computer control via the programmable amplifier. The location of specific signatures to be converted is accomplished under computer acquisition via the shaft encoder (shaft position information heretofore used to provide the BR bearing reference and SR shaft reference information on the printouts); synchronization for the Barkhausen is obtained from the Barkhausen sync pulse. A different time base for sampling or digitization operations is required for Barkhausen, magnetic perturbation background, and laser surface finish sampling and is a function under the command of the computer or CPU.

Also shown in Figure B2 is a data transfer selector block. This module has been added to the system to provide 3 different modes of system operation. During normal inspection operation, the data transfer selector is placed in the 4051 calculator/terminal-to-CPU position which permits the operator to communicate with the computer which is supervising inspection equipment operation. When it is desired to transfer data or request data from the off-site master data base, the selector is placed in the 4051-to-MODEM mode. In cases where it is desired to printout results from a data cartridge on the teleprinter (TTY), this can be accomplished by selecting the proper mode. It is also possible to operate the bearing inspection equipment via operator communications through the TTY, however, such operation precludes tape cartridge input and output of data and inspection results.

The overall concept of the manner in which flaw signatures are selected for digitization, subsequently analyzed, and a serviceability criteria applied to the processed signature data (accept or reject computations) from a bearing component is presented in the block diagram of Figure B3. In the case of the magnetic perturbation, radial and circumferential and laser pit signature channels, signatures exceeding the pre-set threshold level are digitized; in the case of the Barkhausen and laser surface finish, each signature is digitized or sampled. Pre-defined signature parameters are developed from the digitized data and

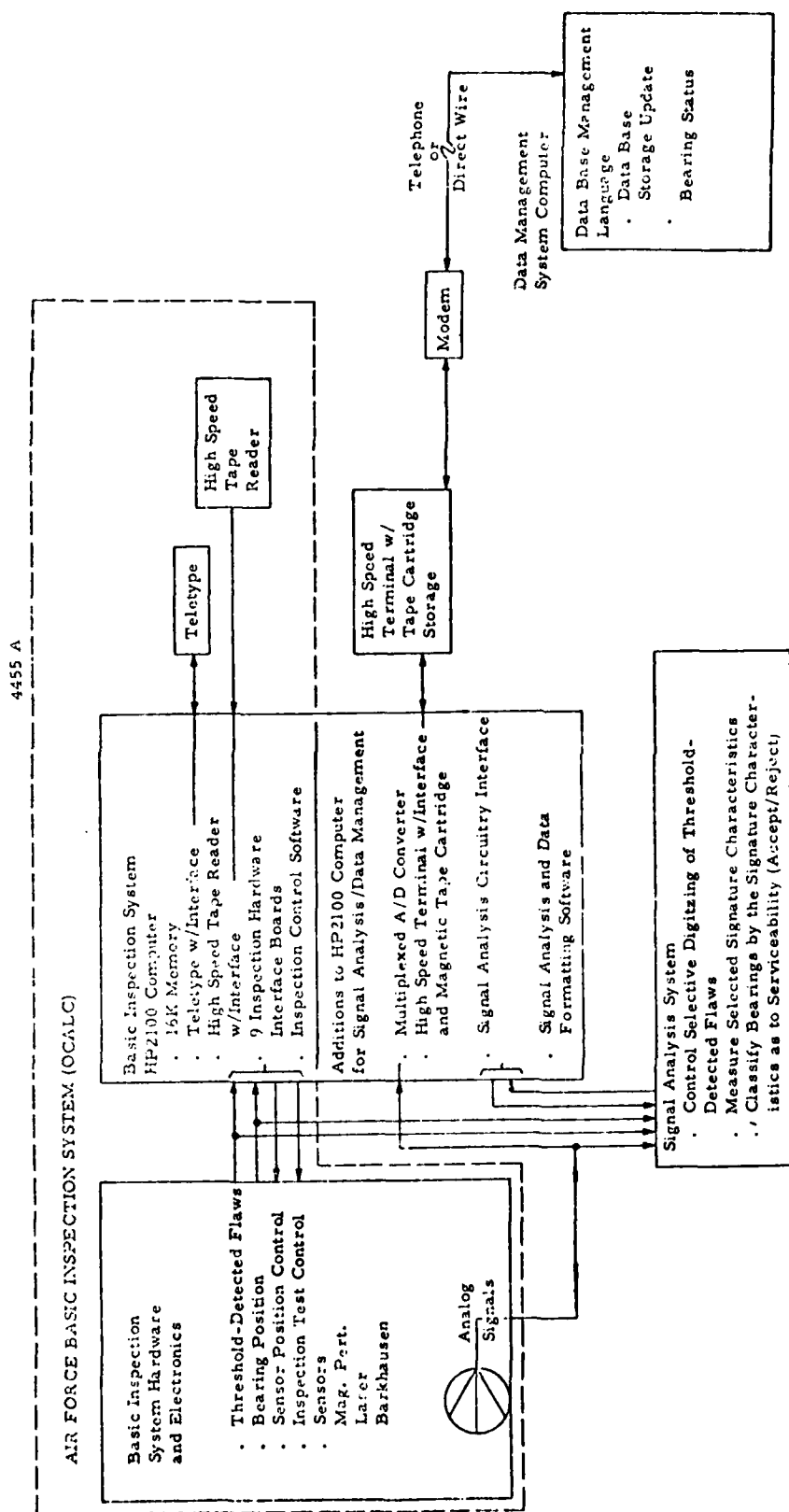


FIGURE B1. BLOCK DIAGRAM OF CIBLE SYSTEM

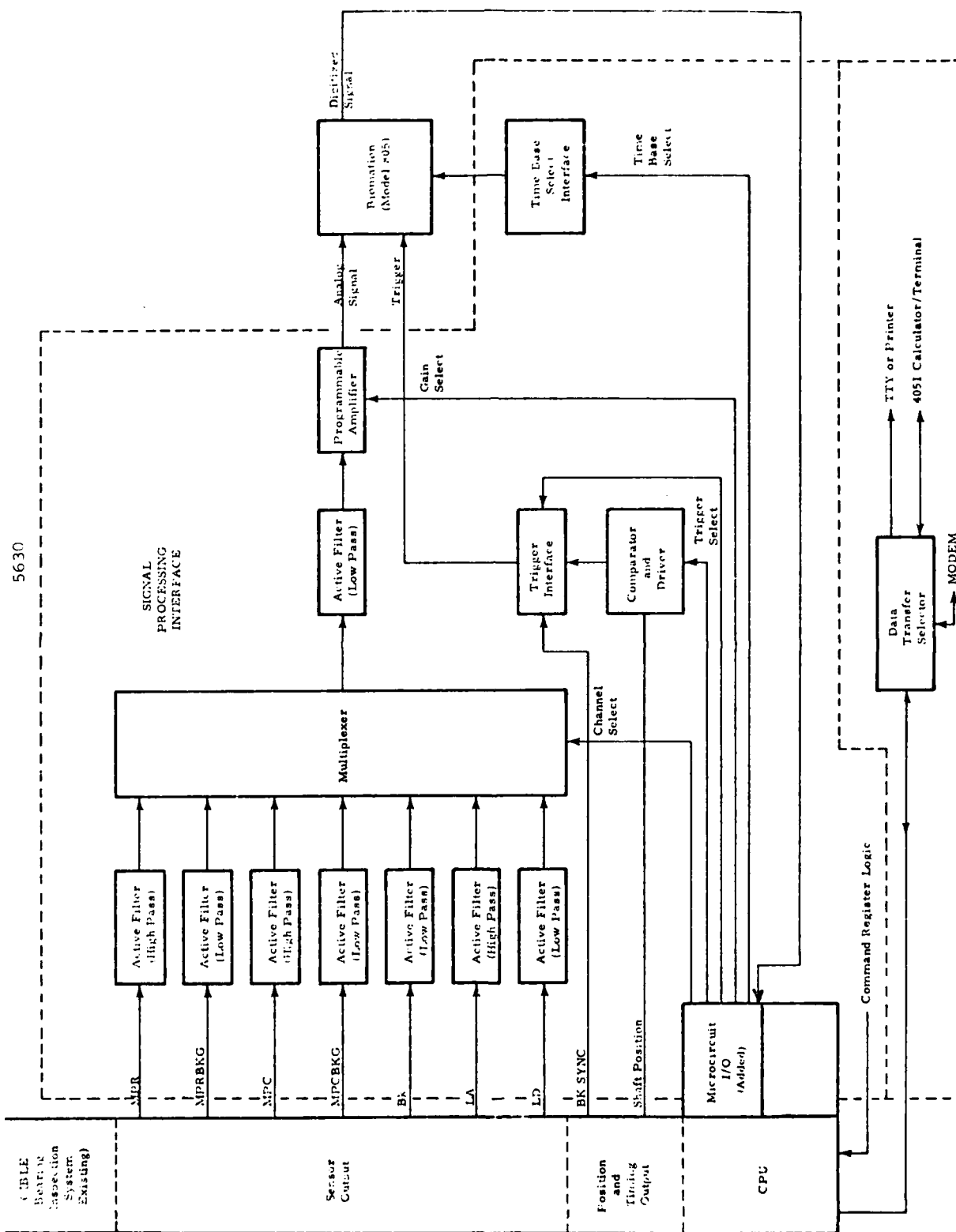


FIGURE B2. BLOCK DIAGRAM OF SIGNAL CONDITIONER

SIGNATURE PROCESSING, ANALYSIS, AND ASSESSMENT

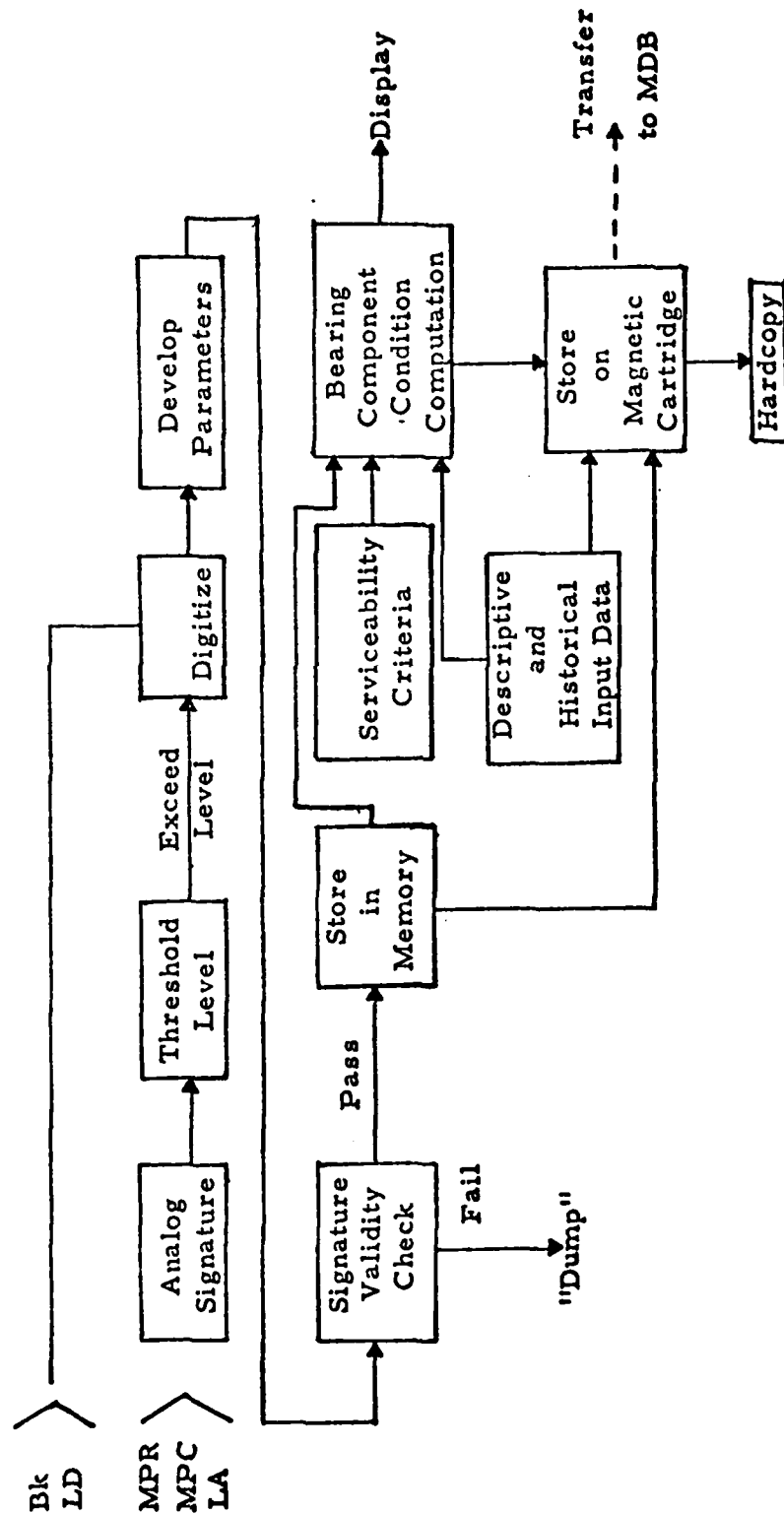
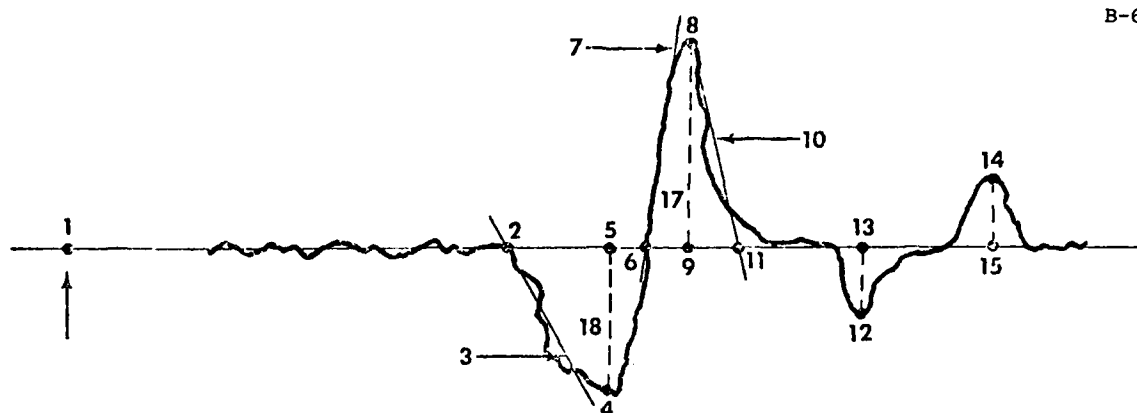


FIGURE B3. BLOCK DIAGRAM OF SIGNATURE PROCESSING, ANALYSIS, AND ASSESSMENT FUNCTIONS

such parameters are used in all subsequent data analyses and the values of such parameters are stored in the data base (the parameters by signature type are defined in Figures B4 through B7). In the case of some signatures, checks are made of certain parameters (signature validity check) and parameters for those signatures which pass are stored in memory for i) transfer to magnetic tape cartridge on the 4051 terminal/calculator and ii) for use in computations of bearing serviceability. The serviceability of the bearing component inspected is computed based upon the values of certain parameters (see the serviceability criteria presented in Figure B8 and reference Figure 29 of this report). The criteria items under which a bearing component is rejected are displayed on the CRT of the 4051 and are also stored on the magnetic tape cartridge for transfer to the Master Data Base (MDB) file. The structure of the files in the MDB is shown in Figure B9.

The threshold level for the analog signatures shown in Figure B3 used as a basis to select the signatures to be digitized is adjustable in the hardware but is not under computer control. The Master Supervisory Program (MSP) contains the routine for developing the values of signature parameters defined in Figures B4 through B7 and the serviceability criteria item values; accordingly, changes in the software routines can be made to perform other analyses and the criteria item values may be changed in the MSP. Currently, the criteria item values programmed into the MSP for balls and rollers are the same values as those used for race components; the race values were used for rolling elements since experience to date in the inspection of rolling elements has not been adequate to develop an independent set of values for the criteria items. For details of actual system operation, the reader is referred to the Operating Manual⁽³⁴⁾.



Data Base Flaw Parameter Identification

4445a

(Pos. Area)
(Neg. Area)
(Symmetry)
(pk-pk amp.)

| Each Flaw | | | Each Track | | |
|-----------|--------------|-------|------------|-----------|-------|
| No. | Name | Alias | No. | Name | Alias |
| 1 | MC CAP. LOC | CO | MC | UNDEFINED | |
| 2 | MC REF. FAC | C1 | MC | | |
| 3 | MC SLP1 | C2 | MC | | |
| 4 | MC EXTR1 AMP | C3 | MC | | |
| 5 | MC EXTR1 LOC | C4 | MC | | |
| 6 | MC SLP2 | C5 | | | |
| 7 | MC ZERO1 LOC | C6 | | | |
| 8 | MC EXTR2 AMP | C7 | | | |
| 9 | MC EXTR2 LOC | C8 | | | |
| 10 | MC SLP3 | C9 | | | |
| 11 | MC SLP3 LOC | CA | | | |
| 12 | MC EXTR3 AMP | CB | | | |
| 13 | MC EXTR3 LOC | CC | | | |
| 14 | MC EXTR4 AMP | CD | | | |
| 15 | MC EXTR4 LOC | CE | | | |
| 16 | MC PEAK SEP | CF | | | |
| 17 | MC SHP FACA | CG | | | |
| 18 | MC SHP FACB | CH | | | |
| 19 | MC SHP FACC | CI | | | |
| 20 | MC SHP FAC1 | CJ | | | |
| | MC SHP FAC2 | | | | |
| | MC SHP FAC3 | | | | |

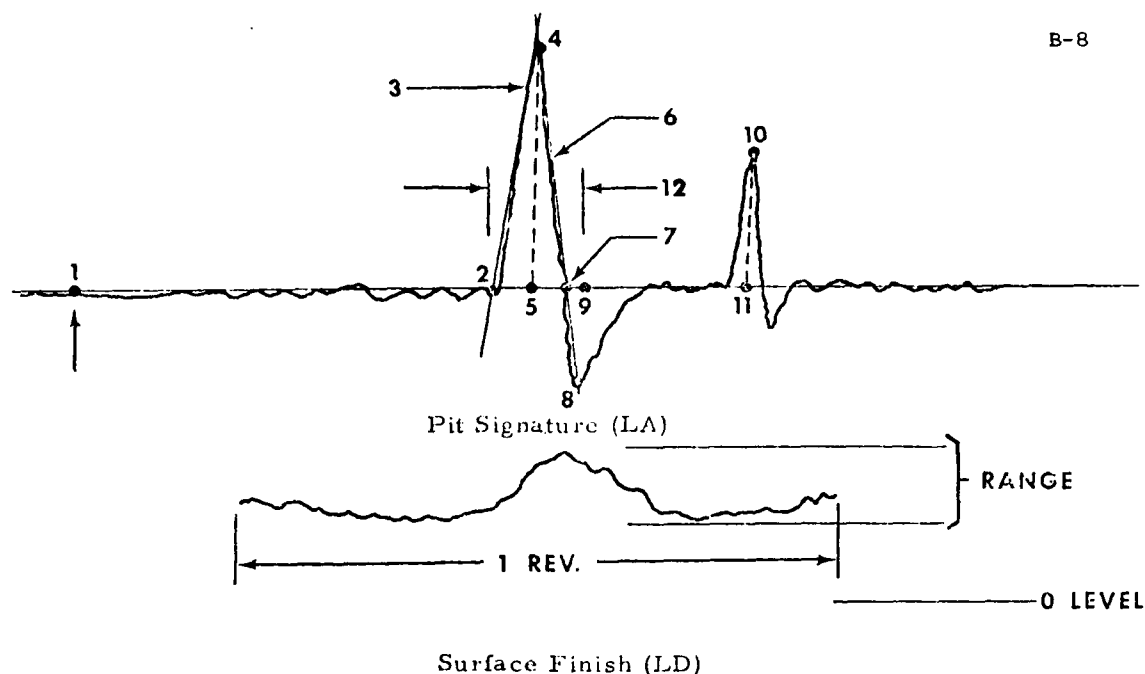
| Each Component | | |
|----------------|-----------|----|
| MC | AVG. MEAN | CV |
| MC | AVG. STDV | CS |
| MC | RANGE | CR |
| MC | CMP. FACA | |
| MC | CMP. FACB | |
| MC | CMP. FAC1 | |
| MC | CMP. FAC2 | |

FIGURE B4. MAGNETIC PERTURBATION CIRCUMFERENTIAL-FLUX-DETECTED FLAW SIGNATURE PARAMETER DEFINITIONS

44466

(Pos. Area)
(Neg. Area)
(Symmetry)

FIGURE B5. MAGNETIC PERTURBATION RADIAL-FLUX-DETECTED
FLAW SIGNATURE PARAMETER

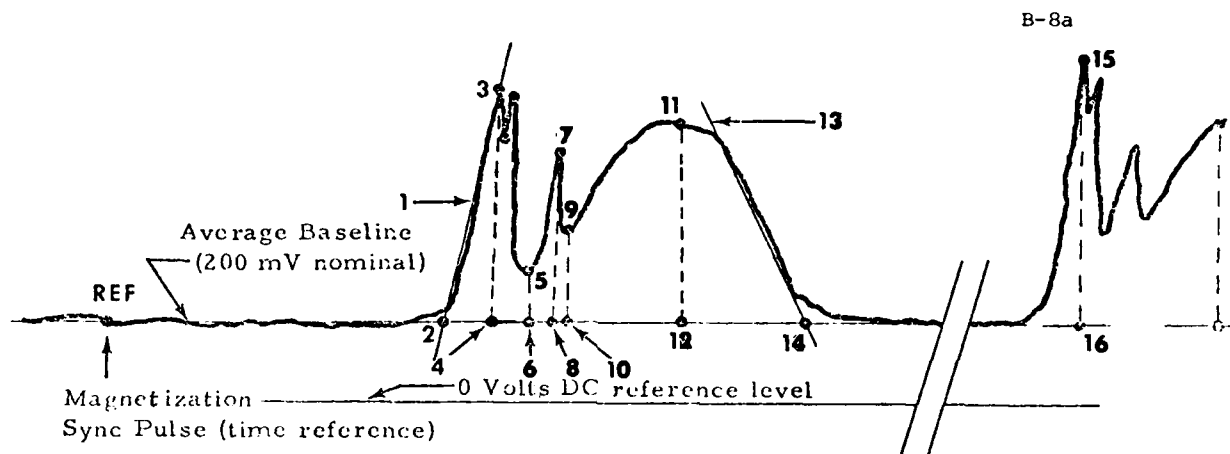


Data Base Flaw Parameter Identification

4447a

| Each Flaw | | | Each Track | | |
|------------------|--------------|-------|----------------|-----------|-------|
| No. | Name | Alias | No. | Name | Alias |
| 1 | LA CAP. LOC | L0 | LD | UNDEFINED | |
| 2 | LA REF. FAC | L1 | LD | | |
| 3 | LA SLP1 | L2 | LD | | |
| 4 | LA EXTR1 AMP | L3 | LD | | |
| 5 | LA EXTR1 LOC | L4 | LD | | |
| 6 | LA SLP2 | L5 | | | |
| 7 | LA SLP2 LOC | L6 | | | |
| 8 | LA EXTR2 AMP | L7 | | | |
| 9 | LA EXTR2 LOC | L8 | | | |
| 10 | LA EXTR3 AMP | L9 | | | |
| 11 | LA EXTR3 LOC | LA | | | |
| (Pulse Width) 12 | LA SHP FACA | LB | | | |
| | LA SHP FACB | | | | |
| | LA SHP FACC | | | | |
| | LA SHP FAC1 | | | | |
| | LA SHP FAC2 | | | | |
| | LA SHP FAC3 | | | | |
| | | | Each Component | | |
| | | | LD AVG. MEAN | | LV |
| | | | LD AVG. STDV | | LS |
| | | | LD RANGE | | LR |
| | | | LD CMP. FACA | | |
| | | | LD CMP. FACB | | |
| | | | LD CMP. FAC1 | | |
| | | | LD CMP. FAC2 | | |

FIGURE B6. LASER SCATTERED LIGHT SIGNATURE
PARAMETER DEFINITIONS



Data Base Signature Parameter Identification

Each Flaw

Each Signature

| No. | Name | Alias | No. | Name | Alias |
|-----|--------------|-------|-----|-------------|-------|
| 1 | BK SLP1 | B0 | 17 | BK SHP FACA | BG |
| 2 | BK SLP1 LOC | B1 | 18 | BK SHP FACB | BH |
| 3 | BK EXTR1 AMP | B2 | | BK SHP FACC | |
| 4 | BK EXTR1 LOC | B3 | | BK SHP FAC1 | |
| 5 | BK EXTR2 AMP | B4 | | BK SHP FAC2 | |
| 6 | BK EXTR2 LOC | B5 | | BK SHP FAC3 | |
| 7 | BK EXTR3 AMP | B6 | | | |
| 8 | BK EXTR3 LOC | B7 | | | |
| 9 | BK EXTR4 AMP | B8 | | | |
| 10 | BK EXTR4 LOC | B9 | | | |
| 11 | BK EXTR5 AMP | BA | | | |
| 12 | BK EXTR5 LOC | BB | | | |
| 13 | BK SLP2 | BC | | | |
| 14 | BK SLP2 LOC | BD | | | |
| 15 | BK EXTR6 AMP | BE | | | |
| 16 | BK EXTR6 LOC | BF | | | |

(Pos. Area, Int.)
(Baseline Avg.)

FIGURE B7. BARKHAUSEN DETECTED NOISE SIGNATURE
PARAMETER DEFINITIONS

FIGURE B8. SERVICEABILITY CRITERIA (PRELIMINARY), RACES AND ROLLING ELEMENTS

| <u>Item*</u> | *Check that CH, variable 20 is $\geq 80\text{mv}+$ and CL, variable 20 is $\geq 40\text{ mV}+$ before applying criteria. |
|------------------|---|
| A | Reject all with CL peak-to-peak amplitude $\geq 100\text{ mV}+$ |
| B | Reject all CH with CH/CL ratio $< 2.0, \geq 0$ |
| C | Reject all CH with peak-to-peak amplitude $\geq 200\text{ mV}+$ and peak separation $< 150\mu$ |
| D | Reject all CH with peak-to-peak amplitude $\geq 200\text{ mV}+$ and RH peak amplitude $\geq 600\text{ mV}+$ |
| E { Races Only } | Reject if CH $\geq 200\text{ mV}+$ for BR XXXX $\pm (0050)$ for 3 or more ST |
| F | Reject all RH with peak amplitude $\geq 1000\text{ mV}+$ |
| G | If flaw buffer overloads |
| H | BK reject, if SLP1 LOC $< \underline{\hspace{1cm}}$ ms, SLP1 $\geq \underline{\hspace{1cm}}$ and EXTR1 $\geq \text{AMP } \underline{\hspace{1cm}}$ mV See Listing by bearing type. |
| I | Reject, if laser EXTR1 $\geq 3900\text{ mV}+$ |
| J | LD If Mean $\geq \underline{\hspace{1cm}}$ See Listing by bearing type. |

IF REJECTED GIVE ITEM(S)

+ Absolute magnitudes

FIGURE B8 (Con't.)

ITEM H LISTING (races)

| <u>Brg. Code</u> | <u>Brg. Type</u> | |
|------------------|------------------|---|
| 10 | J57-#2 | S1L* \leq 560 ms S1 $>$ 50 (5 mV/ms) E1 \geq 100 mV |
| 11 | J57-#4 | S1L \leq 560 ms S1 $>$ 50 (5 mV/ms) E1 \geq 100 mV |
| 12 | J79-#2 | S1L \leq 560 ms S1 $>$ 50 (5 mV/ms) E1 \geq 100 mV |
| 13 | J85-#2 | S1L \leq 600 ms Inner 560 ms outer S1 $>$ 50 (5 mV/ms) E1 \geq 50 mV Inner 100 mV outer |
| 14 | J57-#6 | S1L \leq 560 ms S1 $>$ 50 (5 mV/ms) E1 \geq 100 mV |
| 15 | J57-#4 1/2 | S1L \leq 560 ms S1 $>$ 50 (5 mV/ms) E1 \geq 50 mV |
| 16 | J57-#3 | S1L \leq 560 ms S1 $>$ 50 (5 mV/ms) E1 \geq 100 mV |

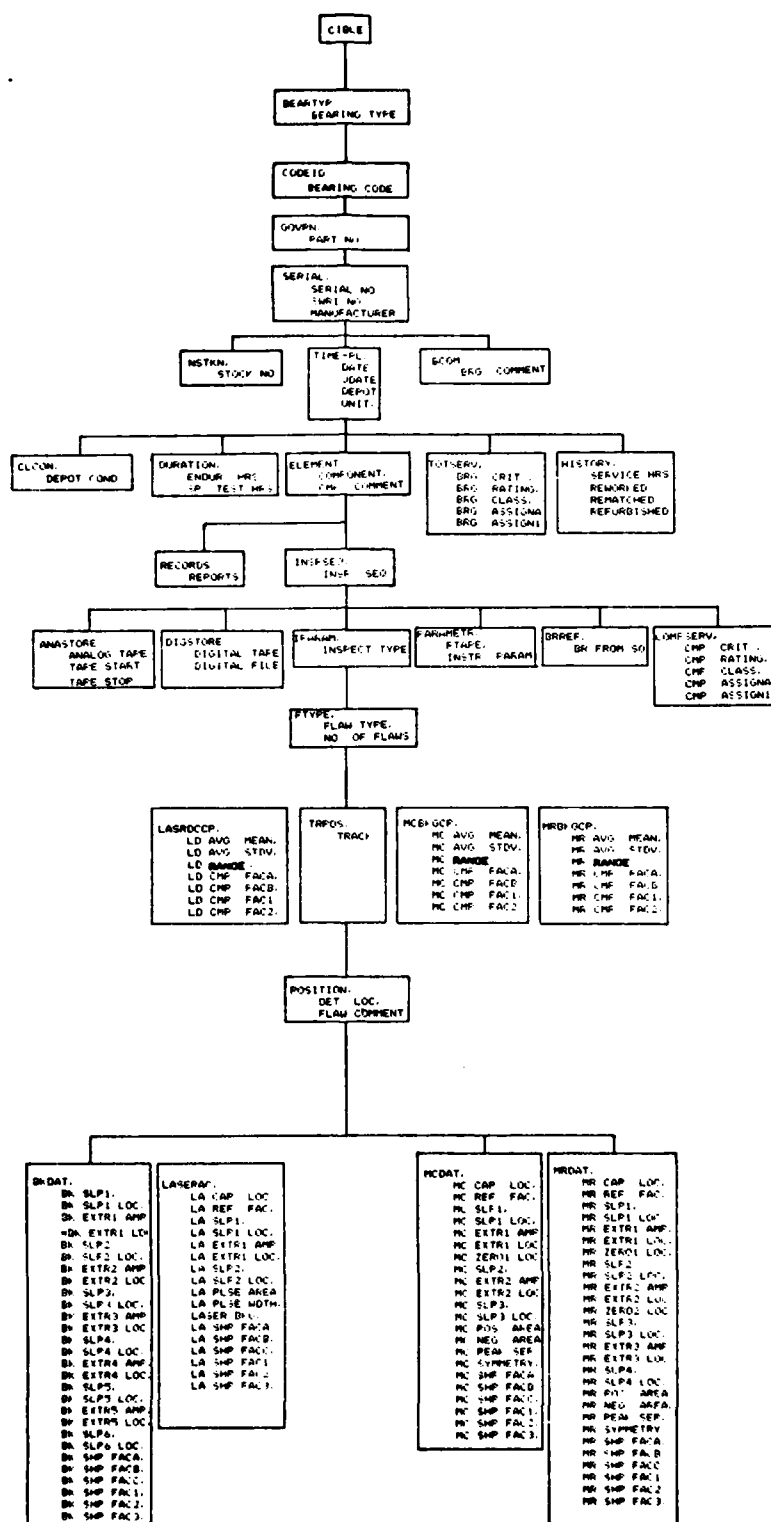
*Notes: S1L = SLP1 LOC
 S1 = SLP1
 E1 = EXTR 1 AMP

FIGURE B8 (Con't.)

ITEM J LISTING (races)

| <u>Brg. Code</u> | <u>Brg. Type</u> | | |
|------------------|------------------|---------|-------|
| 10 | J57-#2 | 720 mV | Inner |
| | | 720 mV | Outer |
| 11 | J57-#4 | 720 mV | Inner |
| | | 720 mV | Outer |
| 12 | J79-#2 | 720 mV | Inner |
| | | 720 mV | Outer |
| 13 | J85-#2 | 1000 mV | Inner |
| | | 1000 mV | Outer |
| 14 | J57-#6 | 720 mV | Inner |
| | | 720 mV | Outer |
| 15 | J57-#4 1/2 | 720 mV | Inner |
| | | 720 mV | Outer |
| 16 | J57-#3 | 720 mV | Inner |
| | | 720 mV | Outer |

Determine level by noting LD levels from several typical bearing components and doubling the average value if inner and outer races nearly the same. If inner and outer race average values not similar compute rejection levels independently. Adjust level as required with experience.



APPENDIX C

SUMMARY REPORT ON
CIBLE BALL INSPECTION

CIBLE
BALL INSPECTION

Summary Report
for
Warner Robins ALC/MMIRDA

Contract No. F09650-74-C-5158

March 1979

TABLE OF CONTENTS

| | <u>Page</u> |
|---|-------------|
| LIST OF ILLUSTRATIONS | iii |
| I. INTRODUCTION | 1 |
| II. INSPECTION PROCEDURE | 2 |
| III. INSPECTION RESULTS | 3 |
| A. General | 3 |
| B. Typical Signatures and Corresponding Flaws | 4 |

LIST OF ILLUSTRATIONS

| <u>Figure</u> | | <u>Page</u> |
|---------------|---|-------------|
| 1 | CIBLE Inspection Signatures and Corresponding Surface Photomicrograph showing Indent on Ball with 3230 hrs. Service, J57-#4 Bearing S/N P9117-1 (Ball #3) | 7 |
| 2 | CIBLE Inspection Signatures and Corresponding Surface Photomicrograph showing Dent on Ball with 3230 hrs. Service, J57-#4 Bearing S/N P9117-1 (Ball #9) | 8 |
| 3 | CIBLE Inspection Signatures and Surface Photomicrographs showing Corresponding Surface Flaws on Ball with 3230 hrs. Service, J57-#4 Bearing S/N 9117-2 (Ball #20, Defects 1 and 2) | 9 |
| 4 | CIBLE Inspection Signatures and Corresponding Surface Photomicrograph showing Gouges on Ball with 3230 hrs. Service, J57-#4 Bearing S/N P9117-2 (Ball #20, Defect #3) | 10 |
| 5 | CIBLE Inspection Signatures and Surface Photomicrographs showing Corresponding Flaws on Two Different Balls from J57-#4 Bearings | 11 |
| 6 | CIBLE Inspection Signatures and Corresponding Surface Photomicrograph showing Inclusion on Surface of New Ball from Vendor Reworked J57-#4 Bearing S/N 3453-2, 5940 hrs. (Ball #12, S11092) | 12 |
| 7 | CIBLE Inspection Signatures and Corresponding Surface Photomicrograph Showing Inclusion on Surface of New Ball from Vendor Reworked J57 J57-#4 Bearing S/N 3453-2, 5940 hrs. (Ball #13, S11092) | 13 |

LIST OF ILLUSTRATIONS

| <u>Figure</u> | | <u>Page</u> |
|---------------|--|-------------|
| 8 | CIBLE Inspection Signatures and Corresponding Surface Photomicrographs Showing Pitted Region on New Ball from Vendor Reworked J57-#4 Bearing S/N 3083-2, 4769 hrs. (Ball #7) | 14 |
| 9 | CIBLE Inspection Signatures and Corresponding Surface Photomicrographs Showing Pitted Region on New Ball from Vendor Reworked J57-#4 Bearing S/N 395-2, 4362 hrs. (Ball #20, S11672) | 15 |
| 10 | CIBLE Inspection Signatures and Corresponding Surface Photomicrograph Showing Anomaly on New Ball from Vendor Reworked J57-#4 Bearing S/N 9191-1, 1500 hrs. (Ball #4, S11911) | 16 |
| 11 | CIBLE Inspection Signatures and Corresponding Surface Photomicrograph Showing Gouge on New Ball from Vendor Reworked J57-#4 Bearing S/N 9293-1, 6651 hrs. (Ball #4, S11931) | 17 |
| 12 | CIBLE Inspection Signatures and Corresponding Surface Photomicrographs Showing Pits and Cracks on New Ball from Vendor Reworked J57-#4 Bearing S/N 395-2, 4362 hrs. (Ball #11, S11672) | 18 |
| 13 | CIBLE Inspection Signatures and Corresponding Surface Photomicrographs Showing Crack Network on New Ball from Vendor Reworked J57-#4 Bearing S/N 395-2, 4362 hrs. (Ball #3, S11672) | 19 |
| 14 | Typical Barkhausen Signatures from J57-#4 Main Shaft Bearing Balls | 20 |
| 15 | Barkhausen Signatures for Four Balls from J57-#4 Vendor Reworked Bearing S/N 395-2 (S11672), 4362 hrs. | 21 |

I. INTRODUCTION

Inspection of 1000 balls from J57-#4 main shaft engine bearings was undertaken and completed over the period 22 May 1978 through 16 August 1978. The balls inspected were supplied by the bearing shop at OCALC; balls were removed from the retainers of each bearing and stored as rolling element sets for inspection. The ball inspection was conducted by Mr. Don Heihn, SwRI, on the Ball/Roller Unit of the Air Force CIBLE Bearing Inspection System previously delivered under Contract F09650-74-C-0200.

A breakdown of the lot of balls inspected according to bearing condition and ball condition is given in Table I below.

TABLE I

| <u>Quantity of Balls</u> | <u>Bearing Condition</u> | <u>Ball Condition</u> |
|------------------------------|------------------------------|---------------------------|
| 200 | Serviceable* | Serviceable* |
| 800 | Vendor Reworked | New |

*The term serviceable refers to a bearing which has been removed from an engine at overhaul and processed through the OCALC bearing shop and accepted as serviceable without being vendor reworked. Vendor reworked bearings are, of course, also serviceable but have been processed through vendor facilities and a complement of new balls installed in each bearing.

Further details relating to specific balls will be related in the discussion of inspection results which follows a brief description of the inspection procedure.

II. INSPECTION PROCEDURE

As previously mentioned, balls to be inspected were removed from their retainers and maintained in sets according to individual bearing serial number. Sets of balls anticipated to be inspected at the start of an inspection day were cleaned to remove the protective oil film. Near the end of the day balls were recoated with a light film of oil. All balls were initially inspected in the automatic mode; magnetic perturbation circumferential and radial flux signatures were monitored on the oscilloscope during this auto-inspection. Those balls having printouts with outstanding signals were individually noted with appropriate comments on inspection "run" forms and retained according to an arbitrarily assigned, unique ball number for special data acquisition. Several balls were also selected at random to characterize magnetic perturbation background. Special data acquisition on the selected balls was conducted in the computer-assisted manual mode via an auto mode re-inspection.

In the manual mode, the physical location on the ball of outstanding signatures of interest was marked using the following procedure:

- 1) During re-inspection in the auto mode for a particular ball orientation, the probe scan track location and azimuthal printout locations were noted for subsequent evaluation in the manual mode.

- 2) Subsequently, the laser was indexed to the magnetic perturbation scan track of interest so that the incident laser beam projected a spot of light corresponding to the magnetic perturbation scan track of interest, rotation of the spindle disabled, and the spindle manually rotated until the shaft reference digital display readout corresponded with the printed out azimuthal location.

- 3) The incident laser light spot was then encircled on the ball using a marking pen, thereby providing an approximate physical location on the ball corresponding with the magnetic perturbation signature of interest for later visual examination under optical magnification.

Subsequent to the completion of ball inspection including special data acquisition and signature location marking at OCALC, 64 selected balls were returned to SwRI, 41 of these balls had marked regions for microscopic examination and surface photomicrography. The following section summarizes the automatic inspection printout results and typical inspection signatures including surface photomicrographs of selected regions of interest.

III. INSPECTION RESULTS

A. General

Table II below summarizes the printout from the initial automatic inspection of the 1000 balls according to two categories: (1) service balls (those balls from bearings with accumulated service time which have not been vendor reworked) and (2) the new balls from vendor reworked bearings.

TABLE II

| Ball Condition | % with MPR* Printouts | % with MPC* Printouts |
|----------------|--------------------------|--------------------------|
| Serviceable | 89 | 4 |
| New | 33 | 12 |

*MPR - magnetic perturbation, radial flux

MPC - magnetic perturbation, circumferential flux

Detection threshold is twice average magnetic background

Of special interest are the magnetic perturbation radial and circumferential flux printouts, since these indicate the probable presence of surface and near-surface flaws of interest. Note that the service balls (balls with service time) have almost three times the number of radial flux, high field (RH) printouts as that for new balls. Conversely, the new balls have three times the number of circumferential high field printouts as the balls with service time. The ball sample selected for a more detailed study is summarized in Table III below.

TABLE III

| Data Category | Serviceable | New |
|------------------------------------|-------------|-----|
| Special data with photomicrographs | 15 | 26 |
| Characterization | 6 | 17 |

Semiquantitative comments on the inspection data sheets indicate the following results regarding magnetic perturbation signature response; 43% of the service balls produced fair to large amplitude signatures while only 9% of the new balls produced similar sized signal amplitudes. Of the 200 service balls, approximately 85, therefore, had significant signatures based on these statistics; 15 of these (18% of this population) were examined. Similarly, 72 of the 800 new ball population were estimated to have significant signatures; 20 of these (28% of this population) have been investigated in detail. Approximately 8% of the new ball population was estimated to have unusual, "poor shape" magnetic perturbation signatures (broad, opposite polarity CH signatures with correspondingly broad RH signatures with essentially no accompanying RL signatures*) associated with them; 6 of this estimated population were examined in detail. No "service" balls were noted with such "poor shape" signatures. Typical results of the detailed investigation of selected balls including reproductions of signatures and surface photomicrographs are presented next.

B. Typical Signatures and Corresponding Flaws

Reproductions of signatures and surface photomicrographs typical of the inspection results obtained are presented in this section. Figure 1 presents typical magnetic perturbation, radial and circumferential, high and low field (RH, RL, CH, CL) signatures from a broad, shallow indent on a service ball (3,230 hours service). The outline of one edge of the long, broad, shallow indent is pointed out by the arrow in the surface photomicrograph E at the bottom of Figure 1. It is also pointed out that the general surface, fine-scale features shown in the photomicrograph are typical of the surface observed for service balls. Figure 2 shows an indentation in another service ball from the same bearing (S/N P9117-1). Note in this case that the radial signatures are significantly greater in amplitude and the circumferential signatures slightly greater in amplitude than that for the indent in Ball #3 (see Figure 1), indicating the indentation in Ball #9 (Figure 2) to be of greater depth. The radial signatures and corresponding photomicrographs in Figure 3 show typical results from a corrosion region and also from a large pit; accompanying circumferential signatures are low amplitude indicating the flaws to be shallow, probably less than 0.001 inch deep. The photomicrograph in Figure 4 illustrates gouges which may also be introduced as a result of service. In the case of Figure 4, note that the distance between the two gouges corresponds to the

*Typically, RL signature amplitudes are between 40% and 80% (approximately) of the RH signature amplitudes.

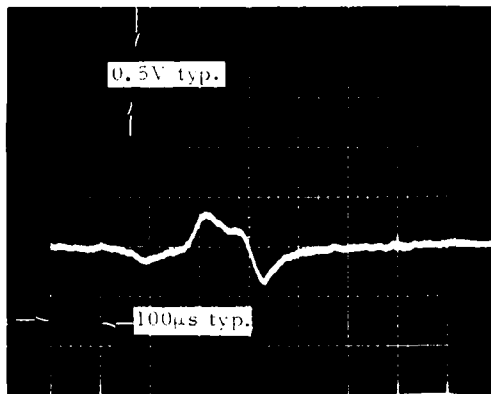
separation between the resulting radial signatures. These gouges have sufficient depth to produce small, circumferential signatures also (see Records C and D in Figure 4). Figure 5 shows pit and gouge type defects in two other service balls. Again, note the large radial signatures; the small circumferential, high field (CH) signature in the case of the gouge indicates that this flaw does not have significant depth.

Figure 6 illustrates the magnetic response obtained from a surface inclusion pit (see surface photomicrograph E). The surface finish surrounding the pit in Figure 6 is typical of that observed for the new balls examined from reworked bearings. A comparison of the surface finish in Figure 6 with that for the service ball in Figure 1 indicates that the multitude of fine, short and long scratch lines are typical of balls with service. The data in Figure 7 shows evidence of another inclusion pit with significant depth since a relatively large circumferential high field signature is obtained (see record C). Similarly, the data in Figure 8 shows a large group of pits from which two outstanding radial signatures are obtained; the smaller circumferential signature indicates these pits to be shallower in depth than the one previously shown in Figure 7. A significant group of pits in still another new ball is illustrated in Figure 9. Gouges in new balls are also evident as illustrated in Figures 10 and 11; very large radial signatures are evident in both cases.

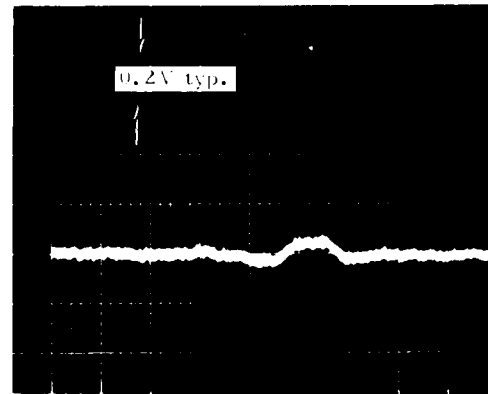
As might be anticipated, essentially no evidence of indentations were observed in the new balls visually examined. Startling evidence, however, was obtained showing large-scale cracking and material loss in two new balls from one bearing (S/N395-2) as illustrated in Figures 12 and 13. The radial and circumferential signatures presented in Figure 12 are typical of those previously described as unusual, "poor shape" signatures (note the broad, opposite polarity of the CH signature and the broad, complex-shaped RH signature with a small amplitude RL signature). Examination of many regions corresponding to "poor shape" signatures did not yield visual evidence at the surface of flaw conditions similar to that illustrated in the photomicrographs at the bottom of Figure 12. Note the even more significant material loss and extensive cracking evident in case of the flaw illustrated in Figure 13 and corresponding magnetic perturbation response (typical of that obtained from inclusions and gouges); the complex CH signature shape is attributed to the complex nature of the flaw. It is anticipated that the flaw illustrated in Figure 13 resulted from the heat treating process, possibly in combination with an extended inclusion(s). As will be shown next in this section, the Barkhausen signatures from this ball (Ball #3 in Bearing S/N 395-2) also exhibited unusual Barkhausen signatures.

Typical Barkhausen signature shapes obtained from service and new balls are illustrated in Figure 14. The Barkhausen signatures illustrated in Records C and D of Figure 14 are typical of those observed from service balls. The signatures illustrated in Records A and B of Figure 14 are dominantly typical for new balls, although, signatures Type C and D were also observed in the case of the new balls. Significantly, Figure 15 illustrates the Barkhausen signatures obtained from four new balls on Bearing S/N 395-2. Note the leading edge signature feature, as pointed out by the arrow in each case, which is not evident in any of the Barkhausen signatures previously illustrated in Figure 14. Furthermore, the signature shown in Record A of Figure 15 was obtained from the ball containing the extensive crack network, see Figure 13. From the data presented in Figures 12, 13, and 15 the entire ball complement for Bearing S/N 395-2 is questionable (in addition, the ball complement in the mating duplex Bearing S/N 395-1 is also suspect). It is possible that many other balls from the same lot of balls containing those in Bearing S/N 395-2 are also suspect, however, SwRI does not have adequate information for this type of traceability.

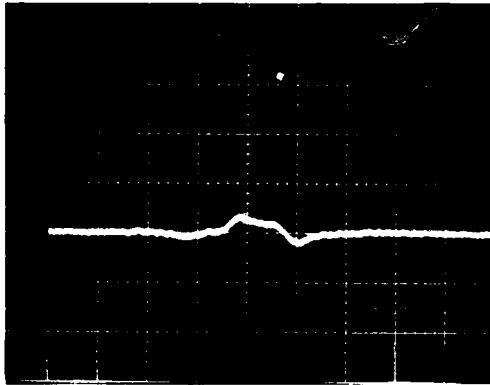
5164



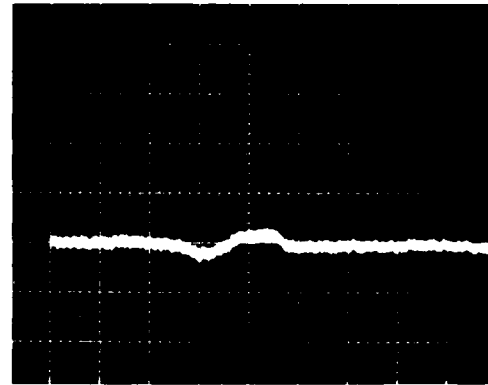
A. RH Signature



C. CH Signature



B. RL Signature



D. CL Signature

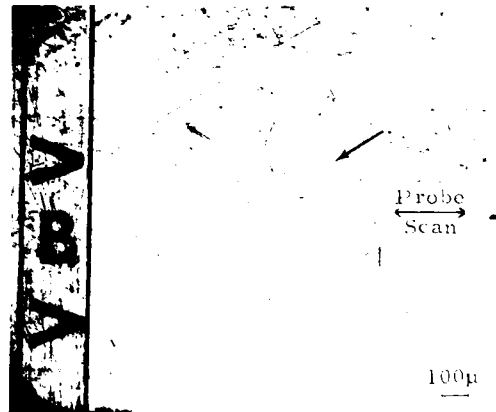
E. Surface Photomicrograph ($\sim 50\times$)

FIGURE 1. CIBLE INSPECTION SIGNATURES AND CORRESPONDING SURFACE PHOTOMICROGRAPH SHOWING INDENT ON BALL WITH 3230 HRS SERVICE, J57-#4 BEARING S/N P9117-1 (Ball #3).

AD-A088 765

SOUTHWEST RESEARCH INST SAN ANTONIO TEX

F/G 13/9

SPECIAL ENGINEERING SERVICES TO ESTABLISH INSPECTION CRITERIA F--ETC(U)

DEC 79 F N KUSENBERGER, J R BARTON

F09603-74-C-5158

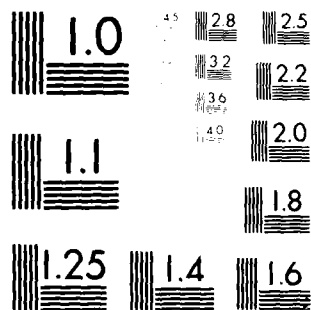
NL

UNCLASSIFIED

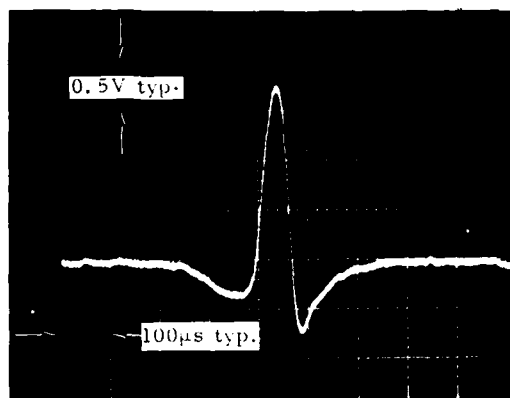
2 of 2

NO
AD-A088 765

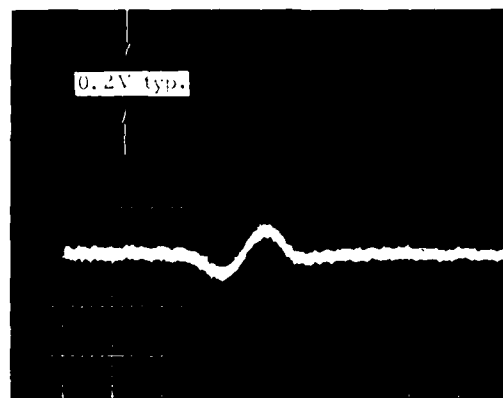




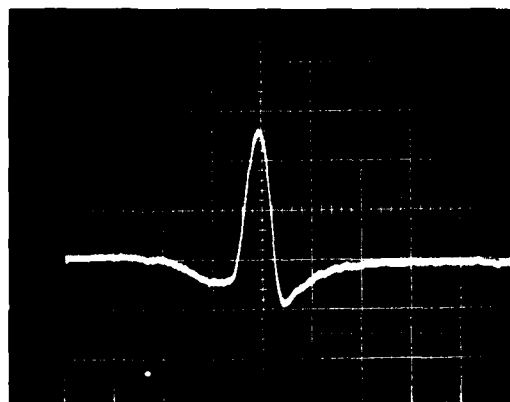
MICROCOPY RESOLUTION TEST CHART
NATIONAL BUREAU OF STANDARDS-1963-A



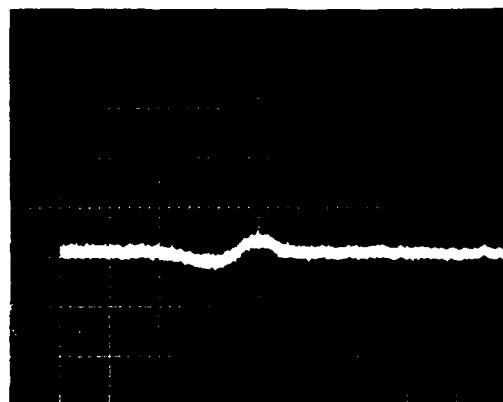
A. RH Signature



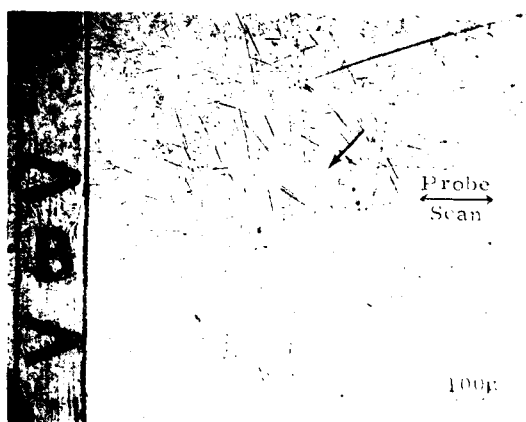
C. CH Signature (200μ peak separation)



B. RL Signature

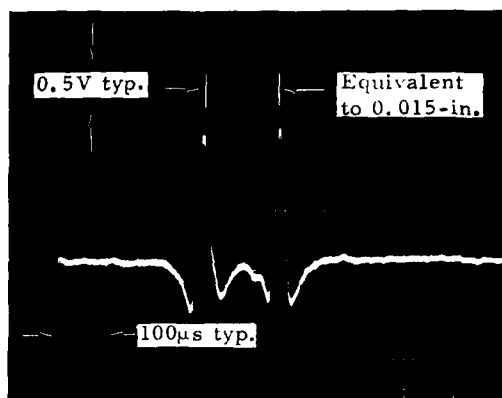


D. CL Signature

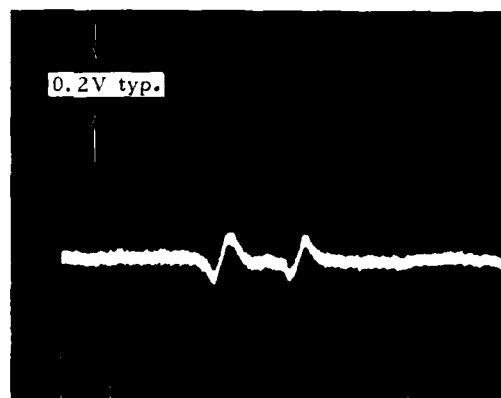


E. Surface Photomicrograph (50X)

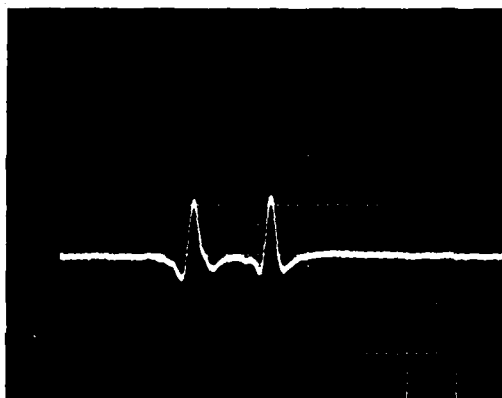
FIGURE 2. CIBLE INSPECTION SIGNATURES AND CORRESPONDING SURFACE PHOTOMICROGRAPH SHOWING DENT ON BALL WITH 3230 HRS SERVICE, J57-#4 BEARING S/N P9117-1 (Ball #9).



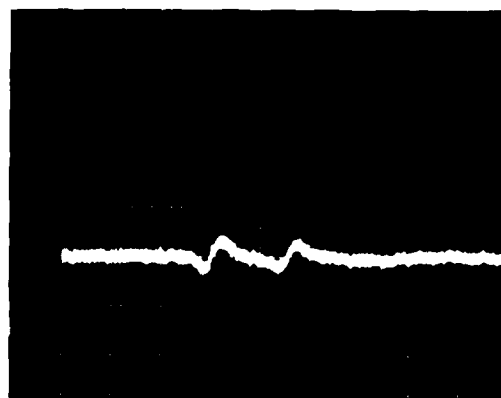
A. RH Signature



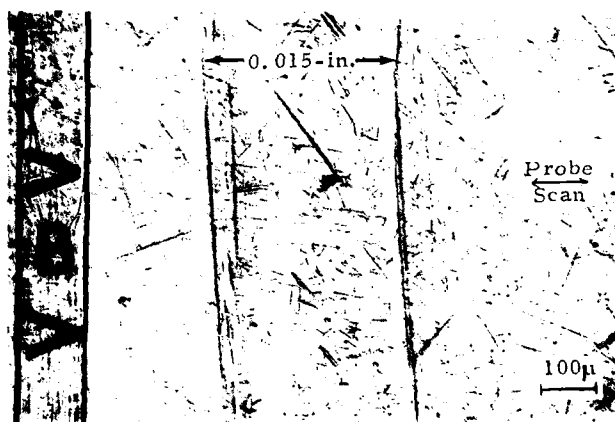
C. CH Signature (68μ peak separation, typ.)



B. RL Signature



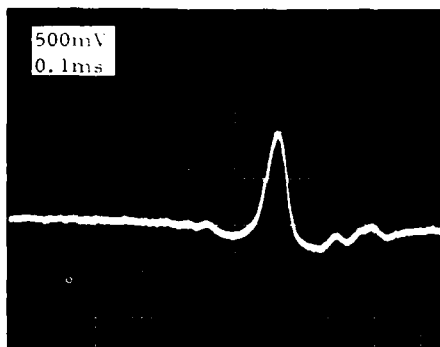
D. CL Signature



E. Surface Photomicrograph (~100X)

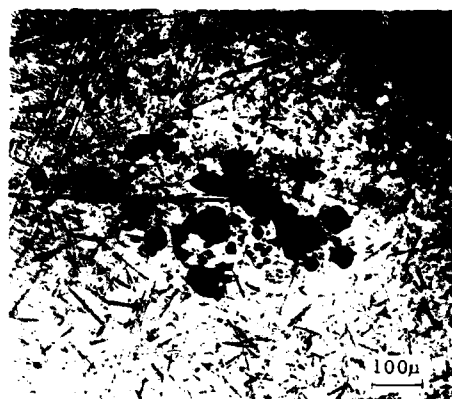
FIGURE 4. CIBLE INSPECTION SIGNATURES AND CORRESPONDING SURFACE PHOTOMICROGRAPH SHOWING GOUGES ON BALL WITH 3230 HRS SERVICE, J57-#4 BEARING S/N P9117-2 (Ball #20, Defect #3).

5161

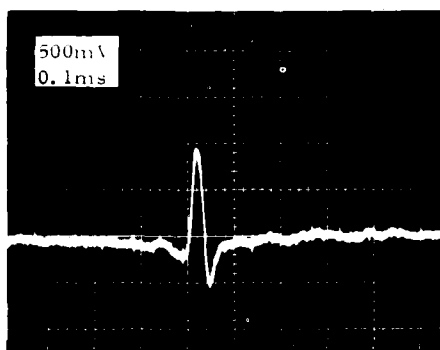


A. RH Signature

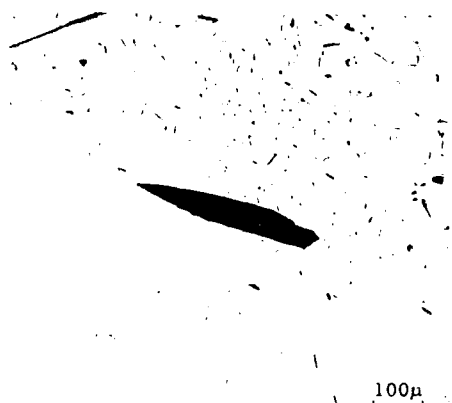
Ball, J57-#4 Bearing, S/N 476T-1, 3555 hrs. service (Ball #3, A00028F)



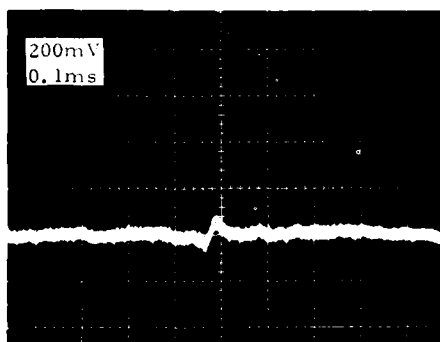
B. Surface Photomicrograph (~100X)



C. RH Signature



E. Surface Photomicrograph (~100X)



D. CH Signature

Ball, J57-#4 Bearing, S/N 9427-2, 1059 hrs. service (Ball #10, S11952)

5045

FIGURE 5. CIBLE INSPECTION SIGNATURES AND SURFACE PHOTOMICROGRAPHS SHOWING CORRESPONDING FLAWS ON TWO DIFFERENT BALLS FROM J57-#4 BEARINGS.

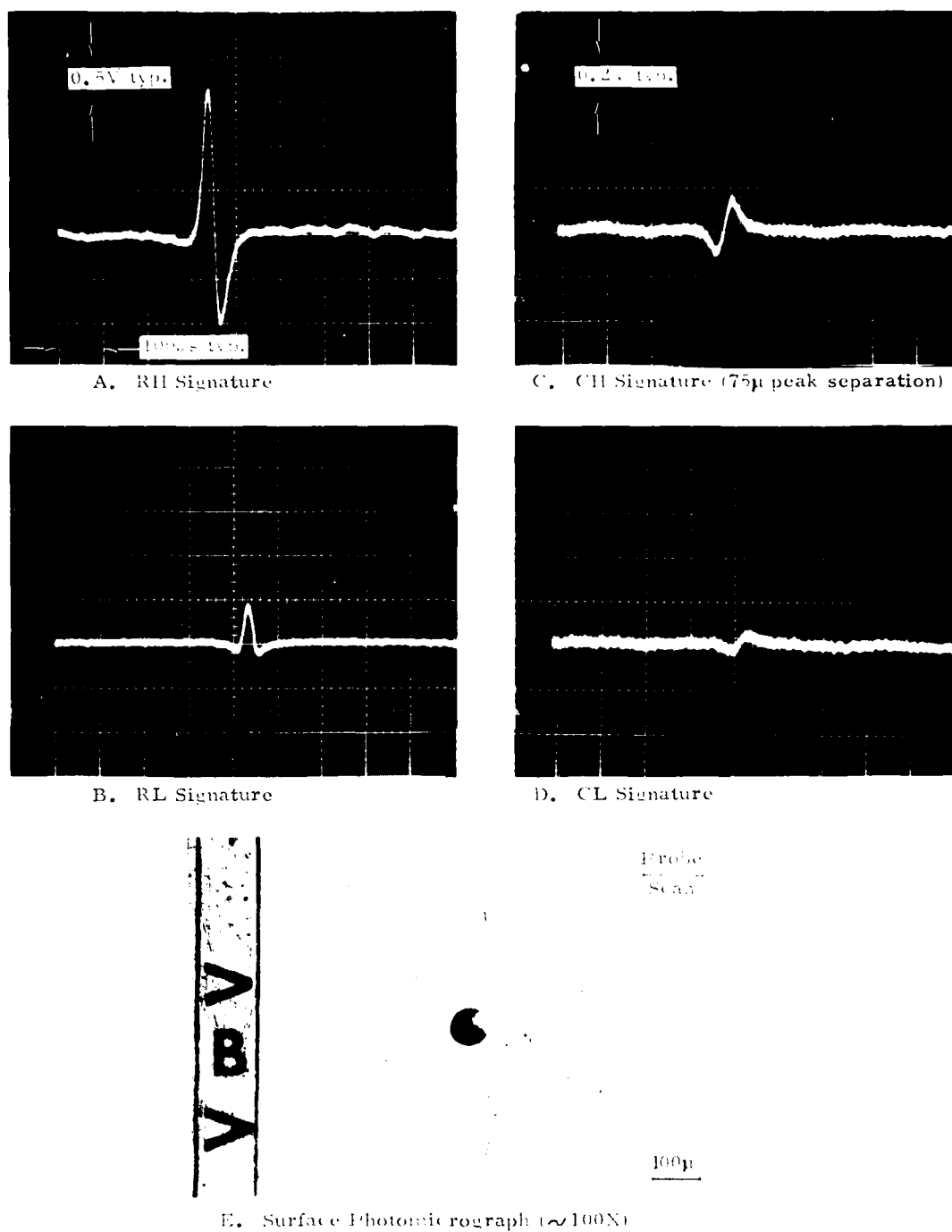


FIGURE 6. CIBLE INSPECTION SIGNATURES AND CORRESPONDING SURFACE PHOTOMICROGRAPH SHOWING INCLUSION ON SURFACE OF NEW BALL FROM VENDOR REWORKED J57-#4 BEARING S/N 3453-2, 5940 HRS (Ball #12, S11092).

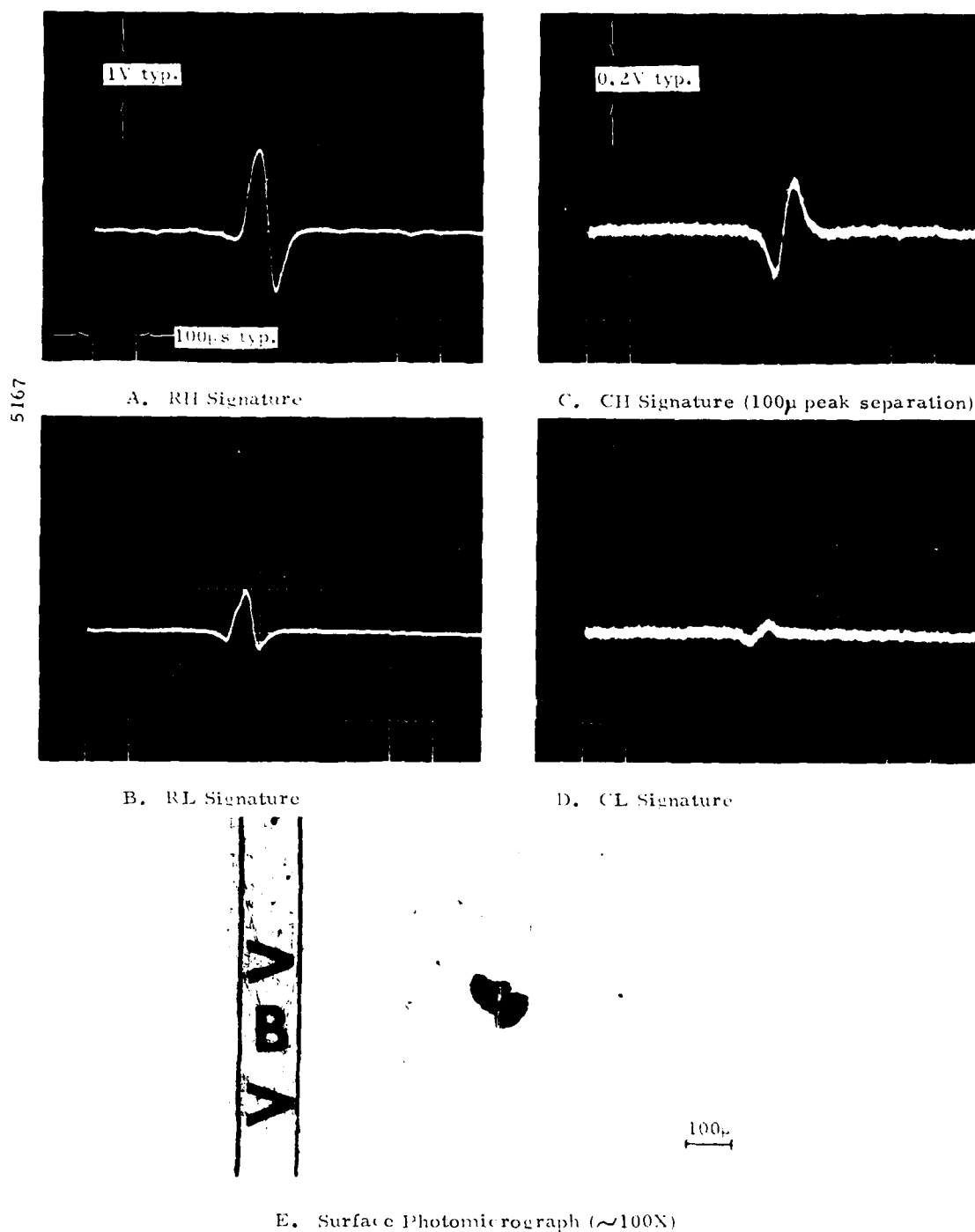


FIGURE 7. CIBLE INSPECTION SIGNATURES AND CORRESPONDING SURFACE PHOTOMICROGRAPH SHOWING INCLUSION ON SURFACE OF NEW BALL FROM VENDOR REWORKED J57-#4 BEARING S/N 3453-2, 5940 HRS (BALL #13, S11092).

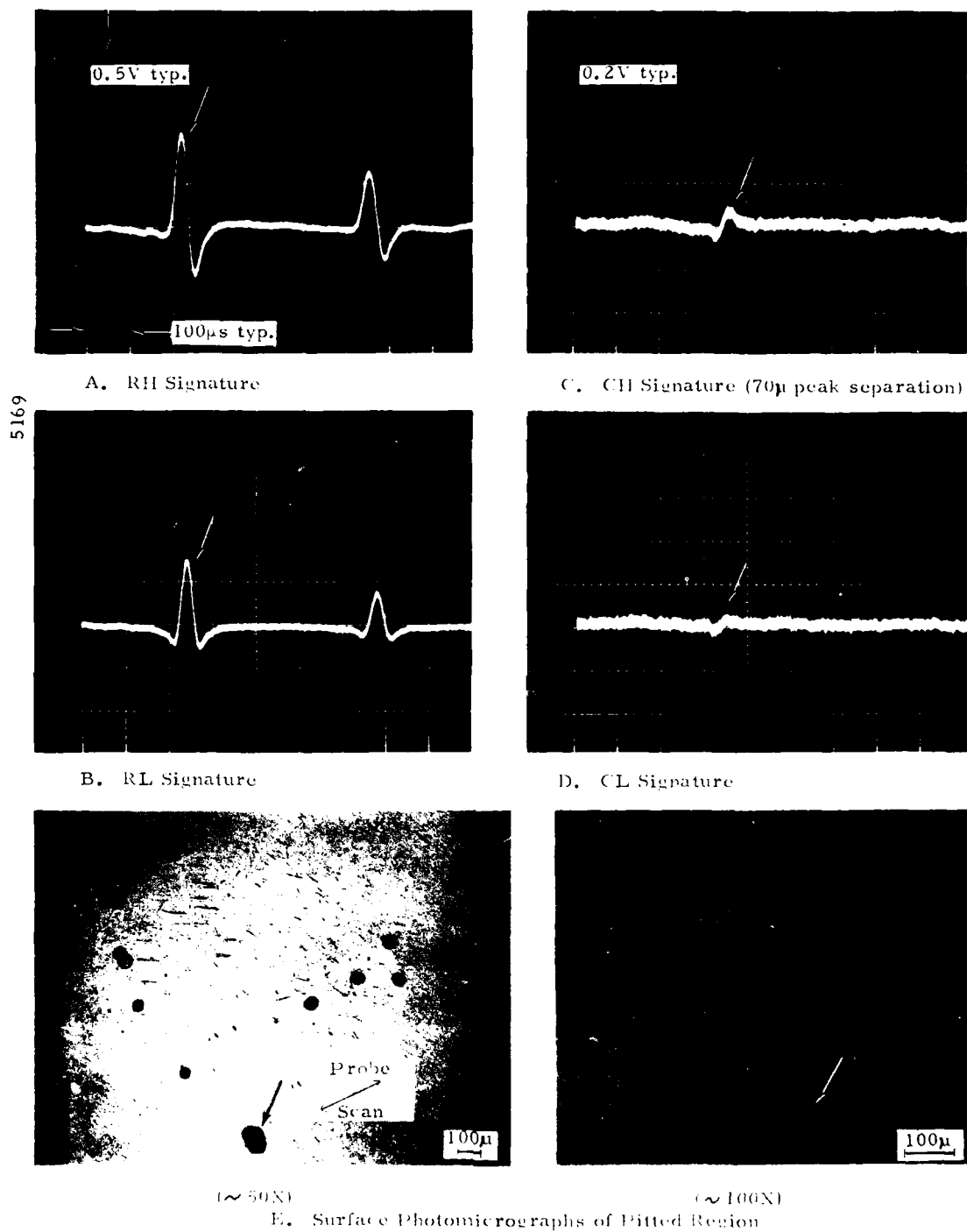


FIGURE 8. CIBLE INSPECTION SIGNATURES AND CORRESPONDING SURFACE PHOTOMICROGRAPHS SHOWING PITTED REGION ON NEW BALL FROM VENDOR REWORKED J57-#4 BEARING S/N 3083-2, 4769 HRS (Ball #7).

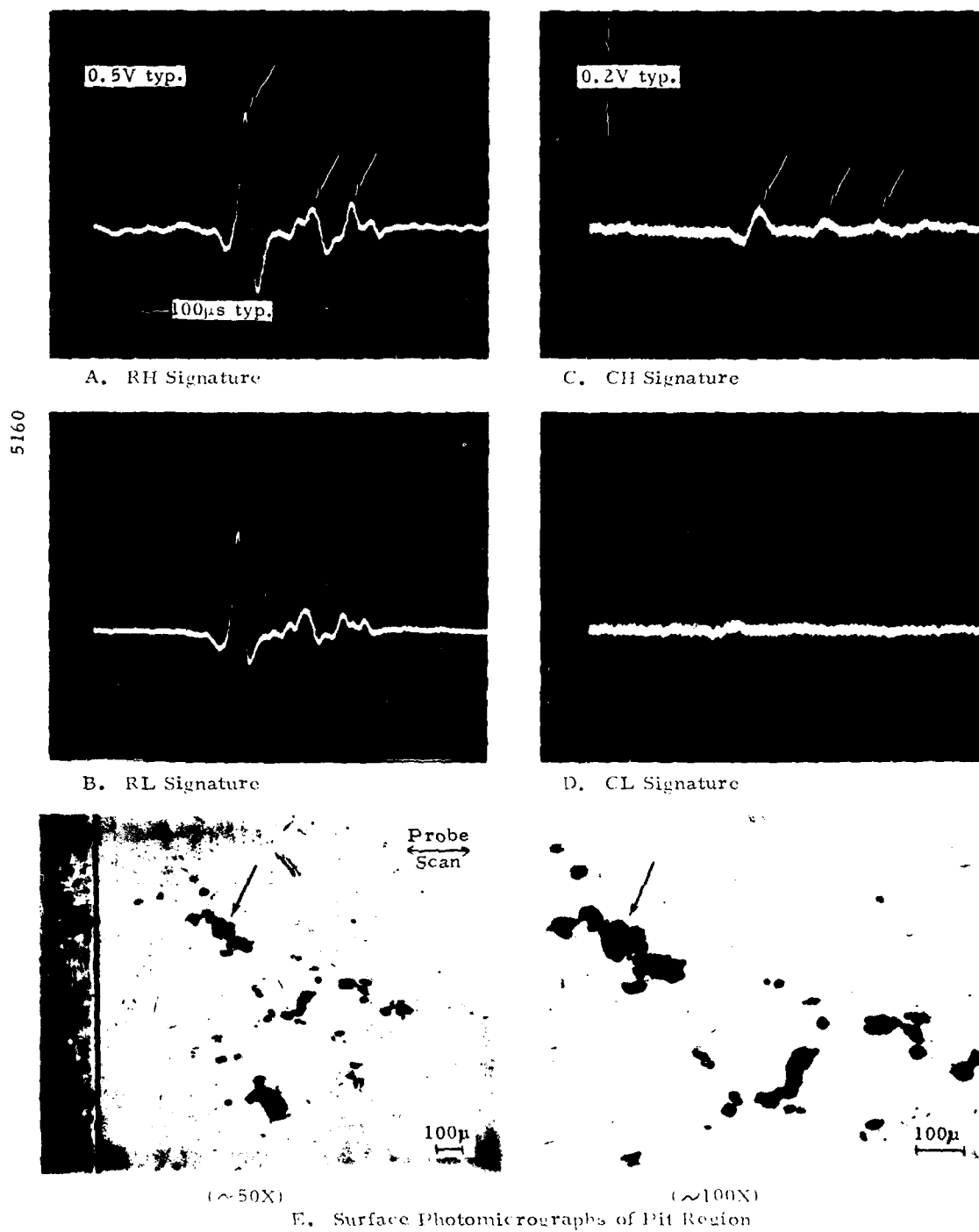
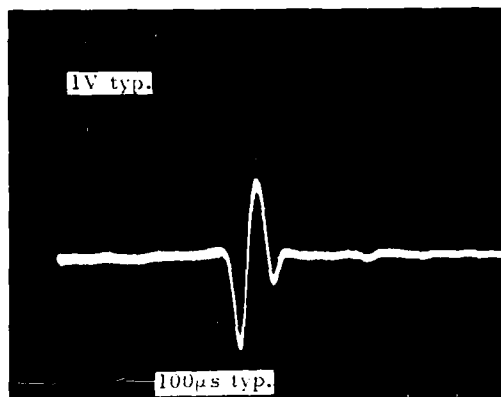
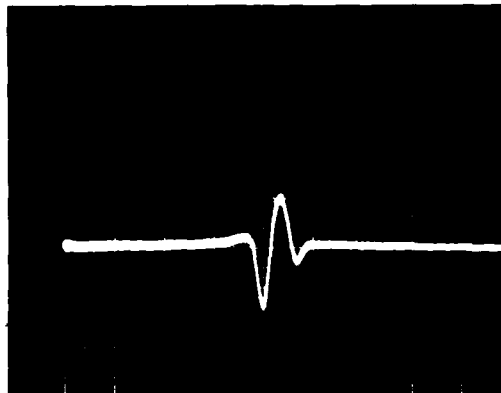


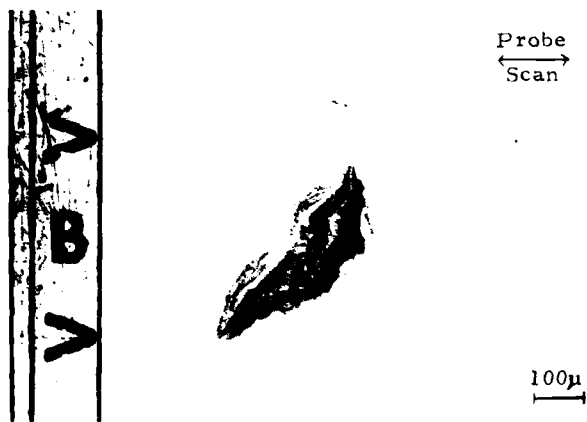
FIGURE 9. CIBLE INSPECTION SIGNATURES AND CORRESPONDING SURFACE PHOTOMICROGRAPHS SHOWING PITTED REGION ON NEW BALL FROM VENDOR REWORKED J57-#4 BEARING S/N 395-2, 4362 HRS (Ball #20, S11672).



A. RH Signature



B. RL Signature



C. Surface Photomicrograph (~100X)

FIGURE 10. CIBLE INSPECTION SIGNATURES AND CORRESPONDING SURFACE PHOTOMICROGRAPH SHOWING ANOMALY ON NEW BALL FROM VENDOR REWORKED J57-#4 BEARING S/N 9191-1, 1500 HRS (Ball #4, S11911).

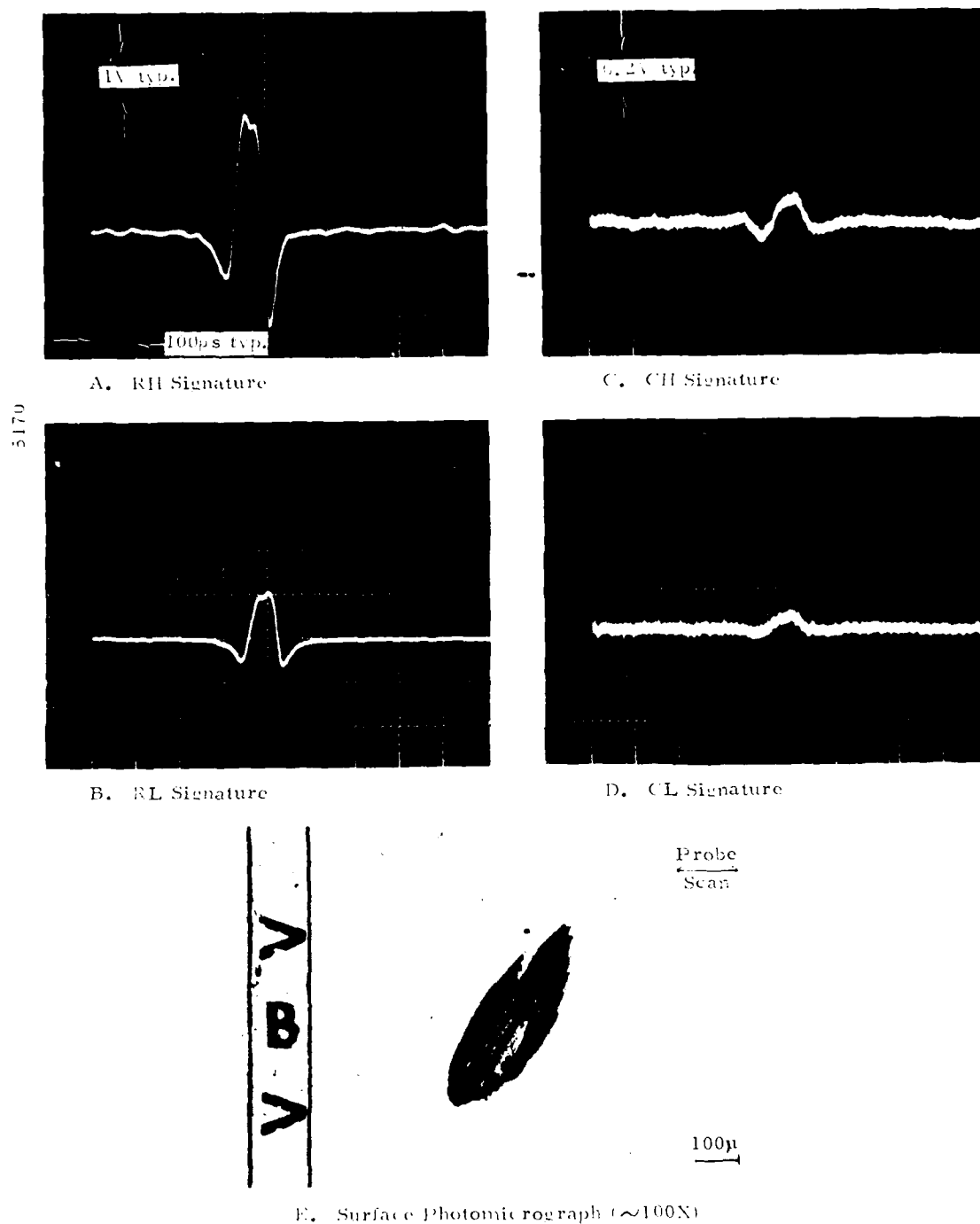
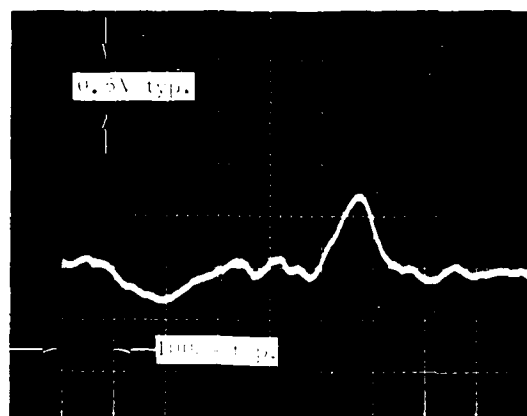


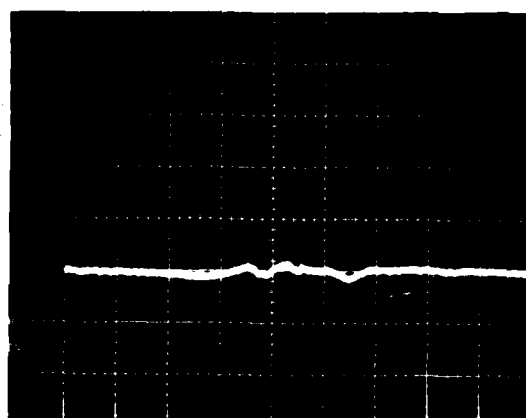
FIGURE 11. CIBLE INSPECTION SIGNATURES AND CORRESPONDING SURFACE PHOTOMICROGRAPH SHOWING GOUGE ON NEW BALL FROM VENDOR REWORKED J57-#4 BEARING S/N 9293-1, 6651 HRS (Ball #4, S11931).



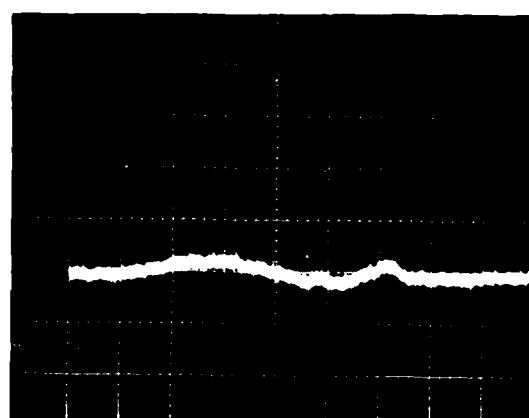
A. RH Signature



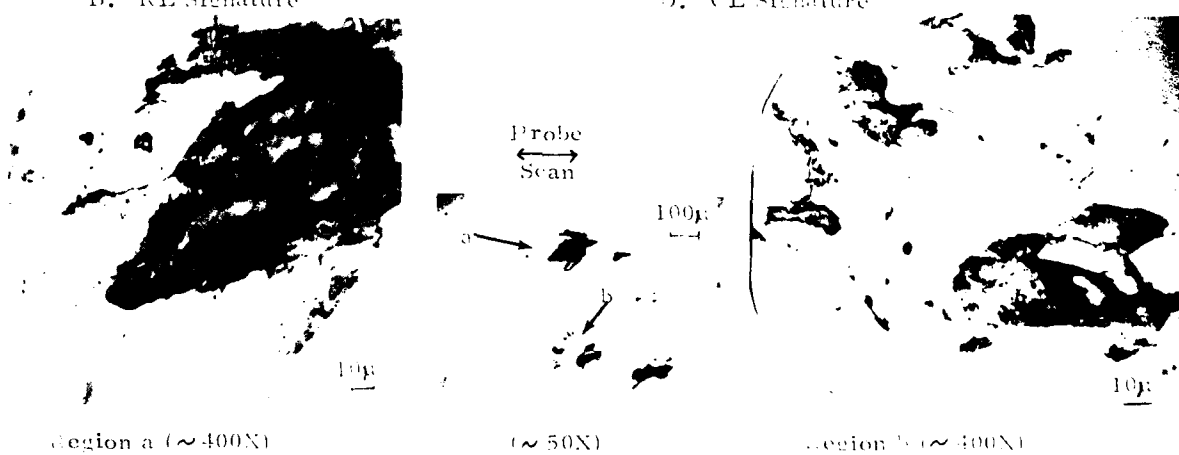
C. CH Signature



B. RL Signature



D. CL Signature



E. Surface Photomicrographs of Flaw Region

FIGURE 12. CIBLE INSPECTION SIGNATURES AND CORRESPONDING SURFACE PHOTOMICROGRAPHS SHOWING PITS AND CRACKS ON NEW BALL FROM VENDOR REWORKED J57-#4 BEARING S/N 395-2, 4362 HRS (Ball #11, S11672).

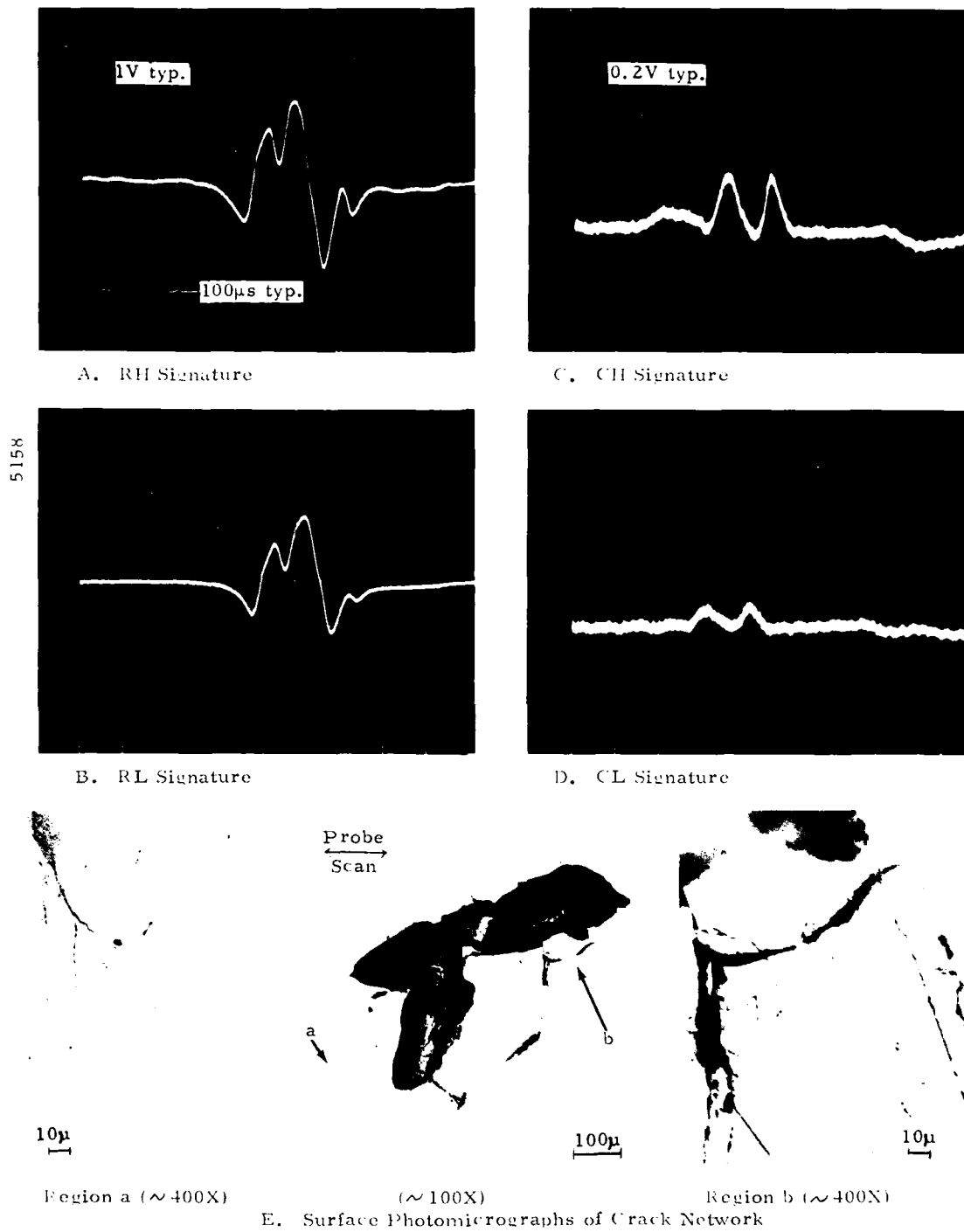
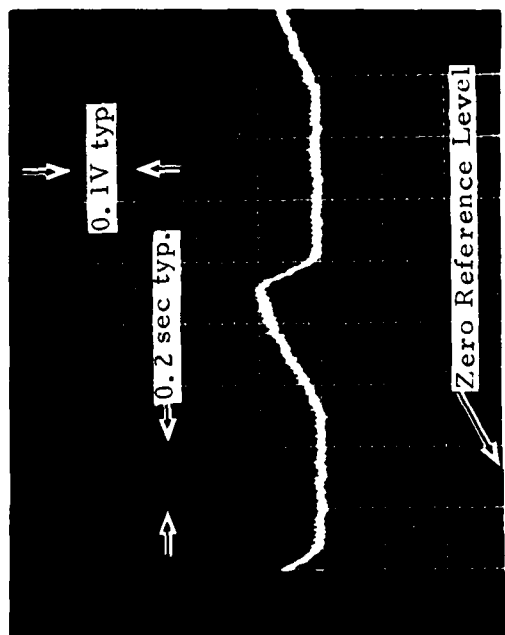
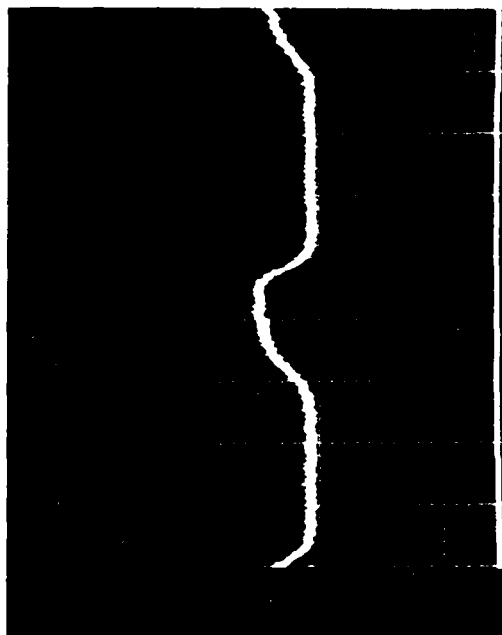


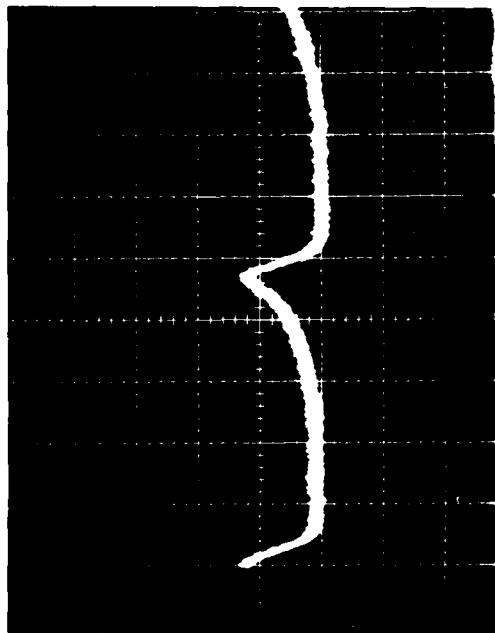
FIGURE 13. CIBLE INSPECTION SIGNATURES AND CORRESPONDING SURFACE PHOTOMICROGRAPHS SHOWING CRACK NETWORK ON NEW BALL FROM VENDOR REWORKED J57-#4 BEARING S/N 395-2, 4362 HRS (Ball #3, S11672).



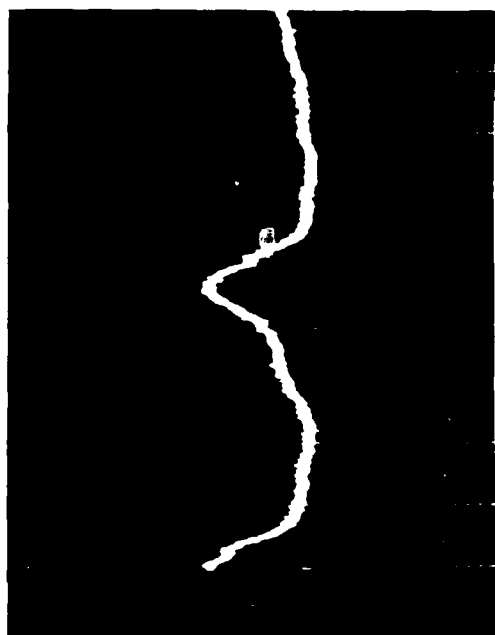
A. Ball No. 4, S/N 9191-1 (S11911), Reworked



B. Ball No. 17, S/N P260A-1 (S11021), Reworked



C. Ball No. 7, S/N 620L-1 (A00031F), 6506 hrs.



D. Ball No. 9, S/N P9117-1, 3230 hrs.

FIGURE 14. TYPICAL BARKHAUSEN SIGNATURES FROM J57-#4 MAIN SHAFT BEARING BALLS.

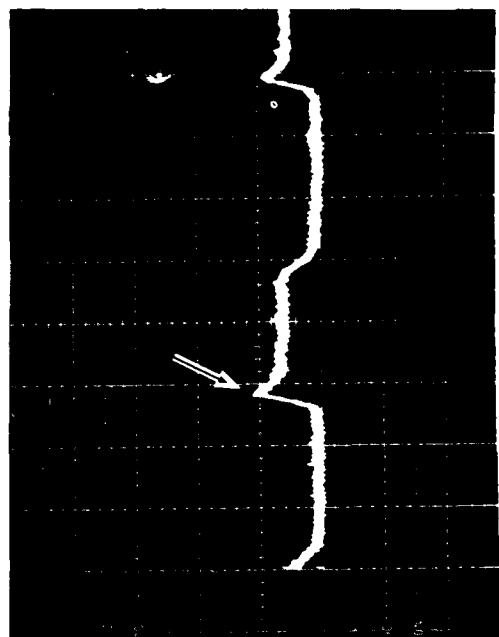
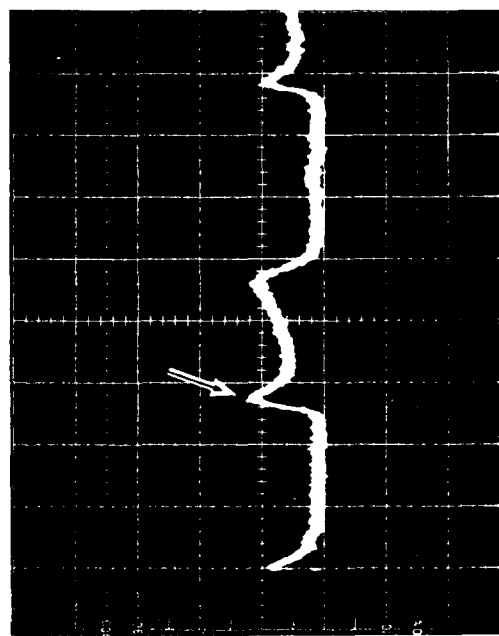
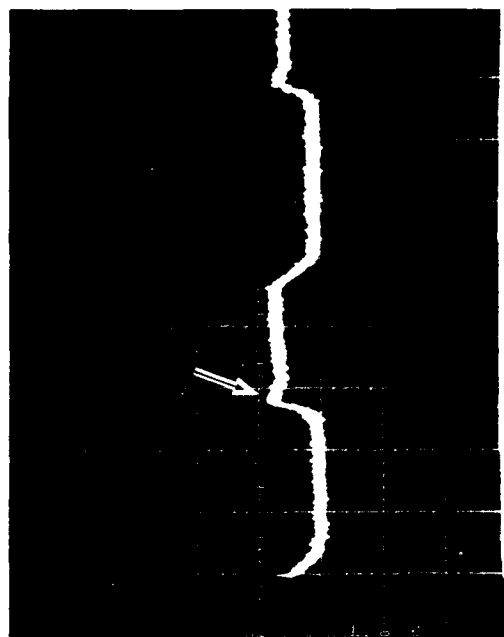
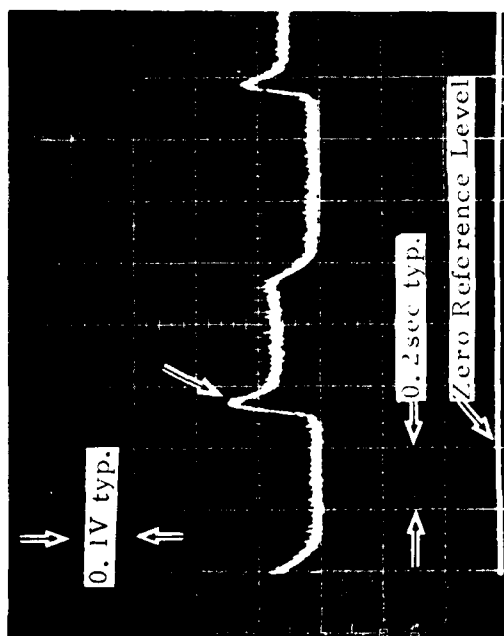


FIGURE 15. BARKHAUSEN SIGNATURES FOR FOUR BALLS FROM J57-#4 VENDOR REWORKED BEARING
S/N 395-2 (S11672), 4362 HRS.

APPENDIX D

TABLE OF ENDURANCE TEST RESULTS

Summary of Endurance Test Results

| Test Results | Prior Signature | Test Data Hrs - Stress | Bearing Type | Remarks | AF S/N (SwRI No.) | Test Ref. No. |
|--------------|-------------------------------|------------------------------|--------------|---|-------------------|---------------|
| Spall | RH, L after 100 hrs 0008-2377 | 314.6-332 ksi | J57-#4 | Outer race, LS; 6173 hrs. service | 5020-1 (S10171) | 1 |
| Spall | CH, 0007-4850 | 16.0-332 ksi | J57-#4 | Inner Race, LH; 6599 hrs. service | 493-1 (S10161) | 2 |
| Spall | CH, 0009-0165 | 26.2-332 ksi | J57-#4 | Inner race, NLH; 5678 hrs. service | 748A-1 (S10981) | 3 |
| Spall | CH, 0005-4853 microcracking | 499.2-204 ksi 4.9-332 ksi | J57-#2 | Inner race, LH; 2053 hrs. service | B1274-2 (S00032) | 6, 11, 13 |
| Spall | Unknown Gross Failure | ~0.2-332 ksi | J57-#2 | Inner race, LH; 3110 hrs. service | B1279-1 (S00041) | 6 |
| Spall | Unknown | 6.0-332 ksi | J57-#2 | Inner race, LH; 3033 hrs. service | Y211-1 (S00701) | 8 |
| Spall | No printout | 50.0-260 ksi | J57-#2 | Outer race, NLS; 891 hrs service | A15-1 (S01551) | 21 |
| Spall | CH, 0013-1762 | 30.0-332 ksi | J57-#4 | Inner race, NLH; 3761 hrs. service | 219A-2 (S12052) | 18 |
| Spall | CH, 0009-3664 | 10.5-286 ksi | J57-#4 | Inner race, LH; 4752 hrs. service | 1604-1 (S11501) | 19 |
| Spall | CH, 0011-0014 | 12.1-260 ksi | J57-#4 | Inner race, LH; 5534 hrs. service (failure not at largest CH signature) | 531A-IRM (S12291) | 23 |
| Spall | CH, 0012-4452 | 19.8-260 ksi | J57-#2 | Inner race NLH; 8192 hrs. service | 360C-2 (S12152) | 22 |
| Cracking | CH, 0008-0548 | 24.0-260 ksi | J57-#2 | Inner race NLH; 1618 hrs. service | 2068-1 (S00871) | 25 |

NOTES:

- LS refers to loaded side of outer race.
- NLS refers to nonloaded side of outer race.
- LH refers to loaded half of inner race.
- NLH refers to nonloaded half of inner race.

Summary of Endurance Test Results

| Test Results | Prior Signature | Test Data Hrs - Stress | Bearing Type | Remarks | AF S/N (SwRI No.) | Test Ref. No. |
|--------------------------------------|--|---------------------------|--------------|---|-------------------|---------------|
| Existing Cracks Propagated | CH 0002, 0007-2291 | 3.0-204 ksi | J57-#2 | Inner race, LH; 6965 hrs. service | 144D-2 (S00762) | 209 |
| Existing Crack Propagated | CH 0003-3216, 3223 | 1.0-204 ksi | J57-#2 | Inner race, LH; 2752 hrs. service | A984-1 (S00591) | 11 |
| Existing Crack Propagated | CH 0007, 0008-2127 | 1.0-204 ksi | J57-#2 | Outer race, LS; 7259 hrs. service | Z916-2 (S00722) | 15 |
| Existing Crack Propagated | CH 0009-2500 RH 0013-1288 | 1.0-204 ksi | J57-#2 | Outer race, LS; 8296 hrs. service | Y704-2RM (S01692) | 15 |
| Existing Crack Propagated | CH, L no printout | 1.0-204 ksi | J57-#4 | Inner race, LH; 1668 hrs. service | 685D-1 (S11281) | 17 |
| Existing Cracks Propagated | CH, L 0006, 1097 | 2.0-204 ksi | J57-#2 | Outer race, LS; 1108 hrs. service Metallurgically examined | Y635-2 (S01682) | 24 |
| Existing Crack Propagated to Failure | See previous sheet listing spalls, J57-#2, S/N B1274-2 | | | | | |

Summary of Endurance Test Results

| Test Results | Prior Signature | Test Data Hrs - Stress | Bearing Type | Remarks | AF S/N (SwRI No.) | Test Ref. No. |
|-----------------------------|-----------------|---------------------------|--------------|--|-------------------|---------------|
| Pit Deterioration | | 12.0-332 ksi | J85-#2 | Inner race, NLS; 1133 hrs. service | A4230 (S30211) | 4 |
| Corrosion Pit Deterioration | | 8.0-332 ksi | J85-#2 | Inner race, LH; 1824 hrs. service vendor reworked 1199 hrs. | 07384 (S31341) | 10 |
| Corrosion Pit Deterioration | | 96.0-332 ksi | J85-#2 | Inner race, LH; 3083 hrs. service vendor reworked 1199 hrs.; BK change | 09997 (S31481) | 7, 14 |
| Corrosion Pit Deterioration | | 96.0-332 ksi | J85-#2 | Inner race, NLH; 2800 hrs. service vendor reworked 1199 hrs.; Bk change | 03017 (S30811) | 7, 14 |

Summary of Endurance Test Results

| Test Results | Prior Signature | Test Data Hrs - Stress | Bearing Type | Remarks | AF S/N (SwRI No.) | Test Ref. No. |
|-----------------|---|------------------------------|--------------|---|-------------------|---------------|
| Test Terminated | RH, RL 0006-1241, 0008-4647 | 314.6-332 ksi | J57-#4 | Inner race, LH; 5049 hrs. service Test terminated, numerous indents from failure of S/N 5020-1 | 8375-2 (S10232) | 1 |
| Test Terminated | CH 0007-0543 | 16.0-332 ksi | J57-#4 | Inner race, LH; 9025 hrs. service Test terminated, numerous indents from failure of S/N 493-1 | 228C-2 (S10102) | 2 |
| Test Terminated | CH 0013-4390 | 83.7-332 ksi | J57-#4 | Inner race, LH; 6769 hrs. service Test terminated, metallurgically examined at CH signatures | 1325-2 (S10782) | 3, 5 |
| Test Terminated | RH, RL four pit locations | 57.5-332 ksi | J57-#4 | Inner race, LH; 7946 hrs. service Test terminated, metallurgically examined at MPR locations | 141C-2 (S10072) | 5 |
| Test Terminated | CH 0007-3782 | 6.0-332 ksi | J57-#2 | Inner race, NLH; 7259 hrs. service Test terminated to load crack region on outer, service loaded region | Z916-2 (S00722) | 8 |
| Test Terminated | CH 0009-2339 Pit and Tiny Crack 0005-0424 | 502.2-204 ksi 4.9-332 ksi | J57-#2 | Inner race, LH; 4935 hrs. service | Z512-2 (S00712) | 9, 20, 13 |
| Test Terminated | CH 0003-1366 and 0005-1391 | 20.0-332 ksi | J85-#2 | Inner race, NLH; 945 hrs. service Test terminated, metallurgically examined at CH signatures | 06630 (S31121) | 4, 10 |
| Test Terminated | CH, RH 0008-2664, 0007-2989, 0008-3185 | 104.0-332 ksi | J85-#2 | Inner race, NLH; 1072 hrs. service Test terminated, Barkhausen change in load region | A4000 (S30101) | 12 |

Summary of Endurance Test Results (Con't.)

| Test Results | Prior Signature | Test Data Hrs - Stress | Bearing Type | Remarks | AF S/N (SWRI No.) | Test Ref. No. |
|-----------------|--|---|--------------|---|------------------------------|--------------------------|
| Test Terminated | RH 0006-4016 Surface Pit | 104.0-332 ksi | J85-#2 | Inner race, NLH; 2228 hrs. service Test terminated, Barkhausen change in load region. | 02750 (30801) | 12 |
| Test Terminated | CH, RH 0002- 0006, 2536 odd shape | 1.0-204 ksi 67.8-260 ksi 10.5-285.6 ksi 30-332 ksi | J57-#4 | Outer race, LS; 1304 hrs. service Test terminated, no outstanding changes | 4516-2 (S12012) (A00022F) | 17, 18, 19, 22, 26 |
| Test Terminated | CH 0008- 3234 CH/CL = 1.5 | 2.0-204 ksi | J57-#4 | Outer race, LS; 1500 hrs. service Test terminated, no cracks indicated | 32A-1 (S11082) | 29 |
| Test Terminated | CH, RH, RL 0010- 1283 | 50.0-260 ksi | J57-#2 | Inner race, NLH; 4486 hrs. service Metallurgical candidate | A392-2 (S01572) | 21 |
| Test Terminated | CH, CL, RH, RL 2078- 2087 Double signal | 50.0-260 ksi | J57-#2 | Outer race, NLS; 4486 hrs. service Metallurgically examined | A392-2 (S01572) | 21 |
| Test Terminated | CH, RH, RL 0010- 1084 | 4.0-260 ksi | J57-#2 | Inner race, LH; 4486 hrs. service Candidate for metallurgical examination | A392-2 (S01572) | 28 |
| Test Terminated | CH, RH, RL 0008- 2819 | 12.1-260 ksi | J57-#4 | Inner race, LH; 5534 hrs. service Candidate for metallurgical examination | 531A-2RM (S12292) | 23 |
| Test Terminated | CH, RH, RL 0011- 0878 stringer | 4.0-260 ksi Inclusion Pit | J57-#2 | Inner race, LH; 891 hrs. service Metallurgically examined | A15-1 (S01551) | 28 |
| Test Terminated | CH, RH, RL 0004- 1354 | 2.0-204 ksi 24.0-260 ksi | J57-#2 | Inner race, NLH; 4486 hrs. service No significant changes | A392-1 (S01571) | 24, 25 |
| Test Terminated | CH 0012- 4350 | 24.0-260 ksi | J57-#2 | Inner race, LH; 4486 hrs. service | A392-1 (S01571) | 27 |
| Test Terminated | CH, Double 0008-3817 | 24.0-260 ksi | J57-#2 | Inner race, LH; 1500 hrs. service | 369K-2 (S01052) | 27 |

Summary of Endurance Test Results (Con't.)

| Test Results | Prior Signature | Test Data Hrs - Stress | Bearing Type | Remarks | AF S/N (SwRI No.) | Test Ref. No. |
|-----------------|----------------------------------|---------------------------|--------------|--|-------------------|---------------|
| Test Terminated | CH, 3 locations also 1 double | 43.0-260 ksi | J57-#4 | Outer race, LS; 777 hrs. service | 3670-2 (S12162) | 26 |
| Test Terminated | CH 0012-1133 | 2.0-204 ksi | J57-#4 | Outer race, LS; 813 hrs. service | 531V-1 (S12301) | 29 |
| Test Terminated | CH, 5 locations | 50.0-260 ksi | J57-#2 | Inner race, NLH; 891 hrs. service Metallurgically examined | A15-1 (S01551) | 21 |
| Test Terminated | CH, Double | 2.0-260 ksi | J57-#2 | Inner race, LH; 6527 hrs. service Candidate for metallurgical examination | 711F-2 (S01292) | 30 |

APPENDIX E

TABLE OF METALLURGICAL RESULTS

Metallurgical Sectioning Results

| Sample No. | Bearing Component | Sample Location | Signature Type | Visual Indication | Sample I.D. | Results | History | Remarks |
|------------|------------------------|-----------------|------------------------------|--|-------------|---|----------------------|---|
| 1 | 141C-1 (S10071) (2) | ST03, BR1682 | RHL Circ. Shape Radial | Grinding Scrape | A-1 | Grinding scrape, no mat'l trans- formation possibly limited micro- cracking in scrape Also SEM Results | 7946 hrs. service | Reparable Reject |
| 2 | 141C-1 (S10071) (2) | ST03, BR1682 | RHL Circ. Shape Radial | Grinding Scrape | A-1a | Microhardness measurements in trailing edge region of circ. shaped radial signature showed uniform distribution | 7946 hrs. service | Reparable Reject |
| 3 | 141C-1 (S10071) (2) | ST01, BR2613 | RHL | Flake Out | B-1 | Material loss or "flaked out". Possibly localized microcracking. No material transformation. Also SEM Results | 7946 hrs. service | Reparable Reject |
| 4 | 427C-1 (S10141) (3) | ST12, BR2818 | RHL Small CH also | Pit | A-2 | Inclusion site at surface with no inclusion material; no crack- ing and no material transforma- tion. Also SEM Results. | 8337 hrs. service | Reparable Reject (Previously Reworked) |
| 5 | 427C-1 (S10141) (3) | ST14, BR3314 | RHL Small CH also | Double Pit | B-2 | Inclusion site at surface with trace of inclusion material; no cracking and no material trans- formation. Also SEM Results | 8337 hrs. service | Reparable Reject (Previously Reworked) |
| 6 | 427C-1 (S10141) (3) | ST14 BR3314+ | Small RH Small CH | Nothing Significant | C-2 | Many apparent large subsurface inclusions - probably sectioning artifacts; X-Ray fluorescence in- dicated porosity | 8337 hrs. service | Reparable Reject (Previously Reworked) |
| 7 | 06498 (S31091) (2) | ST06, BR4968 | RHL | Dig Nick, Surrounding Depression | A-1 | No evidence of microcracking or material transformation. | 2851 hrs. service | Time Limited |

Metallurgical Sectioning Results, (Cont.)

| Sample No. | Bearing Component | Sample Location | Signature Type | Visual Indication | Sample I.D. | Results | History | Remarks |
|------------|------------------------|-----------------|-----------------------|----------------------------------|-------------|--|---|---------------------|
| 8 | 0743A (S31391) (2) | ST05, BR0763 | RHL | Dig Nick, Surrounding Depression | A-2 | No evidence of microcracking or material transformation | 1986 hrs. service | Time Limited |
| 9 | 228C-1 (S10102) (2) | ST07, BR0543 | Small CH No RH P/O | Nothing Significant | B-1 | Nothing significant subsurface | 9025 hrs. service 16 hrs. Endurance Test at 332 ksi | Reparable Reject |
| 10 | 228C-1 (S10102) (2) | BR1927 | RHL | Indent | B-2 | ~0.0002 in. deep indent, no evidence of microcracking | 9025 hrs. service 16 hrs. Endurance Test at 332 ksi | Reparable Reject |
| 11 | 228C-1 (S10102) (2) | BR2341 | RHL | Indent | B-3 | ~0.0002 in. deep indent, no evidence of microcracking ~0.0005 in. deep surface pit and "butterfly" ~.006 in. deep in region. | 9025 hrs. service 16 hrs. Endurance Test at 332 ksi | Reparable Reject |
| 12 | 228C-1 (S10102) (2) | BR4332 | RHL | Indent | B-4 | ~0.0002 in. deep indent, no evidence of microcracking Small group of surface inclusions (~.001 in.) about 2.5 tracks from indent. | 9025 hrs. service 16 hrs. Endurance Test at 332 ksi | Reparable Reject |

Metallurgical Sectioning Results, (Con't.)

| Sample No. | Bearing Component | Sample Location | Signature Type | Visual Indication | Sample I.D. | Results | History | Remarks |
|------------|------------------------|-----------------|----------------|---------------------|-------------|--|---|---|
| 13 | 748A-1 (S10981) (5) | ST26, BR2505 | RHL | Indent | A-1 | ~0.0004 in. deep indent, no evidence of microcracking but some structural differences near surface; small inclusions (0.0005-0.001 in. dia.) X 0.008 in. deep and material transformation in same area. | 26.2 hrs. Endurance Test at 332 ksi on service non-loaded region. 5678 hrs. service | Vendor Reworked |
| 14 | 748A-1 (S10981) (5) | ST15, BR2530 | LA | Pit | A-2 | Sharp contour at bottom of pit; no evidence of microcracking; small inclusions (<0.0005 in. dia.) in same area. | 26.2 hrs. Endurance Test at 332 ksi on service non-loaded region. 5678 hrs. service | Vendor Reworked |
| 15, 24 | 748A-1 (S10981) (5) | ST23, BR4462 | RHL | Indent | A-3 | Indent ~0.0002 in. deep; no evidence of microcracking; small subsurface inclusions or voids in same area. Many subsurface inclusions in trailing edge region of indent with material transformation ranging in depths from 0.0006 to 0.013 in. with sizes ranging from 0.0004 to 0.0012 in. dia. | 26.2 hrs. Endurance Test @ 332 ksi on service non-loaded region. 5678 hrs. service | Vendor Reworked |
| 16 | 07384 (S31341) (3) | BR1977 | CH, RHL | Nothing Significant | A-2 | Complete - no single defect. Entire zone tiny inclusions along flow lines. Signature result of clump, isolated - see planes .4282 and .4272 (SEM possibly, plane .4242, similar results on S31121-0) | 1824 hrs. service 8 hrs. Endurance | Time Limited Vendor Reworked at 1199 hrs. |

Metallurgical Sectioning Results, (Con't.)

| Sample No. | Bearing Component | Sample Location | Signature Type | Visual Indication | Sample I.D. | Results | History | Remarks |
|------------------------|------------------------|-----------------|--------------------------------|---------------------|-------------|--|---|-----------------|
| 17 | 144D-2 (S00762) (3) | BR2291 | CH, L; RH, L | Extensive Cracking | D-1 | Subsurface cracking and large stringer type inclusions. | 6965 hrs ser-vice, 3.0 hrs End. Test @ 204 ksi | Vendor Reworked |
| 18 | 144D-2 (S00762) (3) | BR1041(1st) | 210 mv CH 80 mv RH, complex | Small Crack | B-1a | Extensive subsurface cracking and inclusions with material transformation | 6965 hrs ser-vice, 3.0 hrs End. Test @ 204 ksi | Vendor Reworked |
| 19 | 144D-2 (S00762) (3) | BR1041(2nd) | 360 mv CH 400 mv RH | Nothing Significant | B-1b | Subsurface inclusions, no material transformation or cracking | 204 ksi | Vendor Reworked |
| 20 | 144D-2 (S00762) (3) | BR1120 | 180 mv CH 200 mv RH | Small Pit | C-1 | Surface inclusion extending ~0.6 mil deep and thin stringer extending deeper | End. Test @ 204 ksi | Vendor Reworked |
| 21 | 144D-2 (S00762) (3) | BR0352 | 90 mv CH 120 mv RH | Inclusion Pit | A-1 | Surface inclusion pit with small piece of material remaining ~0.4 mil deep | 6965 hrs ser-vice, 3.0 hrs End. Test @ 204 ksi | Vendor Reworked |
| 22 | 144D-2 (S00762) (3) | BR4274 | 80 mv CH, complex 100 mv RH | Inclusion Pit | E-1 | Surface inclusion pit ~0.3 mil deep | 6965 hrs ser-vice, 3.0 hrs End. Test @ 204 ksi | Vendor Reworked |
| 23 | 748A-1 (S10981) (1) | ST10, BR1992 | CH, RHL | Surface Anomaly | A-2 | Surface inclusion with microcracking as a result of endurance testing. Subsurface inclusions with microcracking and material transformations from endurance test @ 332 ksi | 26.2 hrs. Endurance Test @ 332 ksi on ser-vice non-loaded re-gion. 5678 hrs service | Vendor Reworked |
| 24 Refer to 15 also | 748A-1 (S10981) (5) | BR4462 | | | A-3 | Additional sectioning beyond indent region - see Sample No. 15 | | |

Metallurgical Sectioning Results, (Con't.)

| Sample No. | Bearing Component | Sample Location | Signature Type | Visual Indication | Sample I.D. | Results | History | Remarks |
|------------|------------------------|-----------------|----------------|-------------------|-------------|--|---|------------------|
| 25 | 1325-2 (S10782) (3) | ST13, BR4390 | CH, RHL | Surface Anomaly | A-1 | Surface anomaly indicative of a pit from a stringer inclusion with no evidence of microcracking. Subsurface stringer inclusion complex silicate, probably Al_2O_3 -CaO (+SiO ₂)/ Al_2O_3 -MgO, in same region with no evidence of material transformation or microcracking. Stringer inclusion extends from ~0.002 in. in depth with a length of ~0.06 in. Connects to region of surface flaw. | 6769 hrs. service 83.7 hrs. Endurance Test @ 332 ksi | Vendor Reworked |
| 26 | 141C-2 (S10072) (2) | BR0463 | RHL | Surface Pit | A-1 | No evidence of material transformation or microcracking in the vicinity of the pit | 7946 hrs. service 57.5 hrs Endurance Test @ 332 ksi | Reparable Reject |
| 27 | 141C-2 (S10072) (2) | BR3509 | RHL | Surface Pit | B-1 | No evidence of material transformation or microcracking in the vicinity of the pit | 7946 hrs. service 57.5 hrs. Endurance Test @ 332 ksi | Reparable Reject |
| 28 | 141C-2 (S10072) (2) | BR3868 | RHL | Surface Pit | C-1 | No evidence of material transformation or microcracking in the vicinity of the pit | 7946 hrs. service 57.5 hrs Endurance Test @ 332 ksi | Reparable Reject |

Metallurgical Sectioning Results, (Con't.)

| Sample No. | Bearing Component | Sample Location | Signature Type | Visual Indication | Sample I.D. | Results | History | Remarks |
|------------|------------------------|---|--|---------------------|-------------|---|--|---------------------------------|
| 29 | 141C-2 (S10072) (2) | BR4512 | RHL | Surface Pit | D-1 | No evidence of material transformation or microcracking in the vicinity of the pit | 7946 hrs. service 57.5 hrs. Endurance Test @ 332 ksi | Reparable Reject |
| 30 | 06630 (S31121) (0) | ST03, BR1366 | CH, RHL | Nothing Significant | A-1 | Complete - no singular defect. Entire zone has tiny inclusions along flow lines. Signature attributed to isolated clump of tiny inclusions (see planes .4312, .4272; SEM possibly, plane .4242) (similar results on S31341-3) | 20 hrs. Endurance Test @ 332 ksi over service non-loaded region. 945 hrs. service. | Reparable |
| 31 | 06630 (S31121) (0) | ST05, BR1391 Tentative target plane .3788 starting plane .3824 | CH, RHL | Nothing Significant | A-1b | Complete - no singular defect. Entire zone has tiny inclusions along flow lines. Signature attributed to isolated clump of tiny inclusions (see plane .3788) | 20 hrs. Endurance Test @ 332 ksi over service non-loaded region. 945 hrs service | Reparable |
| 32 | 07384 (S31341-3) | BR0000 | Random location to observe generality of inclusion clustering along flow lines | | B-3 | Inclusion clustering along flow lines noted as for Samples Nos. 16 and 30 | 1824 hrs. service, 8 hrs. Endurance Test @ 332 ksi | Vendor Reworked 1199 hrs. |

Metallurgical Sectioning Results, (Con't.)

| Sample No. | Bearing Component | Sample Location | Signature Type | Visual Indication | Sample I.D. | Results | History | Remarks |
|------------|------------------------|-------------------|------------------------------|---------------------|-------------|--|---|---|
| 33 | Y635-2 (S01682-5) | BR1097 | CH/CL ~1.3 Int. P/O | Tiny Crack | A-1 | Extensive crack network and unusual inclusion appearance | 1108 hrs. service, Vendor Reworked | 2 hrs. Endurance Test @ 204 ksi |
| 34 | Y635-2 (S01682-5) | BR1964 ST11+17 | CH CH/CL ~2 | Nothing Significant | B-1 | Double subsurface inclusions 2-3 mil dia. X 2-3 mil deep. | 1108 hrs. service, Vendor Reworked | 2 hrs. Endurance Test @ 204 ksi |
| 35 | Y635-2 (S01682-5) | BR2020 ST11+17 | RH, RL CH/CL ~2.5 | Small Pits | C-1 | Numerous small inclusions (<1 mil dia) in region. Signature region lost in final setup grind. | 1108 hrs. service, Vendor Reworked | 2 hrs. Endurance Test @ 204 ksi |
| 36 | 531A-IRM (S12291-3) | BR3817 ST07+2 | CH, RH, RL | Tiny Pit | A-1 | Large inclusion 0.003 X 0.004 X .004, 0.0035 Dp slightly breaks to surface, slight mat'l transformation | 5543 hrs. service, Vendor Reworked 12.1 hrs. End. Test @ 260 ksi | Determine what is present since failure occurred at smaller signature |
| 37 | A15-1 (S01551-1) | BR3141 ST13 | CH, CL, RH, RL CH/CL ~4.5 | Nothing Significant | A-1 | Large subsurface inclusion ~0.004 X 0.004 X 0.004 X 0.0035 in. deep | 891 hrs. service, Vendor Reworked | 50 hrs. End. Test @ 260 ksi, NLH |
| 38 | A15-1 (S01551-1) | BR3149 ST02+8 | CH, CL, RH, RL CH/CL ~4 | Small Inclusion Pit | B-1 | Large inclusion to surface ~0.004 X 0.006 X 0.003 in. deep. Smaller inclusions in region, unusual appearance | 891 hrs. service, Vendor Reworked | 50 hrs. End. Test @ 260 ksi, NLH |

Metallurgical Sectioning Results, (Con't.)

| Sample No. | Bearing Component | Sample Location | Signature Type | Visual Indication | Sample I.D. | Results | History | Remarks |
|------------|----------------------|--|---------------------------------|-------------------------------|-------------|---|------------------------------------|-----------------------------------|
| 39 | A15-1 (S01551-1) | BR2759 ST07+16 | CH | Nothing Significant | C-1 | Large subsurface inclusion ~0.0025 X 0.004 X 0.004 in. deep | 891 hrs. service, Vendor Reworked | 50 hrs. End. Test @ 260 ksi, NLH. |
| 40 | A15-1 (S01551-1) | BR2346 | CH, RH | Inclusion Pit | D-1 | Stringer inclusion, angled to surface ~0.002 X 0.007 in. deep, distributed | 891 hrs. service, Vendor Reworked | 50 hrs. End. Test @ 260 ksi, NLH. |
| 41 | A15-1 (S01551-1) | BR3256 | CH, RH | Stringer Pit | E-1 | Long, thin stringer inclusion, angled to surface ~0.001 X 0.020 long, 0.002-0.010 in. deep. | 891 hrs. service, Vendor Reworked | 50 hrs. End. Test @ 260 ksi, NLH. |
| 42 | A15-1 (S01551-3) | BR0878 ST11+4 | CH, CL, RH, RL very large CH | Surface Stringer | A-2 | Stringer inclusion to surface ~0.001 X 0.003 X 0.005 in. deep | 891 hrs. service, Vendor Reworked | 50 hrs. End. Test @ 260 ksi, NLH. |
| 43 | A392-2 (S01572-5) | BR2078 ST 20-22 Double Signature | CH CH/CL ~2+ | Nothing Significant | A-3a | Large subsurface inclusion ~0.004 X 0.006 X 0.006 in. deep | 891 hrs. service, Vendor Reworked | 4 hrs. End. Test @ 260 ksi, LH |
| 44 | A392-2 (S01572-5) | BR2087 ST 20-22 | RH, RL, CH CH/CL ~2+ | Inclusion Pit ~0.005 in. dia. | A-3b | Large inclusion to surface ~0.005 X 0.005 X 0.003 in. deep | 4486 hrs. service, Vendor Reworked | 50 hrs. End. Test @ 260 ksi, NLS |

APPENDIX F

CIBLE RESULTS ON RACES

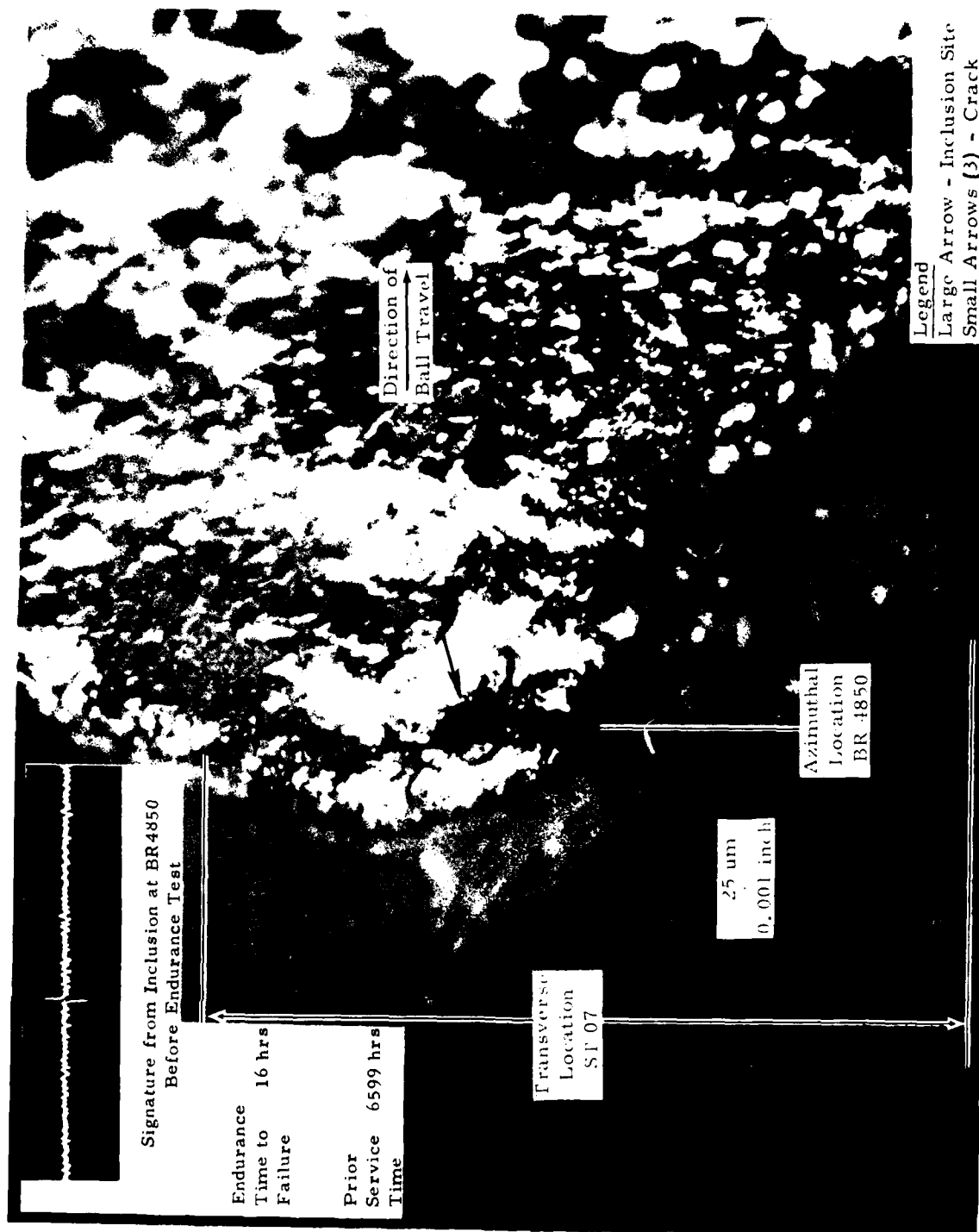


FIGURE F1. PHOTOGRAPH OF LEADING EDGE OF SPALL AND INSPECTION SIGNATURE OBTAINED PRIOR TO ENDURANCE TESTING.

FLAWS

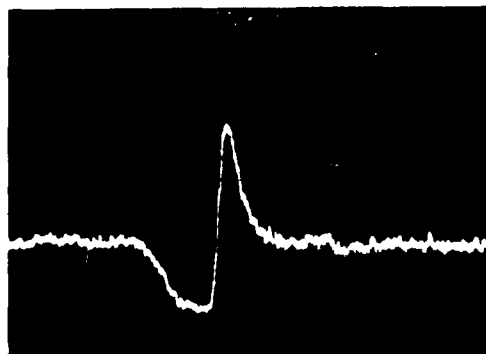
TY S T B R S R
 RH 0004 4858 4871
 CH 0004 4851 4864
 RH 0005 4440 4453
 CH 0005 4851 4864
 RL 0004 4858 4871
 RL 0005 4440 4453
 CL 0005 4851 4864
 END MP.

Legend:

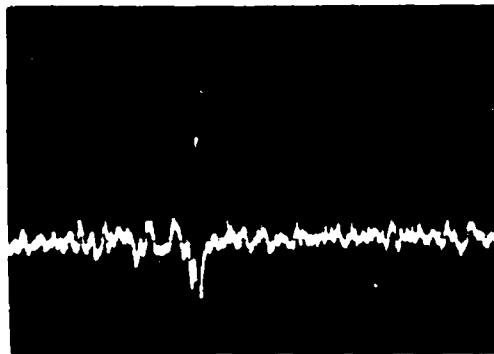
C - circumferential flux
 R - radial flux
 H - high flux density
 L - low flux density
 ST - probe location across race groove
 BR - azimuthal location of signature
 from reference mark on race
 (1 rev = 5000)

Flaw Printout Obtained During Automatic Magnetic Perturbation Inspection

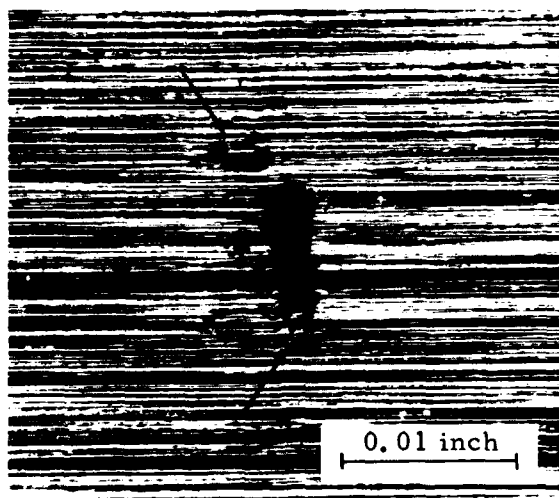
4094



CH Signature @ 0004-4851

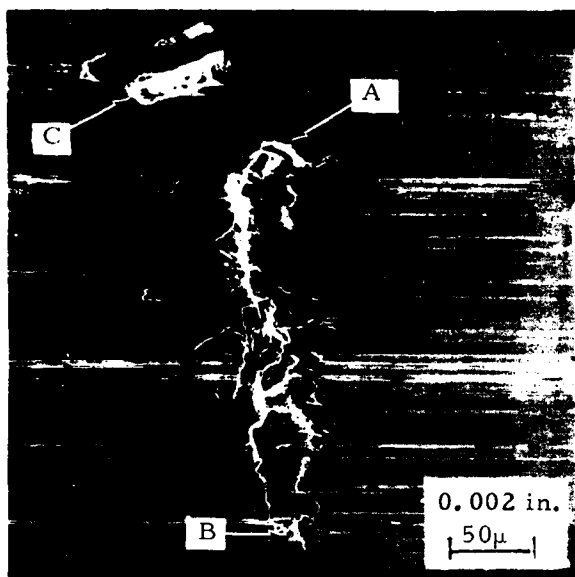


RH Signature @ 0004-4858

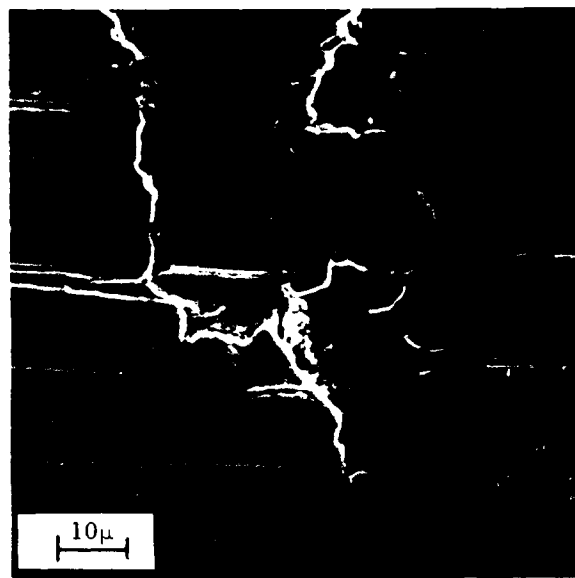


Magnified (100X) View of Surface Showing the Flaw that Caused the CH and RH Signatures

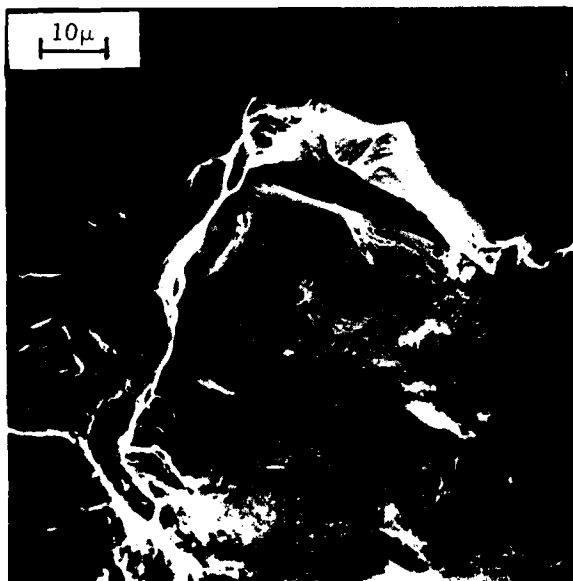
FIGURE F2. CIBLE RESULTS ON J57-#2 BEARING (S/N B1274-2) INNER RACE
 (Reworked bearing accepted by Air Force and considered
 equivalent to new bearing.)



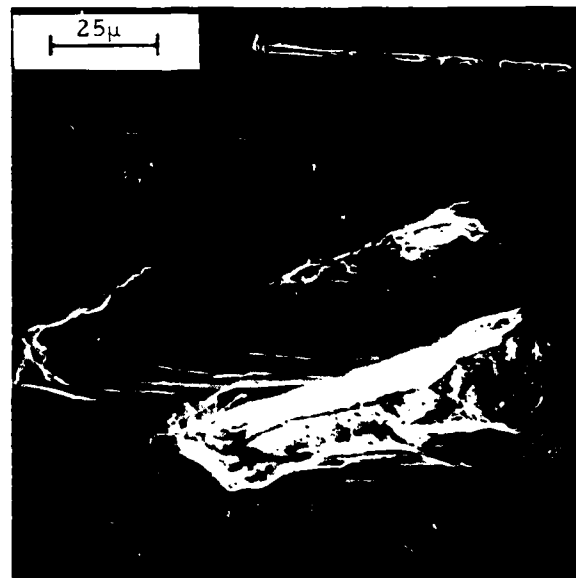
Magnified View ($\sim 250X$) of Surface (SEM) @ 0004-4851



Magnified View ($\sim 1500X$) of Region B (SEM)

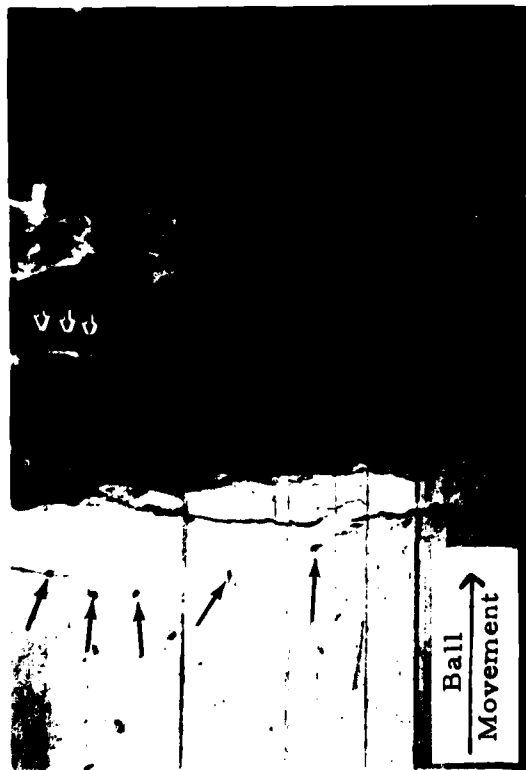


Magnified View ($\sim 1500X$) of Region A (SEM)

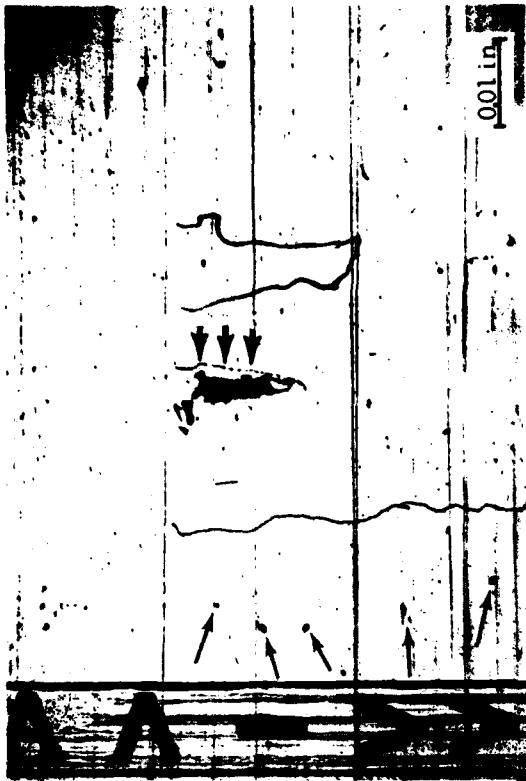


Magnified View ($\sim 600X$) of Region C (SEM)

FIGURE F3. SCANNING ELECTRON MICROSCOPE (SEM) PHOTOGRAPHS OF SURFACE IMPERFECTION (Replica) AT 0004-4851, J57-#2 BEARING (S/N B1274-2) INNER RACE (Reworked Bearing).



A. Magnified View ($\sim 50\times$) of Surface at 0005-4851
4.9 Hrs. (332 ksi) + 499.2 Hrs. (204 ksi)



B. Magnified View ($\sim 50\times$) of Surface at 0005-4851
499.2 Hrs. (204 ksi) Endurance Test Time

Note: Small arrows identify "landmarks" used to establish "spall front" outline in Photograph B.
Bold arrows point to corresponding locations near surface flaw.

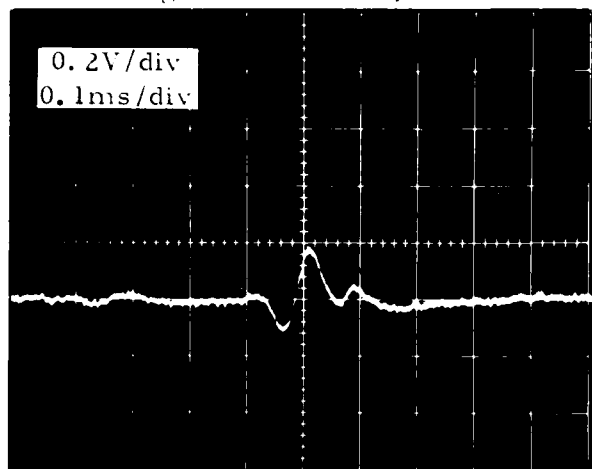
FIGURE F4. SURFACE PHOTOMICROGRAPHS OF FLAW SIGNATURE REGION BEFORE AND AFTER
ENDURANCE TEST FAILURE, J57-#2 BEARING, S/N B1274-2 INNER RACE (S00032-3).

5280



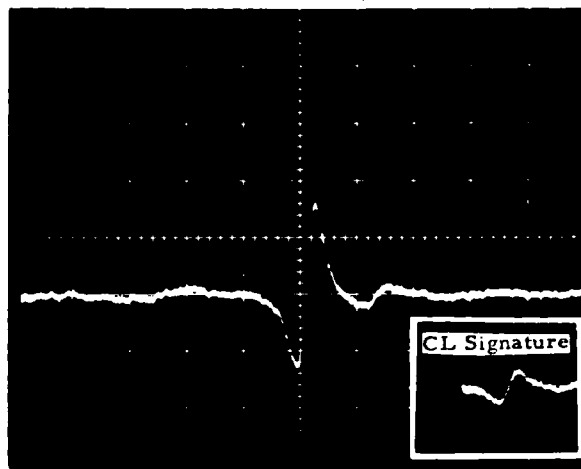
FIGURE F5. SURFACE PHOTOMICROGRAPH OF SPALL REGION ON J57-#2 INNER BEARING RACE, S/N B1274-2 (S00032-3, Service-loaded half).

CH Signature BR0165, ST0009+07

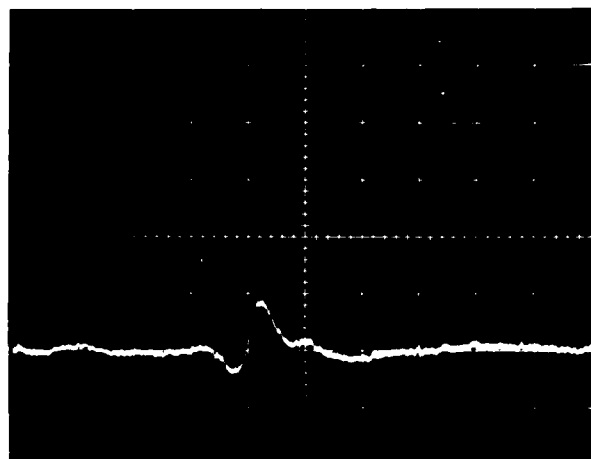


A.

CH Signature BR1992, ST0010+14

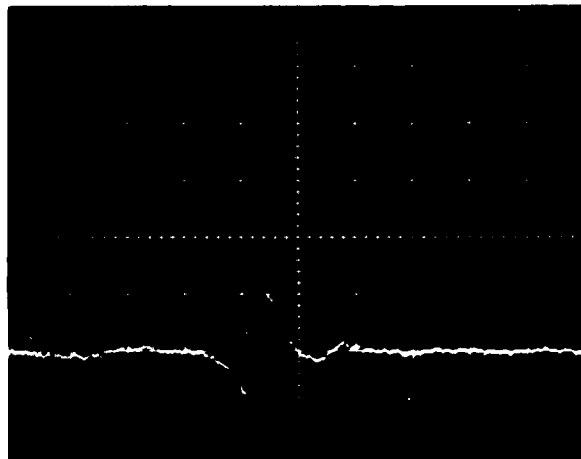


C.



B.

After 19.3 Hrs. Endurance Test Time



D.

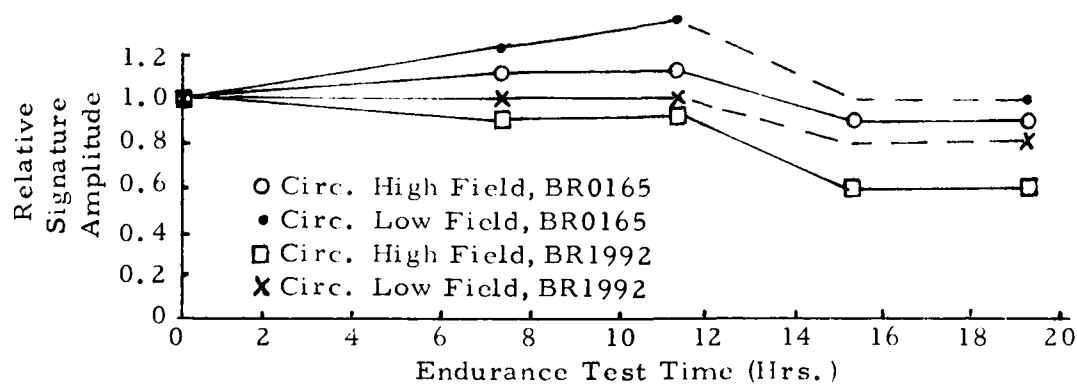
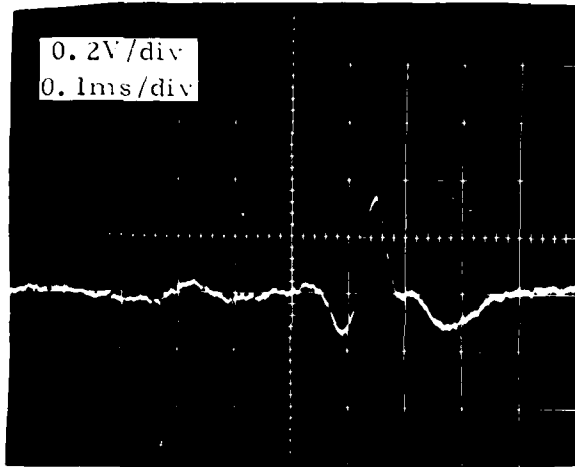


FIGURE F6. MAGNETIC PERTURBATION CIRCUMFERENTIAL FLUX SIGNATURES AT FLAW LOCATIONS 0009-0165 AND 0010-1992 AS A FUNCTION OF ENDURANCE TEST TIME, J57-#4 BEARING S/N 748A-1, INNER RACE S10981(1).

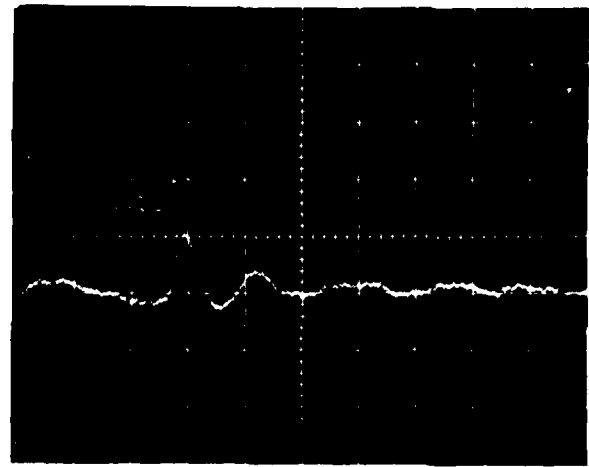
RH Signature BR0165, ST0009107



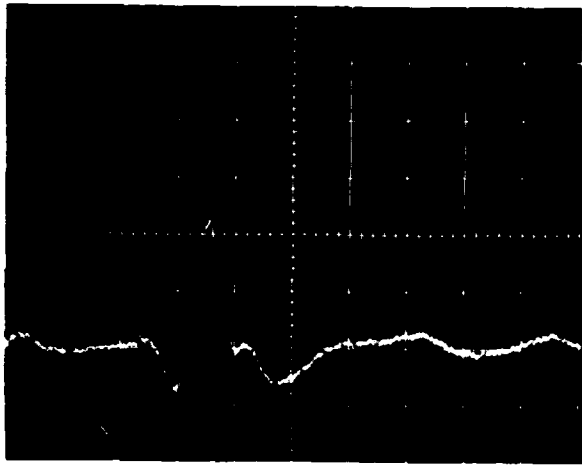
A.

Before Endurance Test

RH Signature BR1992, ST0010114

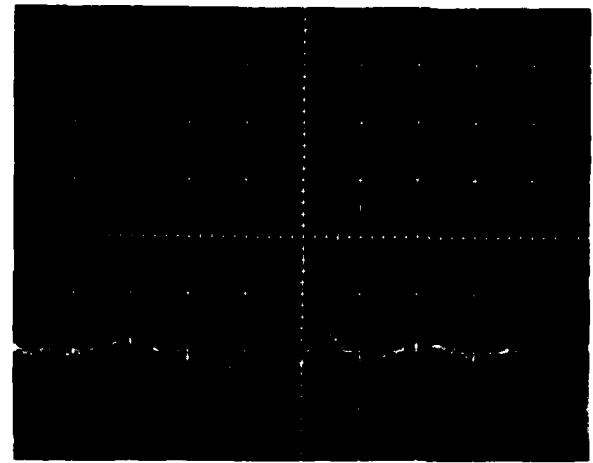


C.



B.

After 19.3 Hrs. Endurance Test Time



D.

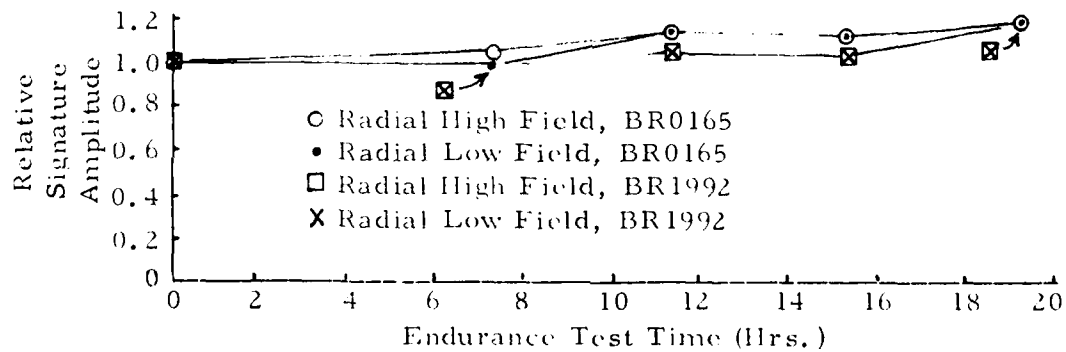


FIGURE F7. MAGNETIC PERTURBATION RADIAL FLUX SIGNATURES AT FLAW LOCATIONS 0009-0165 AND 0010-1992 AS A FUNCTION OF ENDURANCE TEST TIME, J57-#4 BEARING S/N 748A-1, INNER RACE S10981(1).

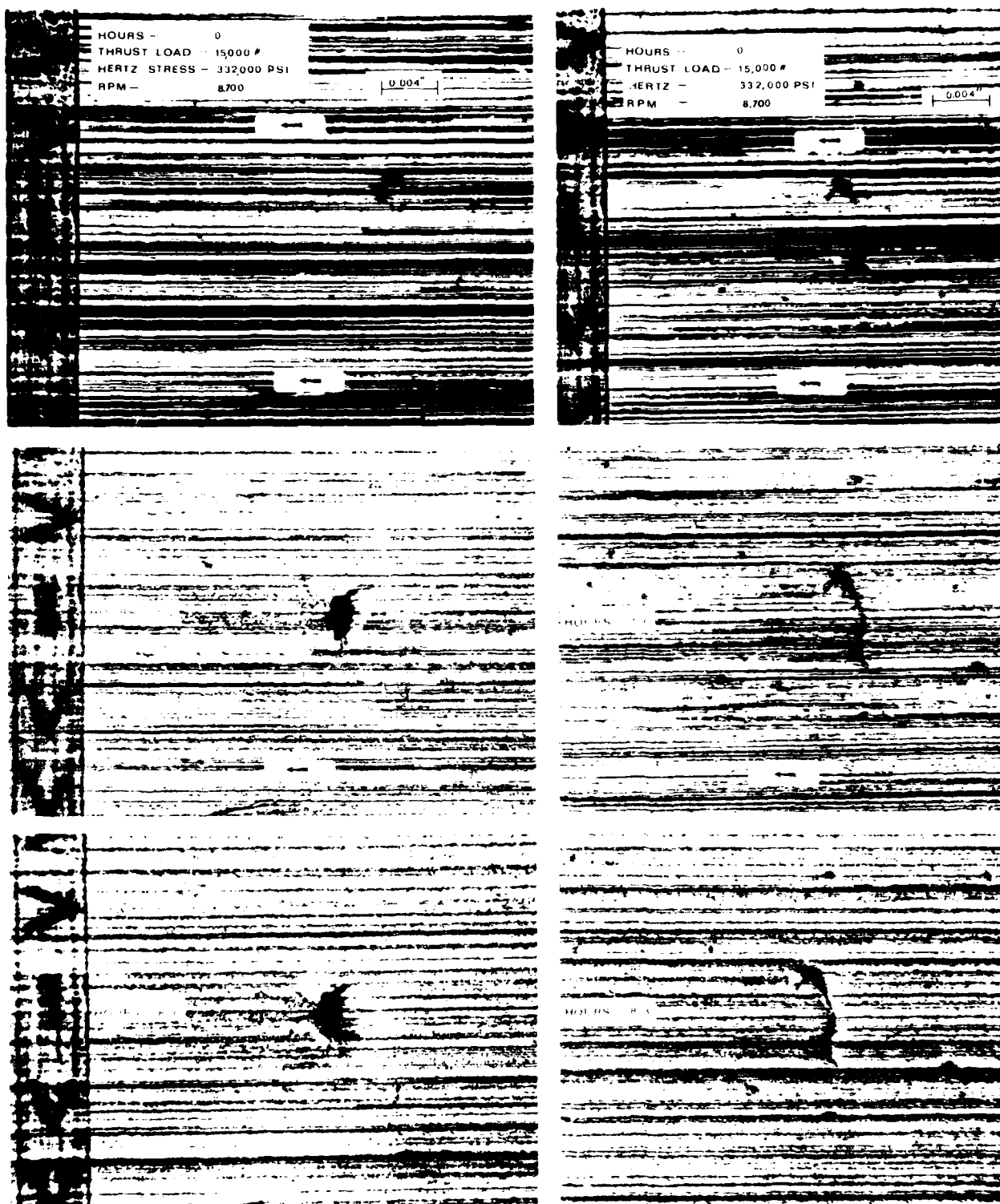


FIGURE F8. SURFACE PHOTOMICROGRAPHS OF TWO FLAW LOCATIONS ON J57-#4 BEARING S/N 748A-1 INNER RACE (nonloaded half in service) "BEFORE" AND "AFTER" 7.3 and 8.3 HRS ENDURANCE TESTING (S10981).

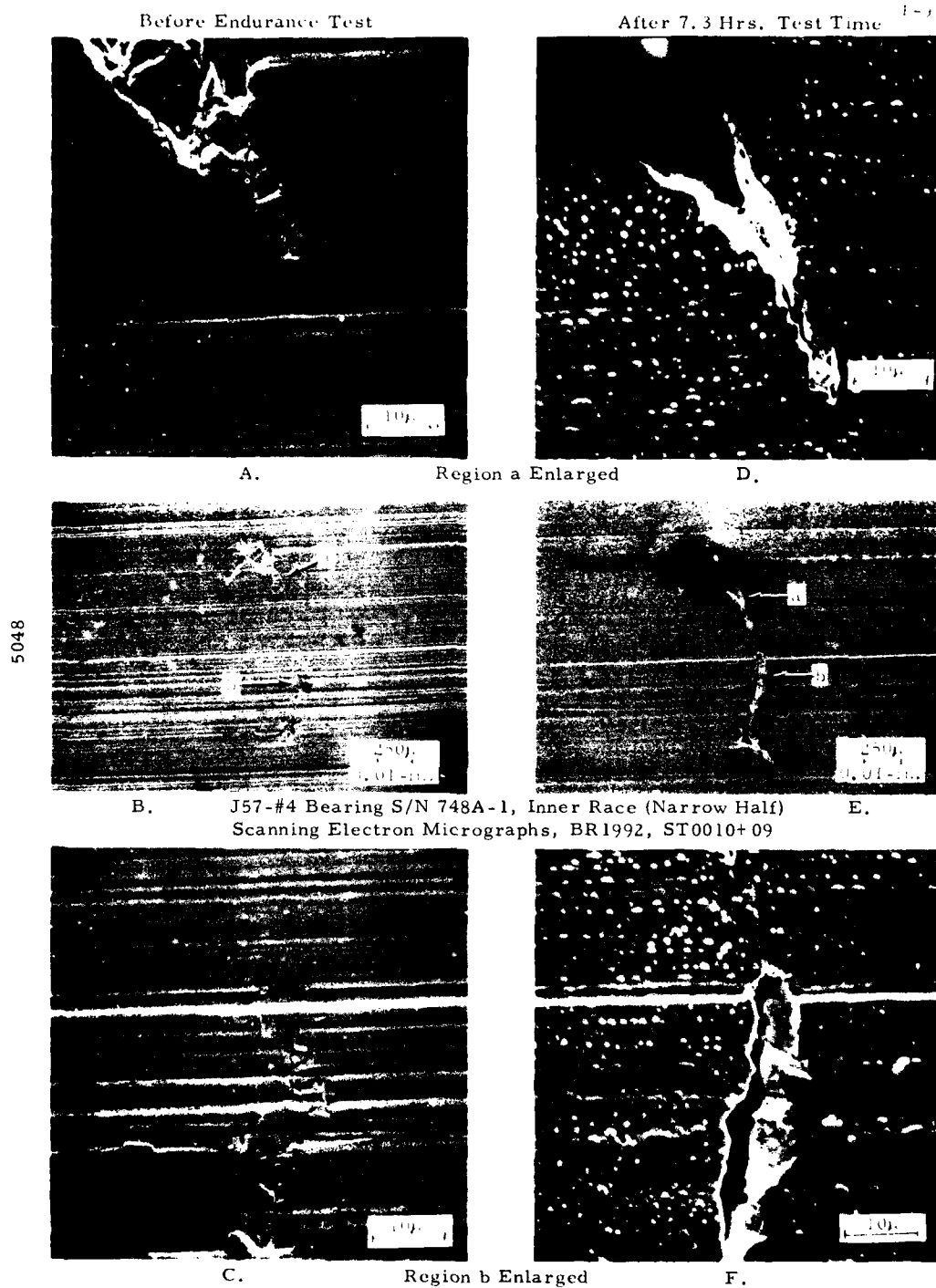
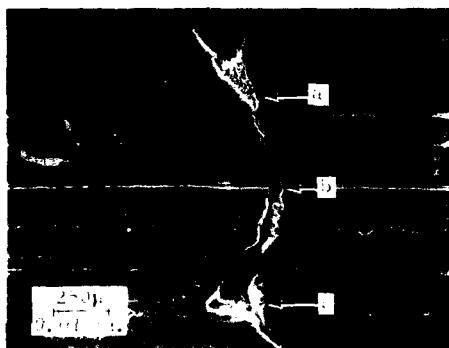
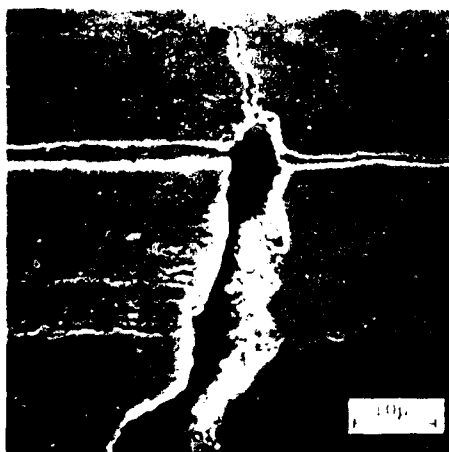


FIGURE P9. REPLICATION (SEM) RESULTS AT 0 HRS AND 7.3 HRS ENDURANCE TEST TIME IN VICINITY OF FLAW SIGNATURE AT 0010-1992, J57-#4 BEARING (S/N 748A-1) INNER RACE S10981(1) (5678 hrs., reworked).

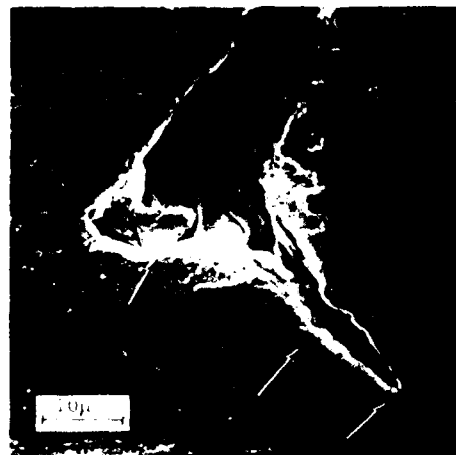
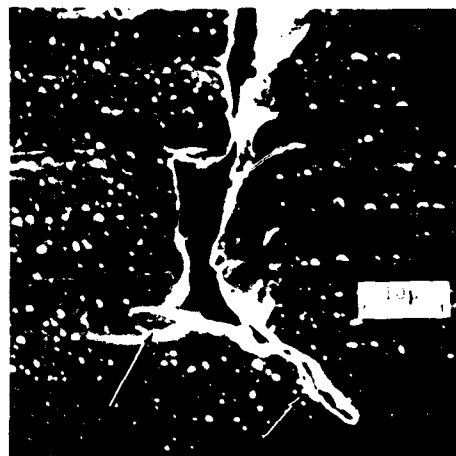
After 26.2 Hrs. Test Time



A. Region a Enlarged

B. J57-#4 Inner Race, S/N 748A-1
(Narrow Half) BR 1992, ST0010+09

C. Region b Enlarged

D. Region c Enlarged
26.2 Hrs. Test TimeE. Region c Enlarged
7.3 Hrs. Test Time

Arrows indicate regions of crack
progression and material loss.

FIGURE F10. REPLICATION (SEM) RESULTS AT 26.2 HRS ENDURANCE TEST
TIME IN VICINITY OF FLAW SIGNATURE AT 0010-1992, J57-#4
BEARING (S/N 748A-1 INNER RACE S10981(1) (5678 hrs., reworked)).



A. Magnified View ($\sim 50X$) of Surface at 0009-0170
26.2 Hrs. Endurance Test Time

B. Magnified View ($\sim 50X$) of Surface at 0009-0165
15.3 Hrs. Endurance Test Time

Notes: Small arrows identify "landmarks" used to establish "spall front" outline in Photograph B.
Bold arrows in Photograph A point out cracks.

Tick marks in Photographs A and B reference location of surface indication present before failure.

F-11

FIGURE F11. SURFACE PHOTOMICROGRAPHS OF FLAW SIGNATURE REGION BEFORE (15.3 HRS) AND AFTER FAILURE (26.2 HRS) ENDURANCE TEST TIME, J57-#4 BEARING, S/N 748A-1, INNER RACE (S10981-1).

5133

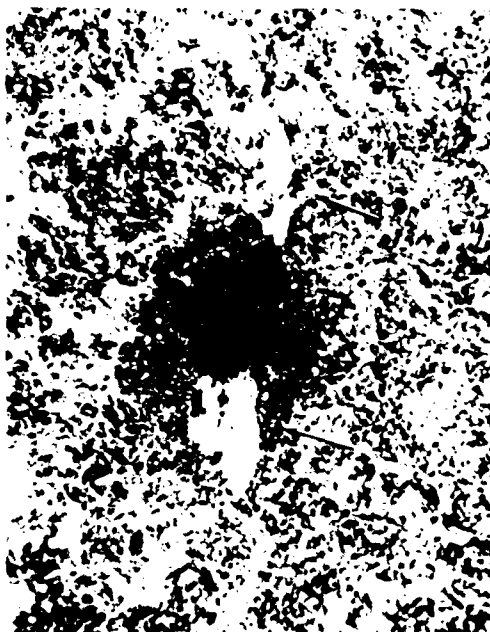


FIGURE F12. SURFACE PHOTOMICROGRAPH OF SPALL REGION ON J57-#4 INNER BEARING RACE, S/N 748A-1 (S10981-1).

5050



A. Surface Photomicrograph ~50X
Plane 0.3991



C. Section Plane 0.3991 1000X



B. Section Plane 0.3991 1000X



D. Section Plane 0.3991 1000X

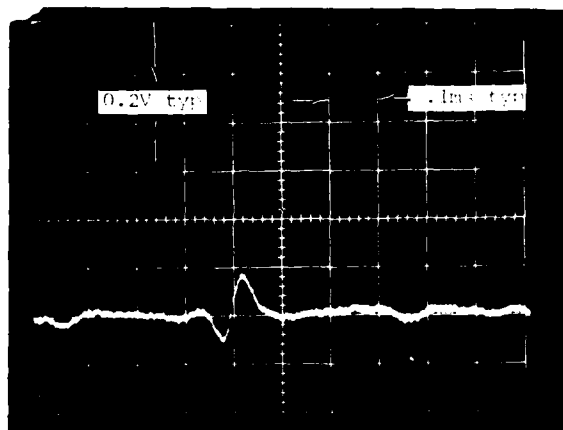
FIGURE F13. METALLURGICAL SECTIONING RESULTS SHOWING MATERIAL TRANSFORMATIONS IN VICINITY OF INDENTATION AT 0023-4462, J57-#4 BEARING S/N 748A-1 OUTER RACE S10981(5) (26.2 hrs. endurance test time).

FLAME
 TY S T E H S R
 CH 0010 4009 4003
 RL 0010 4001 4005

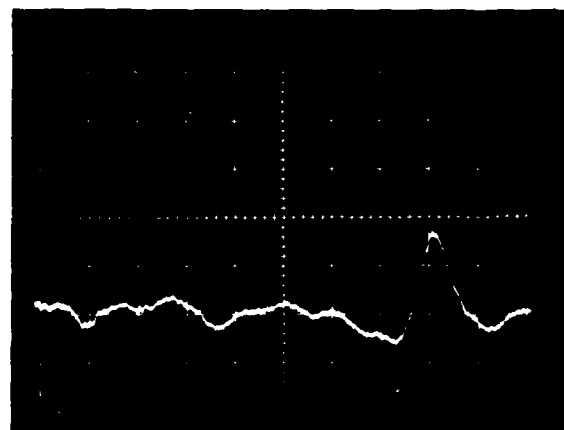
Flaw Printout

Legend:

- C - circumferential flux
- R - radial flux
- H - high flux density
- L - low flux density
- CL - probe location across race groove
- RR - azimuthal location of signature from reference mark on race (1 rev = 5000)



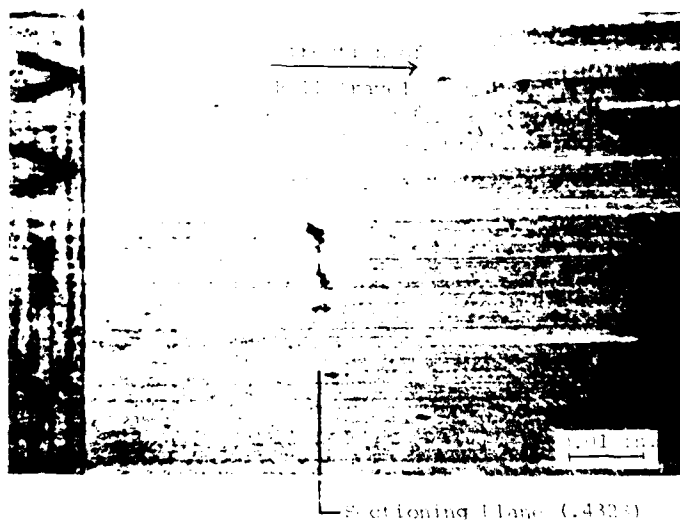
A. CH Signature (13 Hz)



B. RH Signature (13 Hz)

Magnetic Perturbation Signatures After Endurance Test (3.7 hrs., 332 ksi)

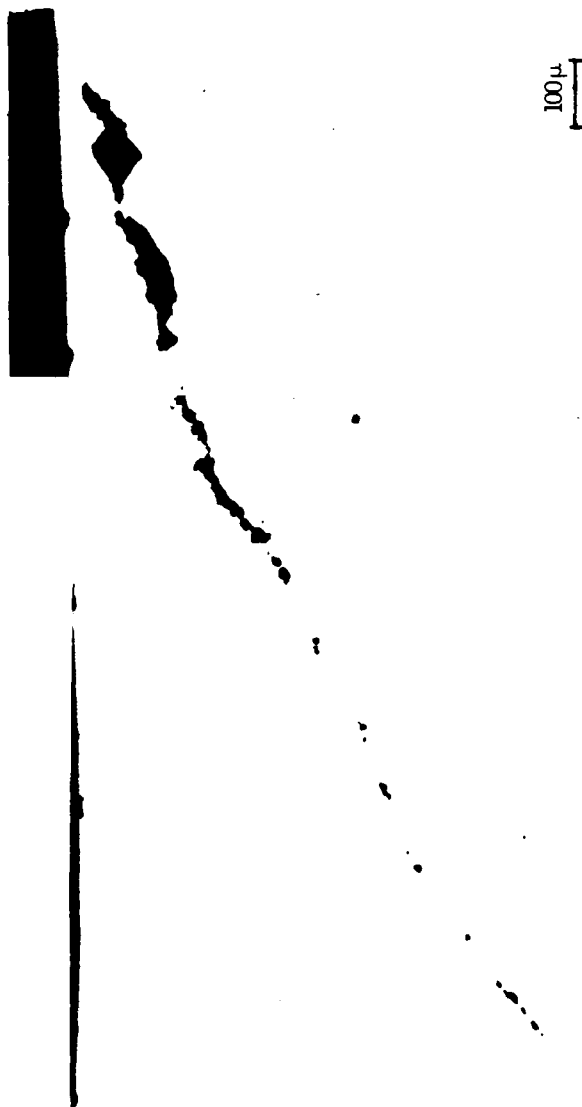
5482



C. Magnified View (50x) of Surface After Endurance Test

FIGURE F14. CIBLE INSPECTION RESULTS ON J57-#4 BEARING (S/N 1325-2) INNER RACE, LOADED HALF, VENDOR REWORKED, 6769 HRS SERVICE AFTER ENDURANCE TEST (S10782-3).

5457

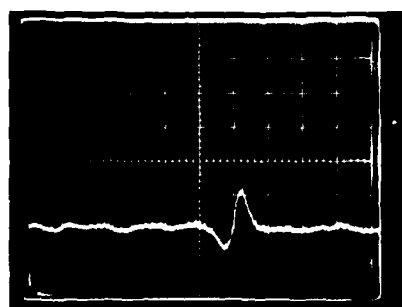
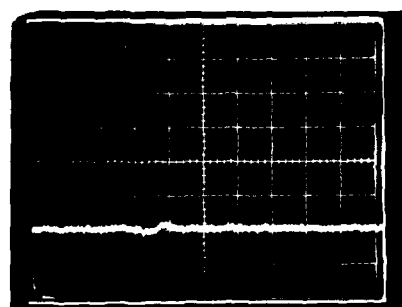
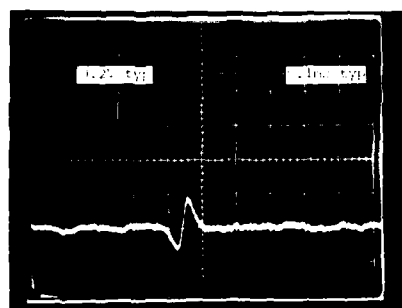


Photomicrograph 100 X (Plane 0.4328)

FIGURE F15. J57-#4 BEARING, INNER RACE, LOADED HALF
S/N 1325-2 (S10782-3) BR 4390, ST13

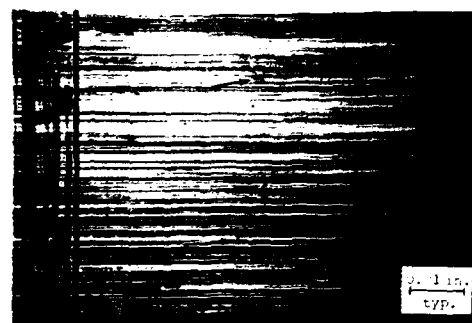
FLW00
TY ST NO SN
CH201 0000 0000 0000
RL202 0000 0000 0000

Flaw Location



Legend:

- 1 = outer race radial flaw
- 2 = inner race radial flaw
- 3 = inner race axial flaw
- 4 = low flux density
- 5 = proper location of signature
- 6 = proper location of signature
- 7 = proper location of signature
- 8 = proper location of signature
- 9 = proper location of signature
- 10 = proper location of signature
- 11 = proper location of signature
- 12 = proper location of signature
- 13 = proper location of signature
- 14 = proper location of signature
- 15 = proper location of signature
- 16 = proper location of signature
- 17 = proper location of signature
- 18 = proper location of signature
- 19 = proper location of signature
- 20 = proper location of signature
- 21 = proper location of signature
- 22 = proper location of signature
- 23 = proper location of signature
- 24 = proper location of signature
- 25 = proper location of signature
- 26 = proper location of signature
- 27 = proper location of signature
- 28 = proper location of signature
- 29 = proper location of signature
- 30 = proper location of signature
- 31 = proper location of signature
- 32 = proper location of signature
- 33 = proper location of signature
- 34 = proper location of signature
- 35 = proper location of signature
- 36 = proper location of signature
- 37 = proper location of signature
- 38 = proper location of signature
- 39 = proper location of signature
- 40 = proper location of signature
- 41 = proper location of signature
- 42 = proper location of signature
- 43 = proper location of signature
- 44 = proper location of signature
- 45 = proper location of signature
- 46 = proper location of signature
- 47 = proper location of signature
- 48 = proper location of signature
- 49 = proper location of signature
- 50 = proper location of signature
- 51 = proper location of signature
- 52 = proper location of signature
- 53 = proper location of signature
- 54 = proper location of signature
- 55 = proper location of signature
- 56 = proper location of signature
- 57 = proper location of signature
- 58 = proper location of signature
- 59 = proper location of signature
- 60 = proper location of signature
- 61 = proper location of signature
- 62 = proper location of signature
- 63 = proper location of signature
- 64 = proper location of signature
- 65 = proper location of signature
- 66 = proper location of signature
- 67 = proper location of signature
- 68 = proper location of signature
- 69 = proper location of signature
- 70 = proper location of signature
- 71 = proper location of signature
- 72 = proper location of signature
- 73 = proper location of signature
- 74 = proper location of signature
- 75 = proper location of signature
- 76 = proper location of signature
- 77 = proper location of signature
- 78 = proper location of signature
- 79 = proper location of signature
- 80 = proper location of signature
- 81 = proper location of signature
- 82 = proper location of signature
- 83 = proper location of signature
- 84 = proper location of signature
- 85 = proper location of signature
- 86 = proper location of signature
- 87 = proper location of signature
- 88 = proper location of signature
- 89 = proper location of signature
- 90 = proper location of signature
- 91 = proper location of signature
- 92 = proper location of signature
- 93 = proper location of signature
- 94 = proper location of signature
- 95 = proper location of signature
- 96 = proper location of signature
- 97 = proper location of signature
- 98 = proper location of signature
- 99 = proper location of signature
- 100 = proper location of signature



1. Magnified View (10x) of Surface of Outer Race Before Endurance Test



2. Magnified View (10x) of Surface of Outer Race After Endurance Test (1.15 typ. 1.15 typ. 1.15 typ.)

FIGURE F16. CIBLE RESULTS ON J57-#4 BEARING (S/N 1604-1), INNER RACE, LOADED HALF VENDOR REWORKED, 4752 HRS. SERVICE, ENDURANCE TESTED TO FAILURE (S11501-3)

FLAWS

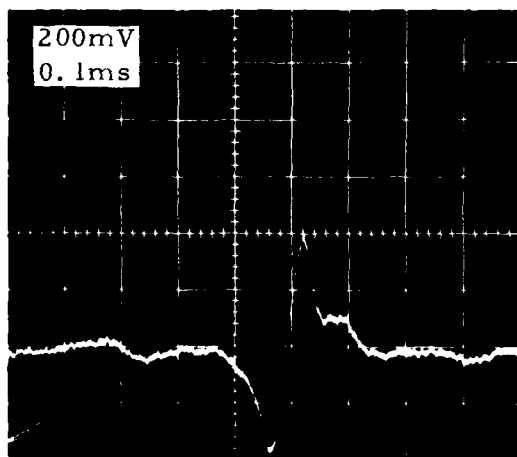
TY ST BR SR
 CH 0002 2291 2306
 RH 0003 2290 2305
 CH 0003 2291 2306
 RH 0004 2290 2305
 CH 0004 2291 2306
 RH 0005 2290 2305
 CH 0005 2292 2307
 RH 0006 2290 2305
 CH 0006 2291 2306
 CH 0007 2291 2306
 CH 0008 1045 1060
 CL 0002 2291 2306
 RL 0003 2291 2306
 CL 0003 2291 2306
 RL 0004 2290 2305
 CL 0004 2291 2306
 RL 0005 2290 2305
 CL 0005 2292 2307
 RL 0006 2291 2306
 CL 0006 2291 2306
 RL 0007 2291 2306
 CL 0007 2291 2306
 CL 0008 1040 1055
 END MP.

Legend:

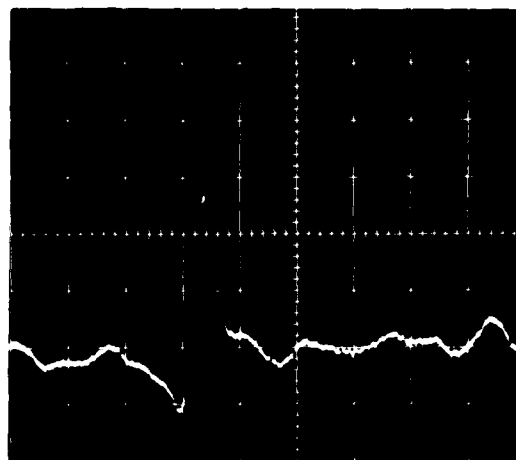
C - circumferential flux
 R - radial flux
 H - high flux density
 L - low flux density
 ST - probe location across race groove
 BR - azimuthal location of signature
 from reference mark on race
 (1 rev = 5000)

4915

Flaw Printout Obtained During Automatic Magnetic Perturbation Inspection

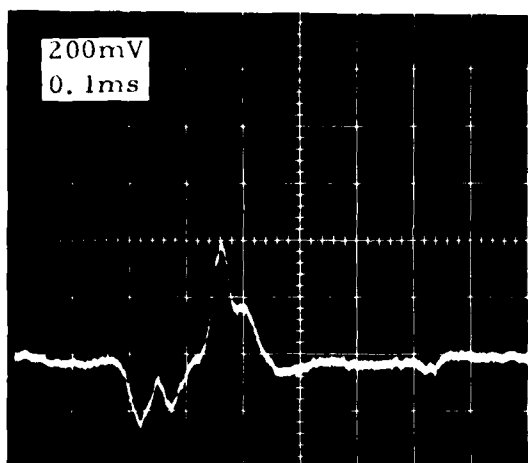


CH Signature @ 0003-2291

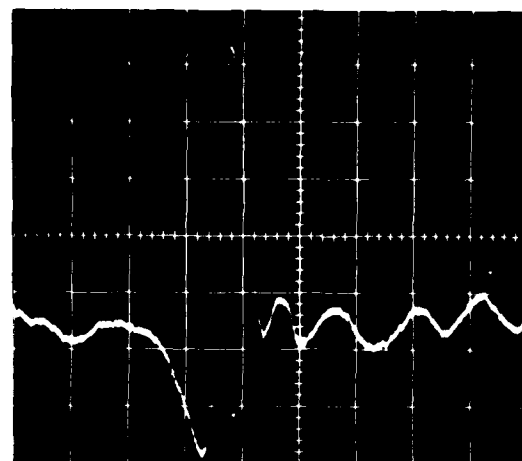


RH Signature @ 0003-2290

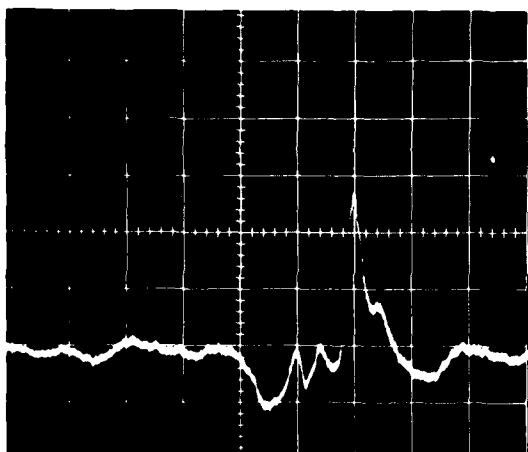
FIGURE F17. CIBLE RESULTS ON J57-#2 BEARING (S/N 1440-2) INNER RACE, LOADED HALF [S00762(3)] (6965 hrs. service - Vendor reworked bearing, accepted by Air Force as serviceable).



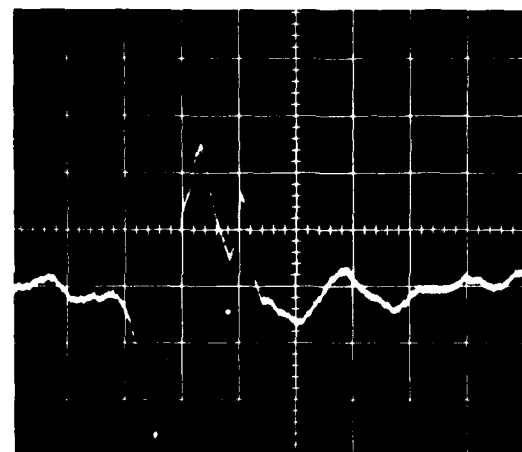
CH Signature @ 0004-2291



RH Signature @ 0004-2290



CH Signature @ 0005-2292



RH Signature @ 0005-2290

FIGURE F18. CIBLE RESULTS ON J57-#2 BEARING (S/N 1440-2) INNER RACE, LOADED HALF [S00762(3)] (6965 hrs. service - Vendor reworked bearing, accepted by Air Force as serviceable).

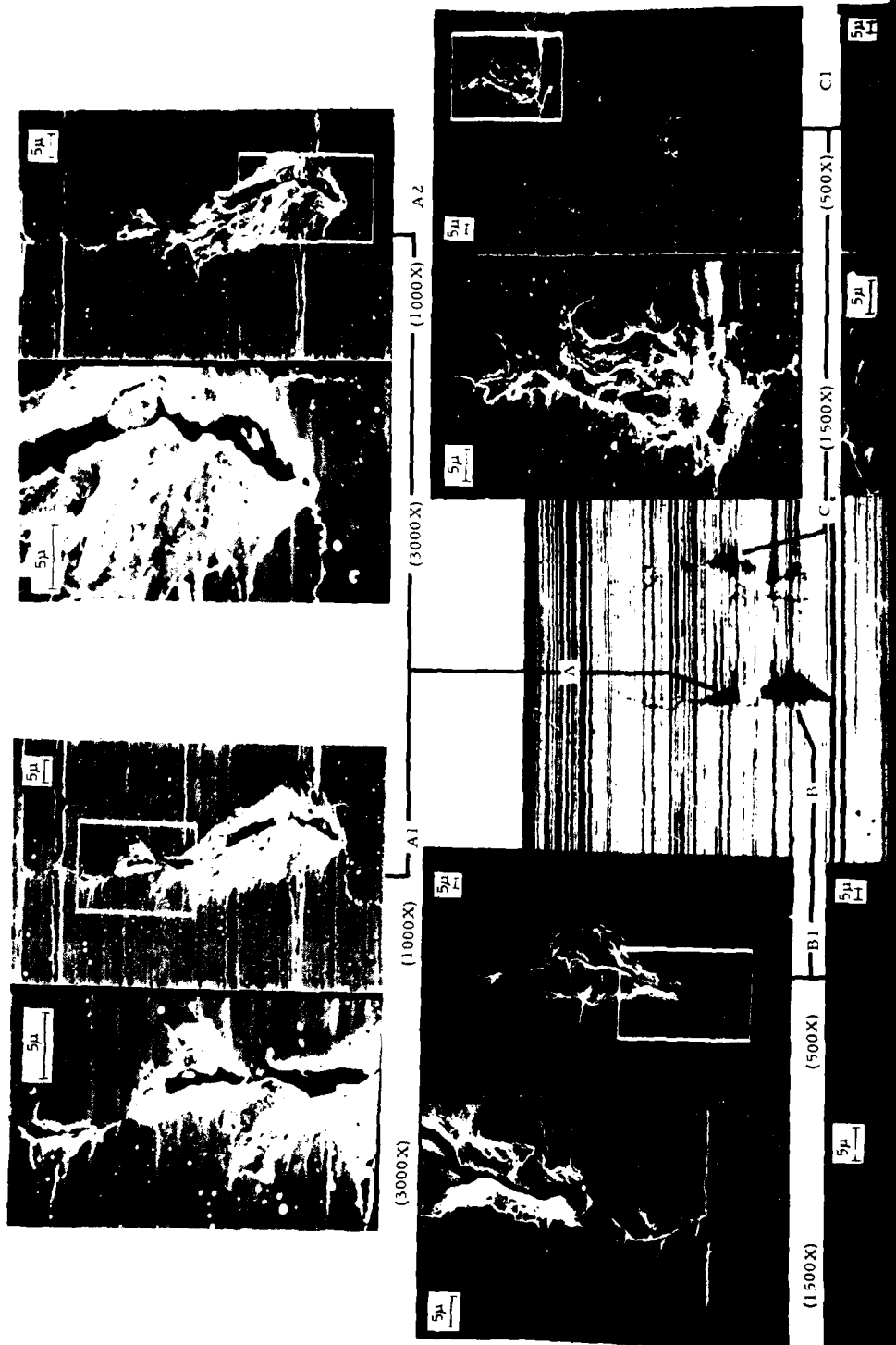
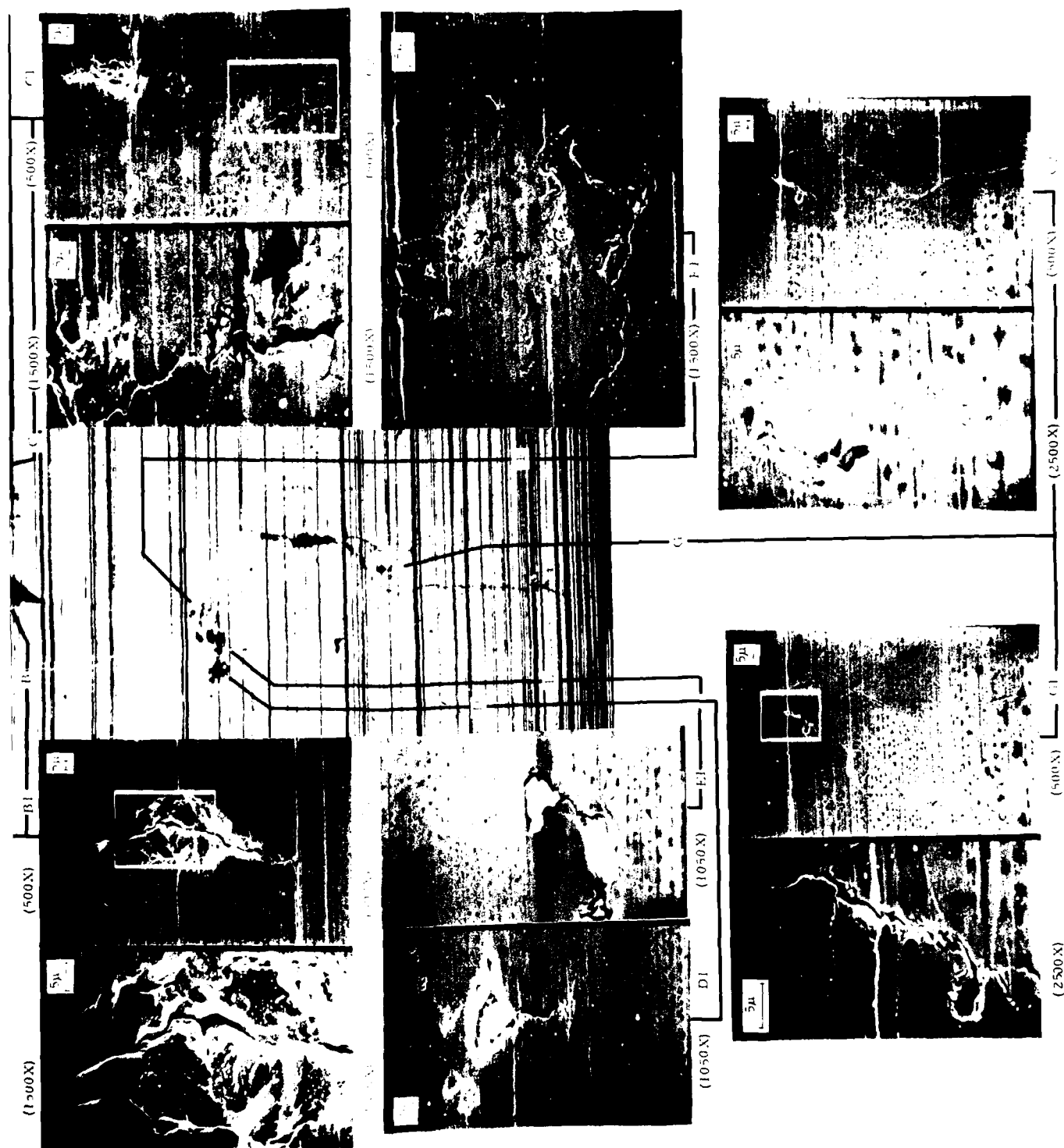
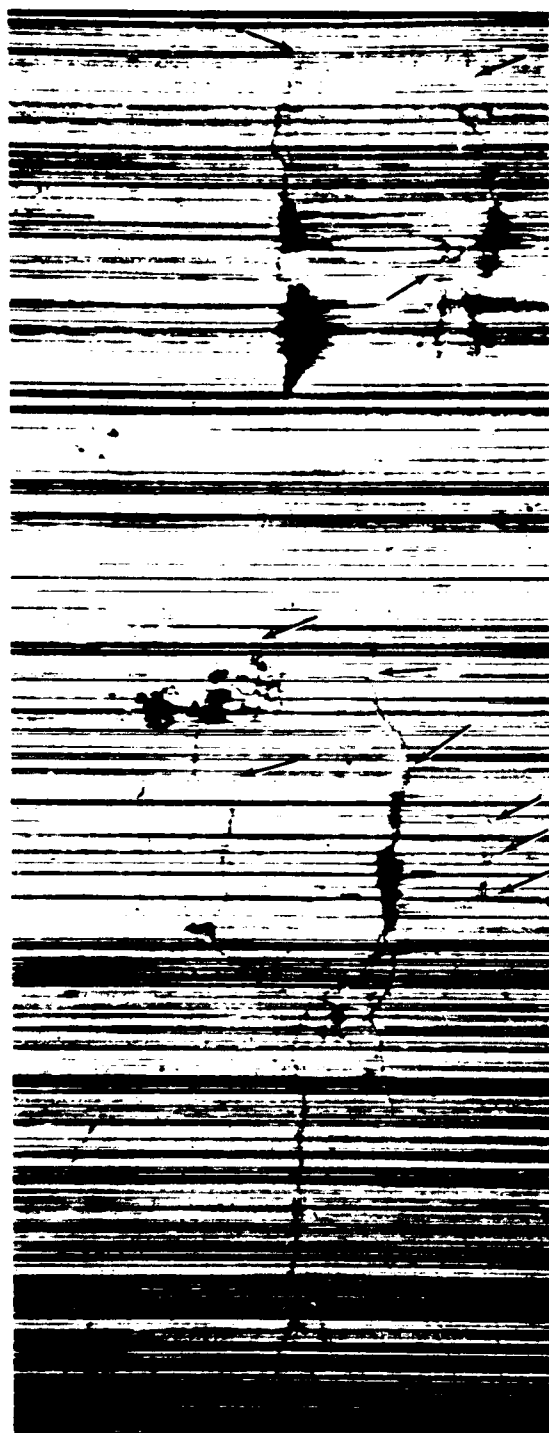


FIGURE F19. REPLICATION
(0002/0008-2)
(S00762) (69)

5035



LOCATION RESULTS FROM LARGE CRACK NETWORK IN VENDOR REWORKED BEARING
 1/0008-2290, J57-#2 Bearing S/N 124 - Inner Race, Loaded Half
 (62) (6965 hrs. service).



Before Endurance Test ($\sim 100\times$)



After 1 Hr. @ 204 ksi Hertz Stress
Endurance Test ($\sim 100\times$)

Small arrows point out regions of crack propagation.

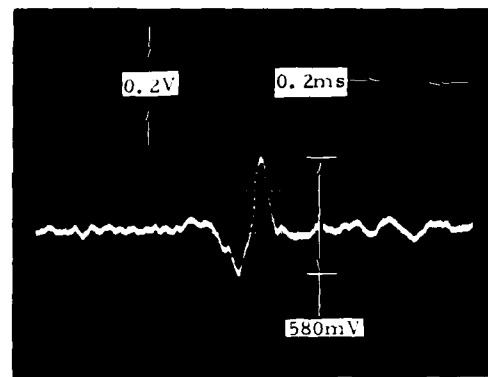
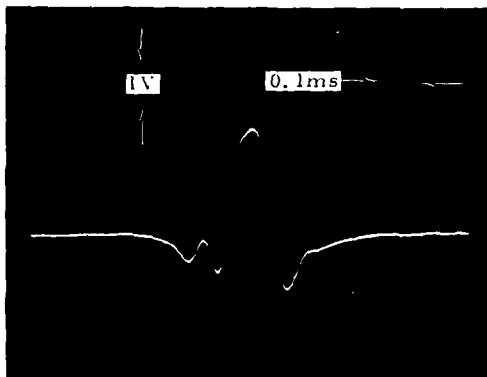
FIGURE F20. SURFACE PHOTOMICROGRAPHS SHOWING CRACK NETWORK "BEFORE" AND "AFTER" 1 HR ENDURANCE TEST [S00762(3)].

Before Endurance Test

F-21

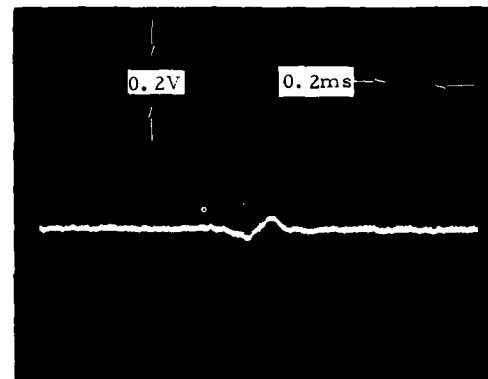
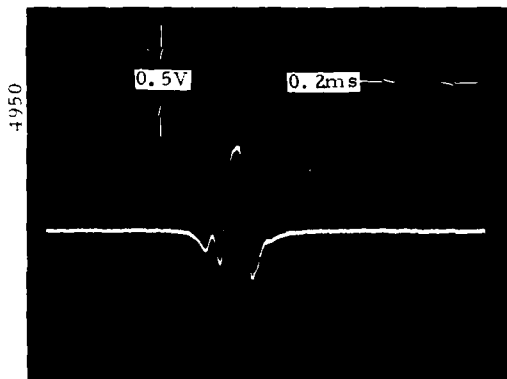
A. Radial Flux, High Field

D. Circumferential Flux, High Field



B. Radial Flux, Low Field

E. Circumferential Flux, Low Field



After 8.0 Hrs. Endurance Test

C. Radial Flux, High Field

F. Circumferential Flux, High Field

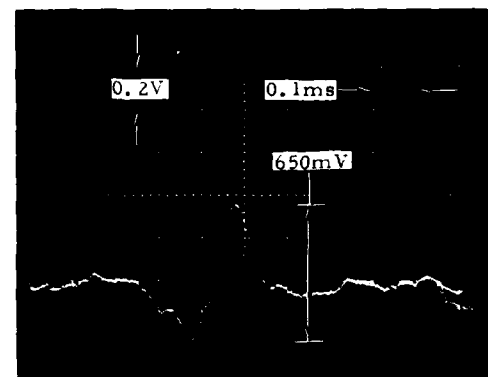
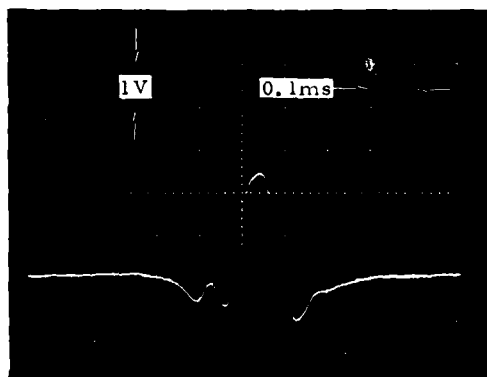
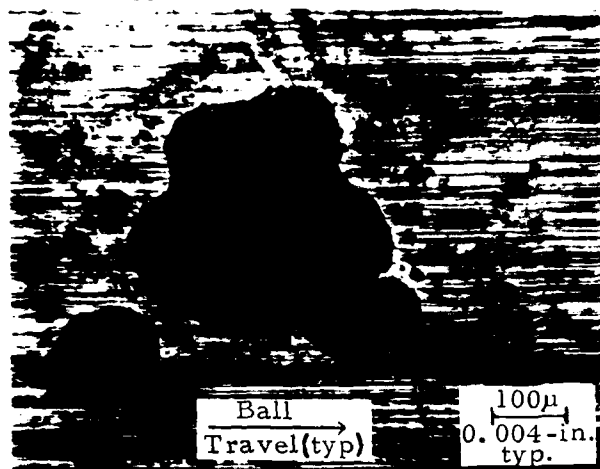


FIGURE F21. MAGNETIC PERTURBATION SIGNATURES AT TWO ENDURANCE TEST INTERVALS FROM LARGE SURFACE FLAW AT 0006+18 IN J85-#2 BEARING S/N A4230, INNER RACE, NONLOADED HALF (1133 hrs. service time) (S30211).

Before Endurance Test

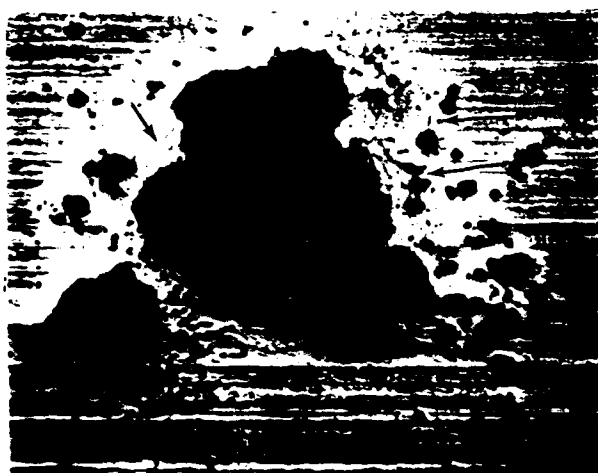
Surface Flaw @ 0006+18-3547



Surface Flaw @ 0007+4-3679



After 8.0 hrs. Endurance Test



After 12.0 hrs. Endurance Test

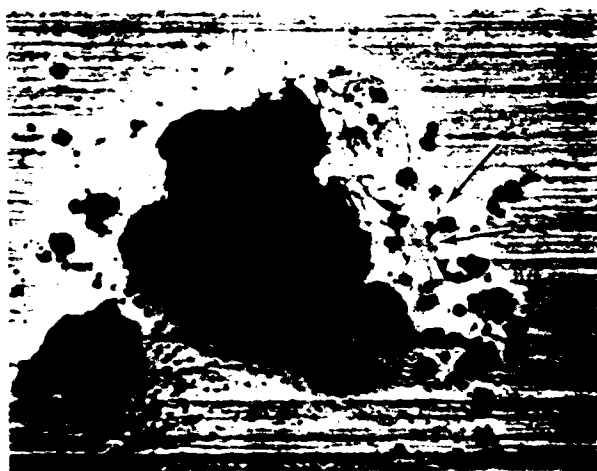
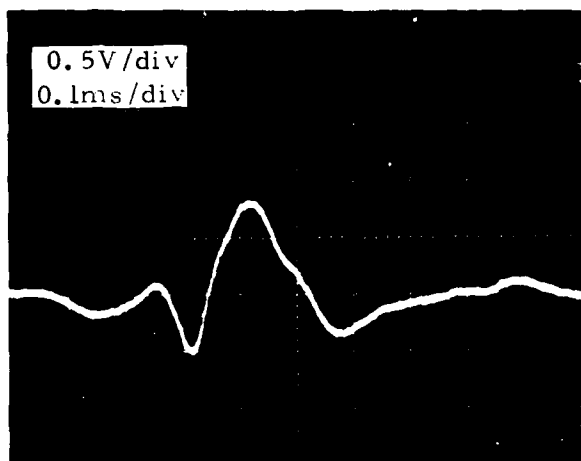
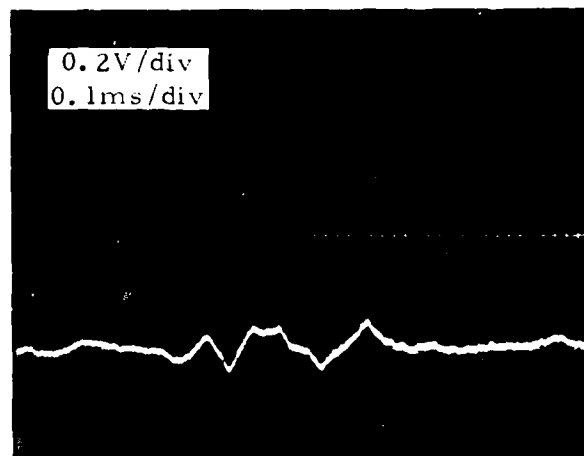


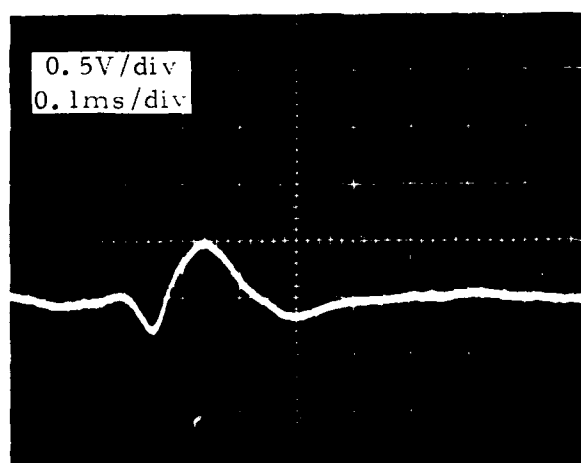
FIGURE F22. SURFACE PHOTOMICROGRAPH OF TWO LARGE FLAWS AT SEVERAL ENDURANCE TEST INTERVALS, J85-#2 BEARING S/N A4230, INNER RACE, NONLOADED HALF (1133 hrs. service time) (S30211).



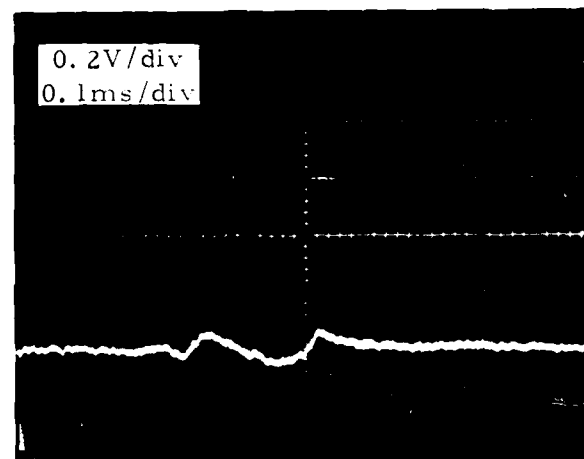
RH Signature



CH Signature



RL Signature



CL Signature

(BR 1288, ST0013+06)

(BR 1288, ST0013+06)

$$\frac{RH}{RL} = \frac{1.4V}{0.8V} = 1.75$$

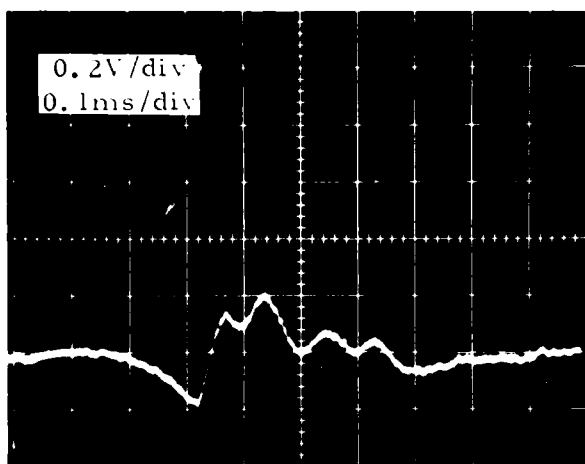
$$\frac{CH}{CL} = \frac{0.2V}{0.14V} = 1.43$$

FIGURE F23. MAGNETIC PERTURBATION SIGNATURES FROM SERVICE INDUCED CRACK NETWORK AT0013-1288 IN J57-#4 BEARING S/N 6857-1, INNER RACE LOADED HALF S11281(3) (1668 hrs. service, Vendor reworked).

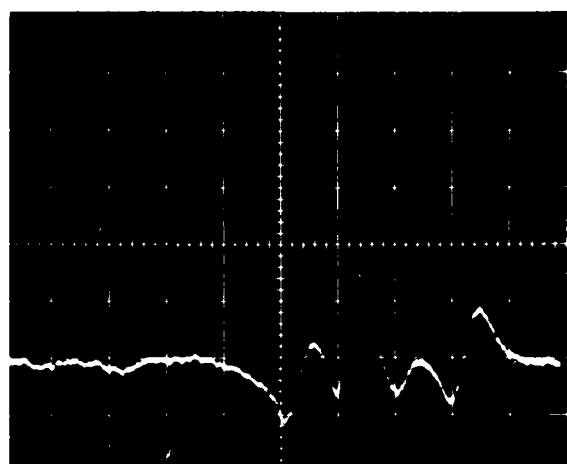
5036



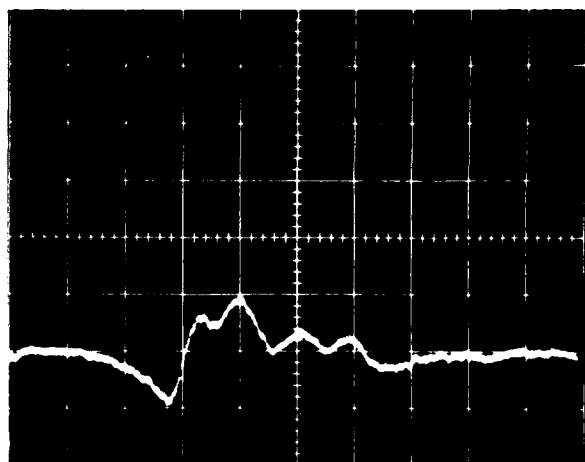
FIGURE F24. SURFACE PHOTOMICROGRAPH OF CRACKS IN VENDOR REMORKED BEARING (Signature Location 0013-1288 on J57-#4 Bearing S/N 6850-1 Inner Race, loaded Half S11281(3), 1668 hrs. service).



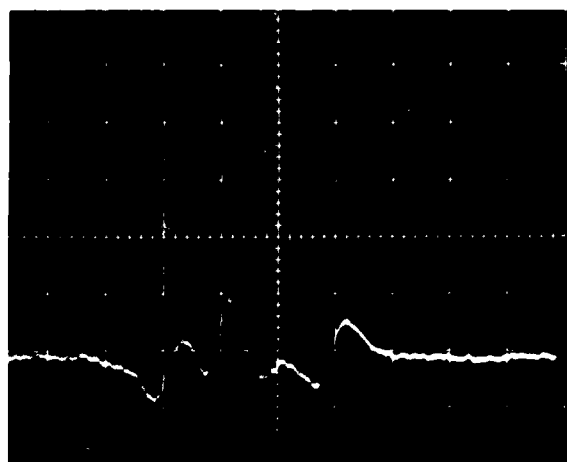
A. RH Signature



C. CH Signature



B. RL Signature



D. CL Signature

(BR 2127, ST0007+08)

(BR 2127, ST0007+08)

$$\frac{RH}{RL} = \frac{0.4V}{0.4V} = 1.00$$

$$\frac{CH}{CL} = \frac{0.56V}{0.38V} = 1.47$$

BR 2127, ST0007+08

FIGURE F25. MAGNETIC PERTURBATION SIGNATURES FROM SERVICE INDUCED CRACK NETWORK AT 0007, 0008-2127 IN J57-#2 BEARING S/N 2916-2, OUTER RACE S00722(5) (7259 hrs. service, vendor reworked).

5039



FIGURE F26. SURFACE PHOTOMICROGRAPH OF CRACKS IN VENDOR REWORKED BEARING (Signature Location 0007, 0008-2127 on J57-#2 Bearing S/N Z916-2 Outer Race S00722 (5), 7259 hrs. service).

5113

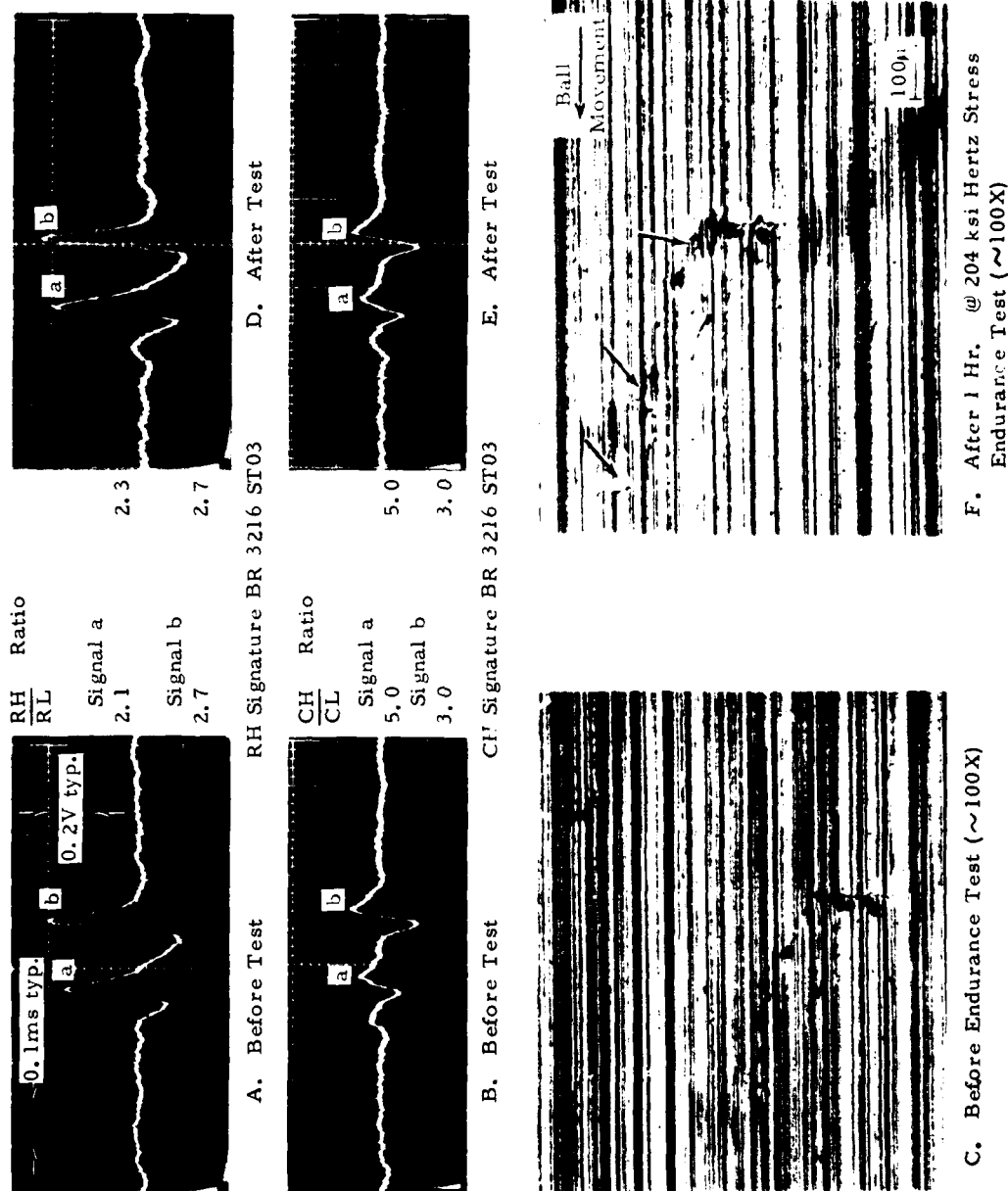


FIGURE F27. MAGNETIC PERTURBATION SIGNATURES FROM AND SURFACE PHOTOMICROGRAPHS OF CRACK NETWORK "BEFORE" AND "AFTER" 1 HR ENDURANCE TEST [S00591(3)].

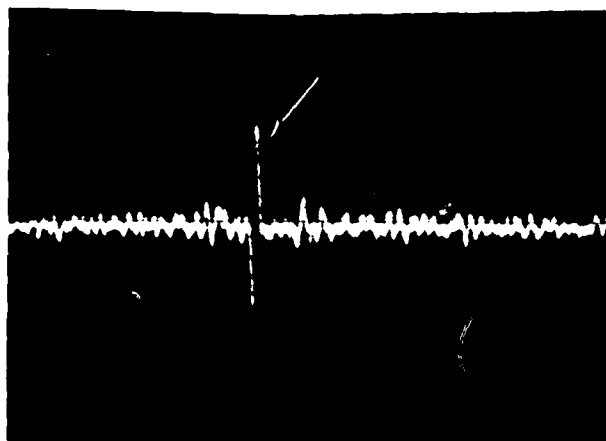
FLAWS

TY S T B R S R
 RH 0005 4405 4427
 RL 0005 4405 4427

Legend:

R - radial flux
 H - high flux density
 L - low flux density
 ST - probe location across race groove
 BR - azimuthal location of signature
 from reference mark on race
 (1 rev = 5000)

Flaw Printout Obtained During Automatic Magnetic Perturbation Inspection



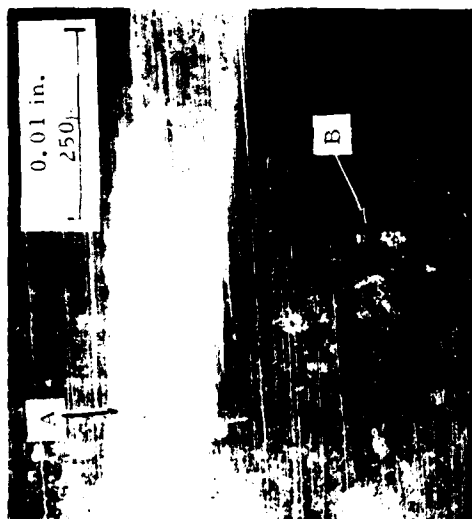
RH Signature @ 0005-4405



Magnified (50X) View of Surface @ 0005-4405

FIGURE F28. CIBLE RESULTS ON J57-#2 BEARING (S/N 704A-1) INNER RACE (New Bearing).

4095



Magnified View (100X) of Surface
(SEM) @ 0005-4405



Magnified View ($\sim 600X$) of Region A (SEM)

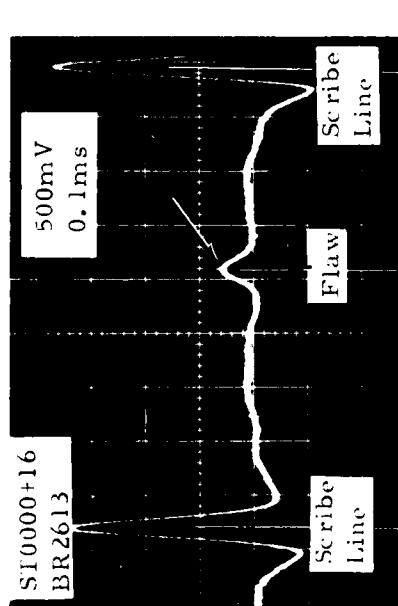


Magnified
View
($\sim 1500X$)
of Region A'
(SEM)

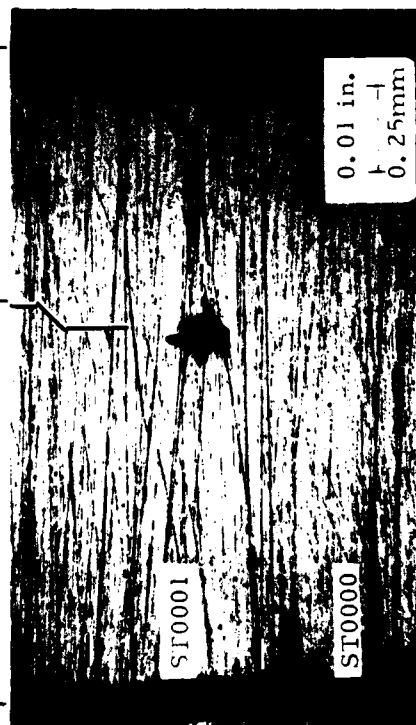
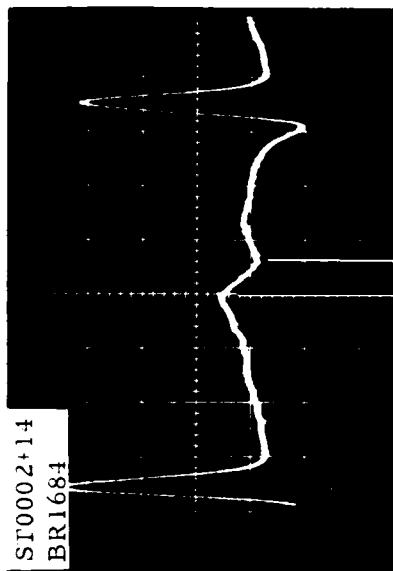


Magnified
View
($\sim 600X$)
of Region B
(SEM)

FIGURE F29. SCANNING ELECTRON MICROSCOPE (SEM) PHOTOGRAPHS OF SURFACE
IMPERFECTION (Replica) AT 0005-4405, J57-#2 BEARING (S/N704A-1)
INNER RACE (New Bearing).



A. Surface Flaw and Scribe Line Signatures

B. Surface Photomicrograph ($\times 50X$)

C. Surface Flaw and Scribe Line Signatures

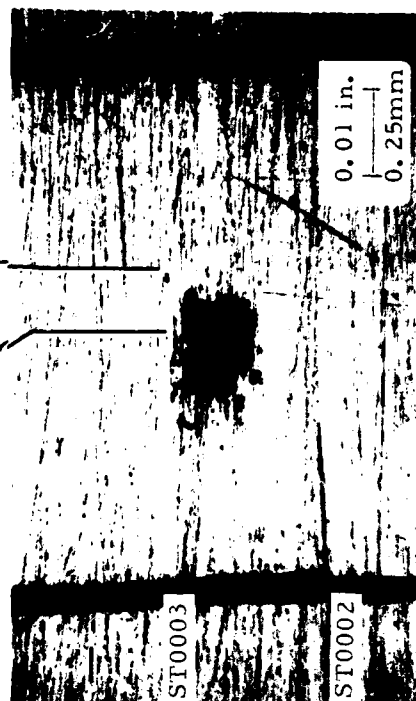
D. Surface Photomicrograph ($\times 50X$)

FIGURE F30. MAGNETIC PERTURBATION RADIAL SIGNATURE RECORDS AND SURFACE PHOTOMICROGRAPHS ILLUSTRATING METHOD FOR ACCURATELY DETERMINING FLAW SIGNATURE LOCATIONS ON J57-#4 BEARING (S/N 141C-1) INNER RACE S10071(2) (reparable bearing, 7946 hrs. service).

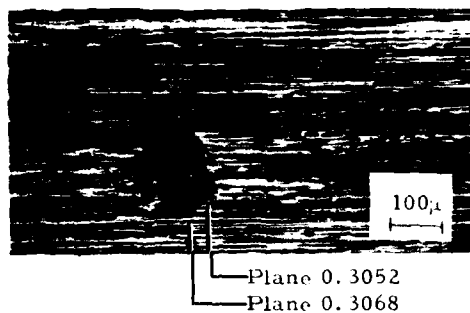
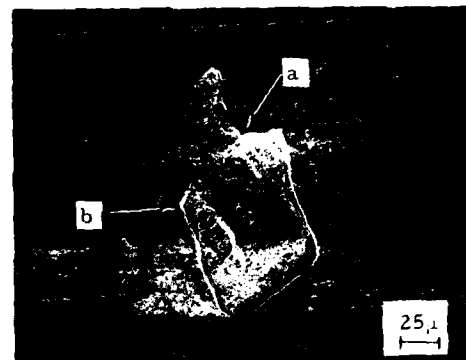
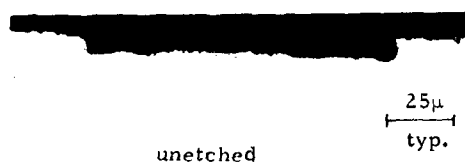
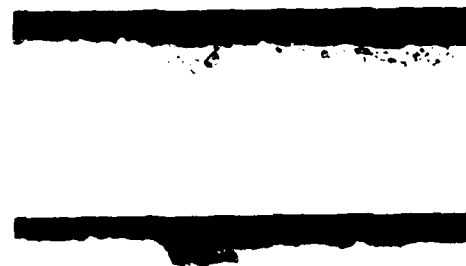
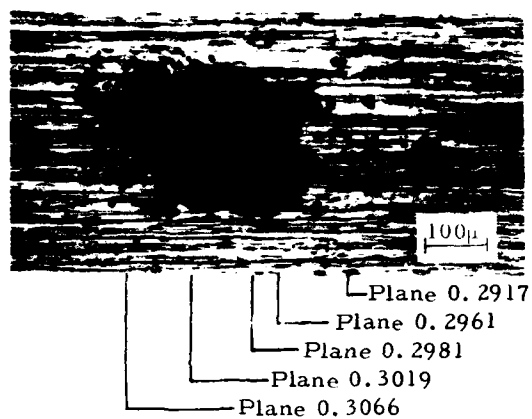
A. Surface Photomicrograph $\sim 100X$ B. Magnified View ($\sim 300X$) of Surface (SEM)
(after 2% nital etch)C. Magnified View ($\sim 1500X$) of Region a (SEM)
(after 2% nital etch)D. Magnified View ($\sim 1500X$) of Region b (SEM)
(after 2% nital etch)E. Section Plane 0.3068 $\sim 500X$ F. Section Plane 0.3052 $\sim 500X$

FIGURE F31. REPLICATION AND METALLURGICAL SECTIONING RESULTS FOR
SURFACE IMPERFECTION AT 0001-2613, J57-#4 BEARING INNER
RACE S/N 141C-1 REPARABLE REJECT S10071(2).



A. Surface Photomicrograph ~100X

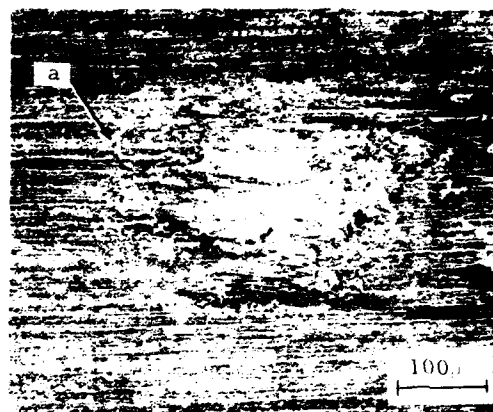
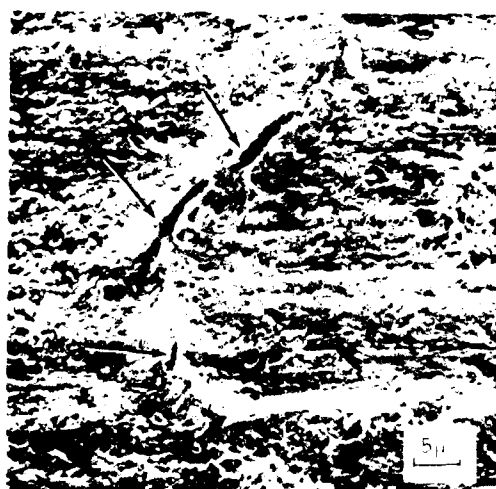
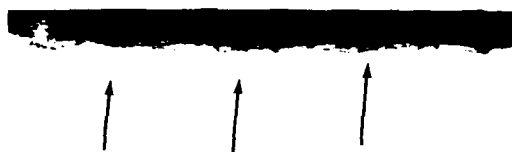
B. Magnified View (~150X) of Surface (SEM)
(after 2% nital etch)C. Magnified View (~1500X) of Region
a (SEM)D. Section Plane 0.3066 ~500X
(2% nital etch)E. Section Plane 0.3019 ~500X
(unetched)F. Section Plane 0.3019 ~500X
(2% nital etch)

FIGURE F32. REPLICATION AND SECTIONING RESULTS FOR SURFACE IMPERFECTION
AT 0003-1684, J57-#4 BEARING (S/N 141C-1) INNER RACE S10071(2)
(Reparable Reject, 7946 Hrs.)

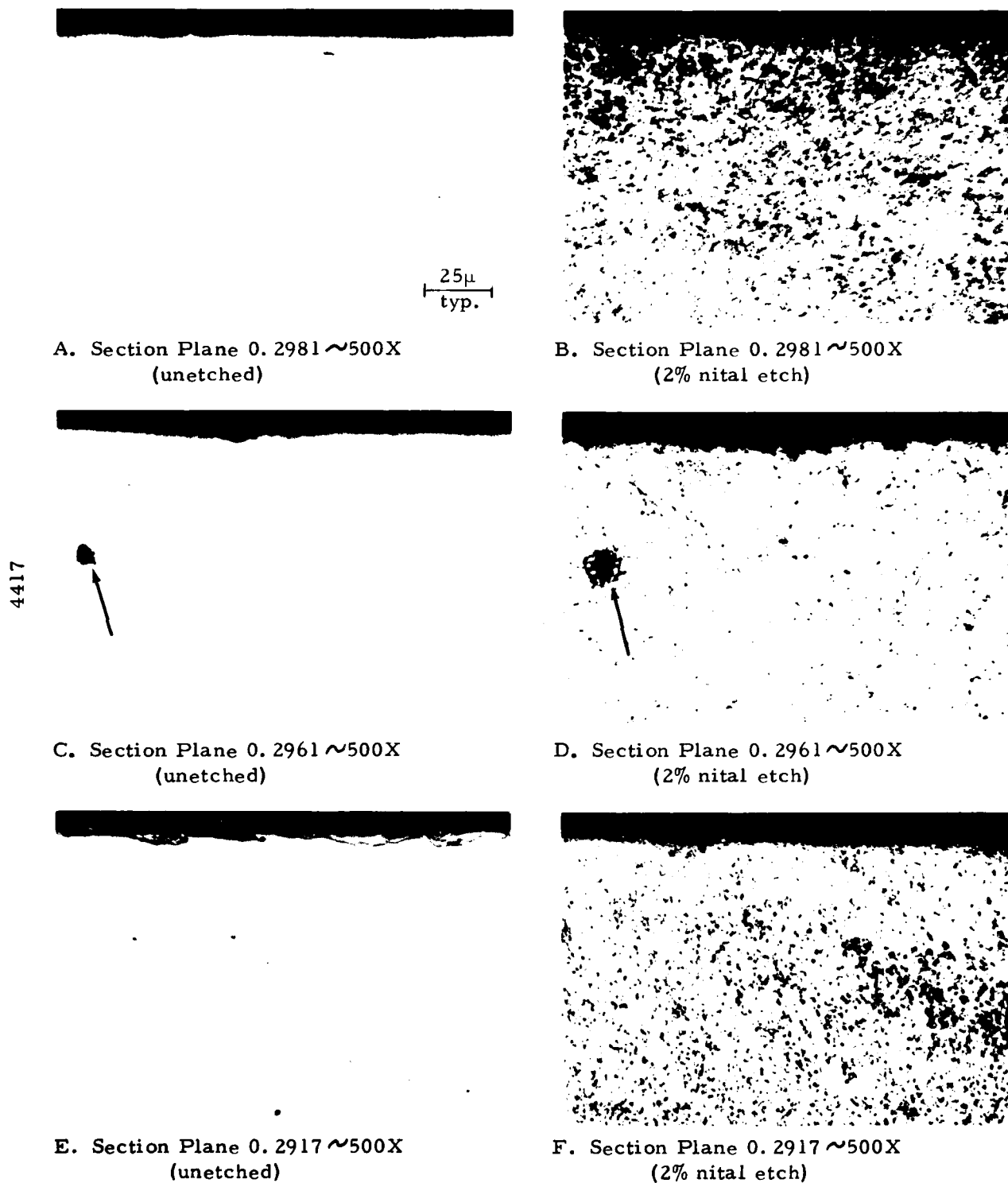
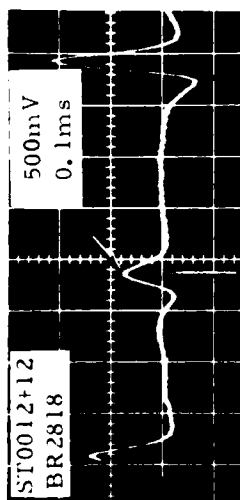
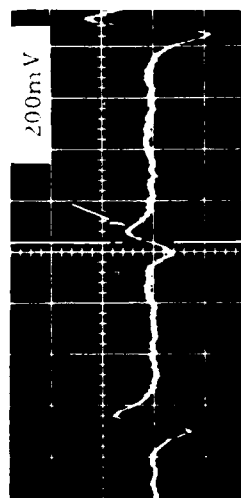


FIGURE F33. REPLICATION AND SECTIONING RESULTS FOR SURFACE IMPERFECTION AT 0003-1684, J57-#4 BEARING (S/N 141C-1) INNER RACE S10071(2) (reparable reject, 7946 hrs.).

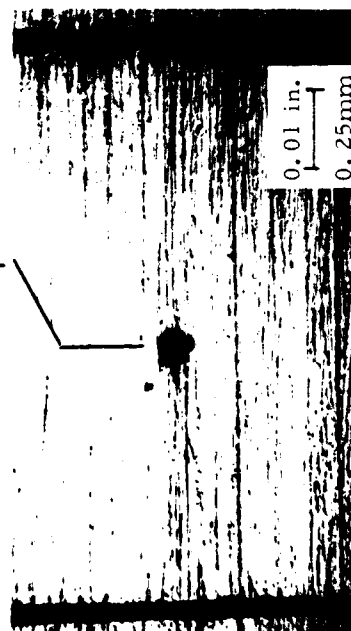
4421



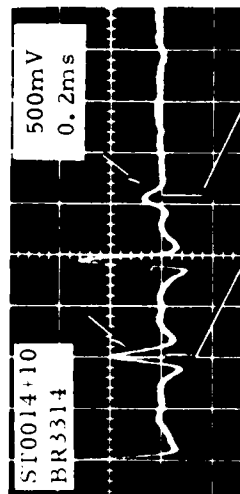
A. RH Signatures



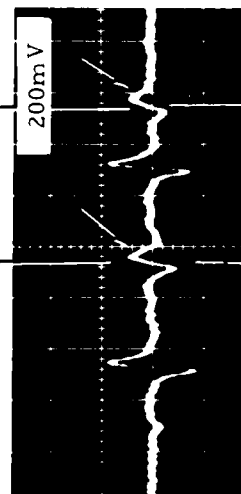
B. CH Signatures
Flaw and Scribe Line Signatures



C. Surface Photomicrograph (~50X)



D. RH Signatures

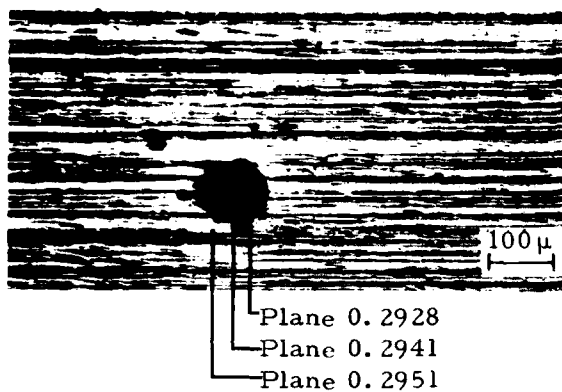
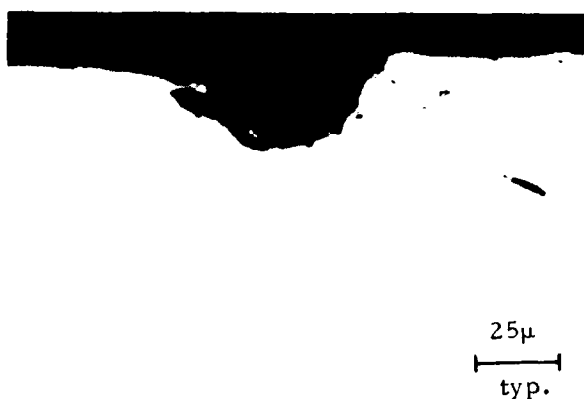


E. CH Signatures
Flaw and Scribe Line Signatures



F. Surface Photomicrograph (~50X)

FIGURE F34. MAGNETIC PERTURBATION RECORDS AND SURFACE PHOTOMICROGRAPHS ILLUSTRATING
CORRESPONDING LOCATIONS OF SIGNATURES ON J57-#4 BEARING (S/N 427C-1) INNER
RACE S10141(3) (reparable bearing, 8337 hrs. service after rework).

A. Surface Photomicrograph $\sim 100X$ B. Magnified View ($\sim 600X$) of Surface (SEM)
(after 2% nital etch)C. Section Plane 0.2951 $\sim 500X$ D. Section Plane 0.2951 $\sim 1000X$ 

E. Section Plane 0.2941 500X



F. Section Plane 0.2928 500X

FIGURE F35. REPLICATION AND METALLURGICAL SECTIONING RESULTS FOR
SURFACE INCLUSION PIT AT 0013-2818, J57-#4 BEARING
(S/N 427C-1) INNER RACE S1014(3) (8337 hrs. after rework,
reparable).

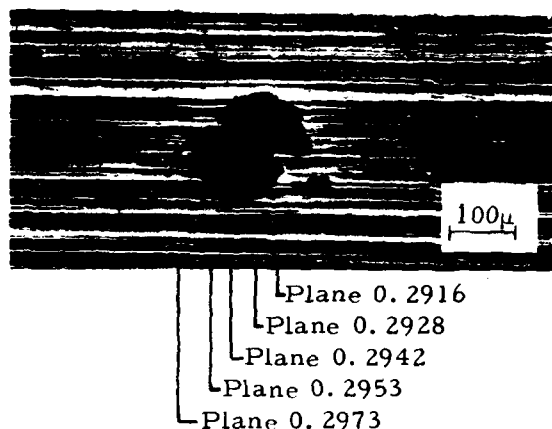
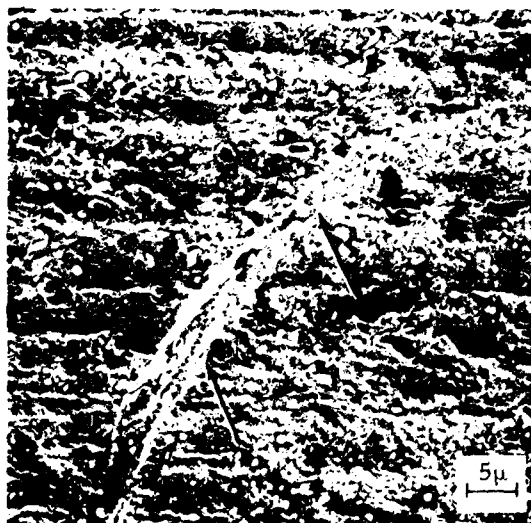
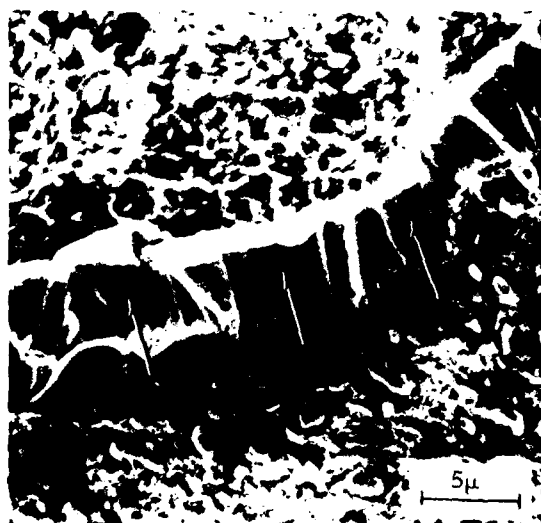
A. Surface Photomicrograph $\sim 100X$ B. Magnified View ($\sim 300X$) of Surface (SEM)
(after 2% nital etch)C. Magnified View ($\sim 1500X$) of Region
a (SEM) (after 2% nital etch)D. Magnified View ($\sim 3000X$) of Region b (SEM)
(after 2% nital etch)E. Section Plane 0.2973 $\sim 500X$ F. Section Plane 0.2953 $\sim 500X$

FIGURE F36. REPLICATION AND SECTIONING RESULTS FOR SURFACE INCLUSION
PIT AT 0014-3314, J57-#4 BEARING (S/N 427C-1) INNER RACE
S10141(3) (8337 hrs. after rework, reparable).

4416



A. Section Plane 0.2942 ~500X
(unetched)

25μ



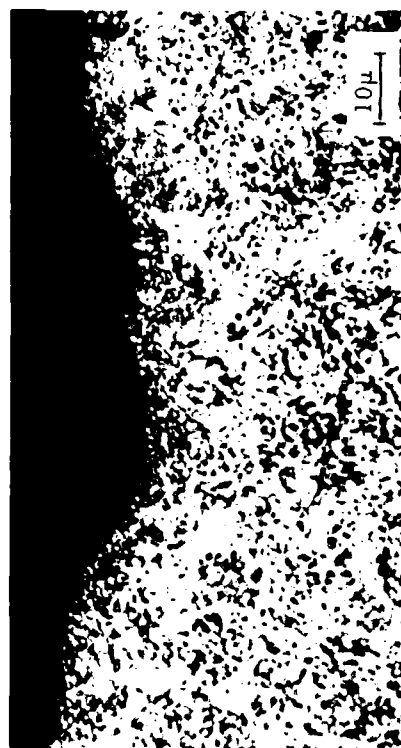
B. Section Plane 0.2928 ~500X
(unetched)

25μ



C. Section Plane 0.2916 ~1000X
(unetched)

10μ



D. Section Plane 0.2916 ~1000X
(2% nital etch)

10μ

FIGURE F37. REPLICATION AND SECTIONING RESULTS FOR SURFACE INCLUSION PIT AT 0014-3314, J57-#4 BEARING (S/N 427C-1) INNER RACE S10141(3) (8337 hrs. after rework, repairable).

FLAWS

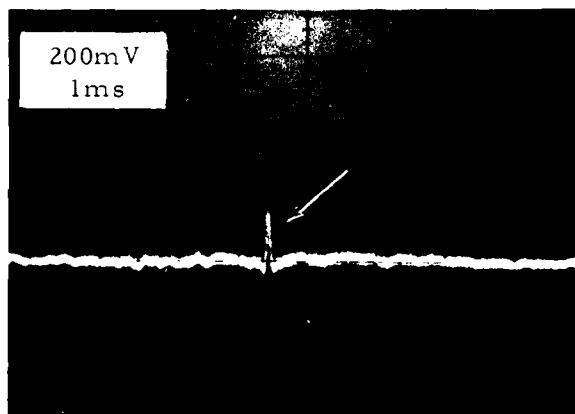
| TY | ST | BR | SR |
|----|------|------|------|
| RH | 0011 | 2469 | 2467 |
| RL | 0011 | 2470 | 2468 |

Legend:

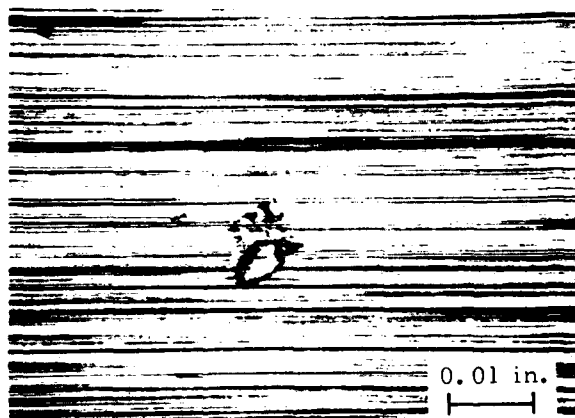
R - radial flux
H - high flux density
L - low flux density
ST - probe location across race groove
BR - azimuthal location of signature
from reference mark on race
(1 rev = 5000)

F-38

Flaw Printout Obtained During Automatic Magnetic Perturbation Inspection



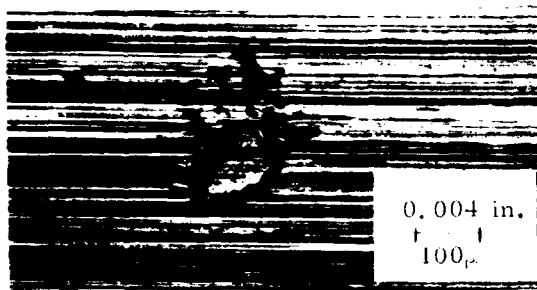
RH Signature @ 0011-2469



Magnified (50X) View of Surface @ 0011-2469

FIGURE F38. CIBLE RESULTS ON J57-#4 BEARING (S/N 7563-2) OUTER RACE S10992(5) (reworked bearing with 700 hrs. service - service prior to rework unknown).

4424



A. Optical Photomicrograph ($\sim 100X$)



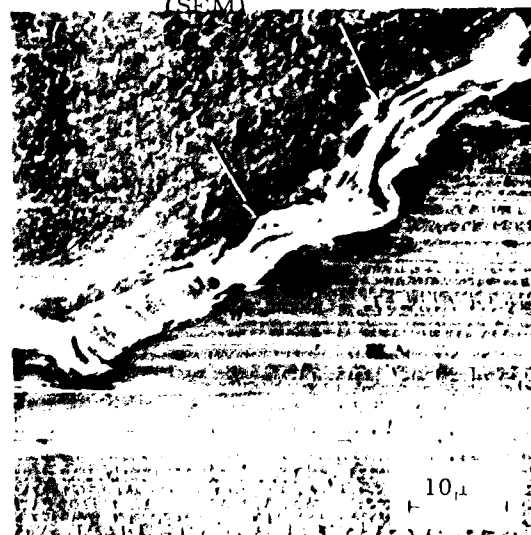
B. Magnified View ($\sim 300X$) of Surface (SEM)



C. Magnified View ($\sim 1500X$) of Region a (SEM)

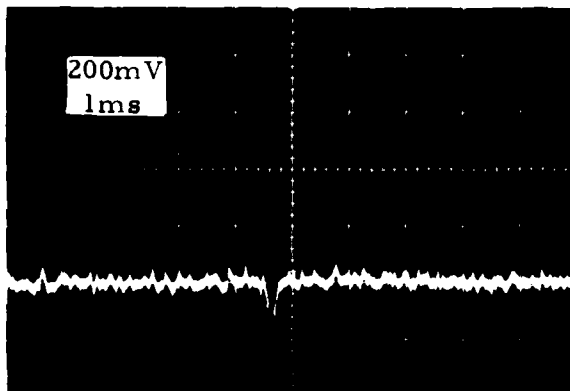


D. Magnified View ($\sim 1500X$) of Region b (SEM)

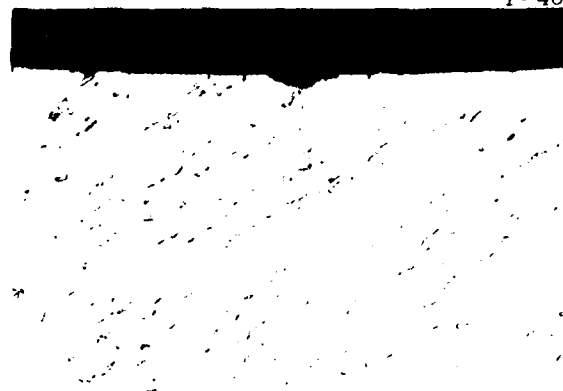


E. Magnified View ($\sim 1500X$) of Region c (SEM)

FIGURE F39. OPTICAL AND SEM PHOTOMICROGRAPHS OF SURFACE IMPERFECTION AT 0011-2469, J57-#4 BEARING (S/N 7563-2) OUTER RACE S10992(5) (Reworked + 700 hrs.).



A. Radial Flux, High Field
Signature (© ST0006+16, BR4968)



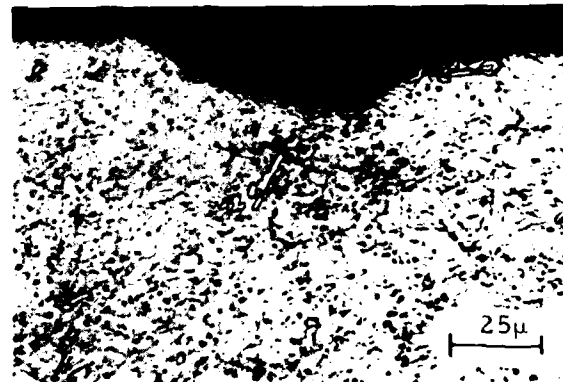
D. Section Plane 0.4266 ~100X
(2% nital etch)

4913



B. Surface Photomicrograph ~100X

Plane 0.4241
Plane 0.4266
Plane 0.4293



E. Section Plane 0.4266 ~500X
(2% nital etch)

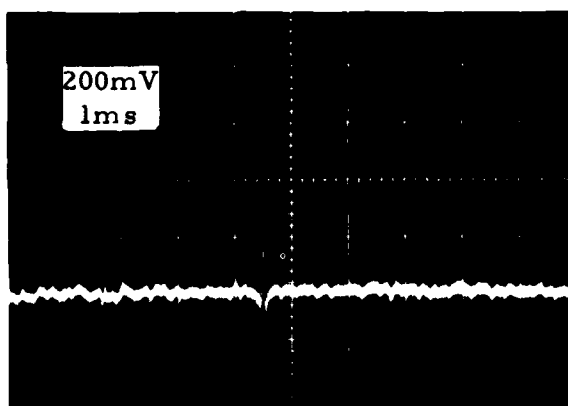


C. Section Plane 0.4293 ~100X
(unetched)



F. Section Plane 0.4241 ~100X
(unetched)

FIGURE F40. METALLURGICAL SECTIONING RESULTS FOR SURFACE IMPERFECTION
AT 0006-4968, J85-#2 BEARING (S/N 06498) INNER RACE
S31091(2) (time limited, 2851 hrs.).



A. Radial Flux, High Field
Signature @ ST0005+ 10, BR0763



Plane 0.4269

B. Surface Photomicrograph ~100X



C. Section Plane 0.4269 ~500X
(2% nital etch)

FIGURE F41. METALLURGICAL SECTIONING RESULTS FOR SURFACE IMPERFECTION
AT 0005-0763, J85-#2 BEARING (S/N 0743A) INNER RACE S31391(2)
(time limited, 1986 hrs.).